

AD-A278 791



PROCESSING AND PROPERTIES OF HIGH TEMPERATURE METAL/FIBER-REINFORCED- THERMOPLASTIC LAMINATES

Jeffrey Cook
Air Vehicle and Crew Systems Technology Department (Code 6063)
NAVAL AIR WARFARE CENTER
AIRCRAFT DIVISION, WARMINSTER
P.O. Box 5152
Warminster, PA 18974-0591

19 OCTOBER 1993



FINAL REPORT

Approved for Public Release; Distribution is Unlimited

94-13206



2198

Prepared for
Air Vehicle and Crew Systems Technology Department
6.2 Aircraft Materials Block
NAVAL AIR WARFARE CENTER
AIRCRAFT DIVISION WARMINSTER
P.O. Box 5152
Warminster, PA 18974-0591

84 8 02 8 6

**Best
Available
Copy**

NOTICES

REPORT NUMBERING SYSTEM — The numbering of technical project reports issued by the Naval Air Warfare Center, Aircraft Division, Warminster is arranged for specific identification purposes. Each number consists of the Center acronym, the calendar year in which the number was assigned, the sequence number of the report within the specific calendar year, and the official 2-digit correspondence code of the Functional Department responsible for the report. For example: Report No. NAWCADWAR-92001-60 indicates the first Center report for the year 1992 and prepared by the Air Vehicle and Crew Systems Technology Department. The numerical codes are as follows:

CODE	OFFICE OR DEPARTMENT
00	Commanding Officer, NAWCADWAR
01	Technical Director, NAWCADWAR
05	Computer Department
10	AntiSubmarine Warfare Systems Department
20	Tactical Air Systems Department
30	Warfare Systems Analysis Department
50	Mission Avionics Technology Department
60	Air Vehicle & Crew Systems Technology Department
70	Systems & Software Technology Department
80	Engineering Support Group
90	Test & Evaluation Group

PRODUCT ENDORSEMENT — The discussion or instructions concerning commercial products herein do not constitute an endorsement by the Government nor do they convey or imply the license or right to use such products.

Reviewed By: Jeffrey Waldman Date: 2/24/94
Branch Head

Reviewed By: Shirley S. Huff Date: 2/25/94
Division Head

Reviewed By: Paul H. Hsu Date: 2/26/94
Director/Deputy Director

REPORT DOCUMENTATION PAGE			Form Approved OMB No. 0704-0188	
Public reporting burden for this collection of information is estimated to average 1 hour per response, including the time for reviewing instructions, searching existing data sources, gathering and maintaining the data needed, and completing and reviewing the collection of information. Send comments regarding this burden estimate or any other aspect of this collection of information, including suggestions for reducing this burden, to Washington Headquarters Services, Directorate for Information Operations and Reports, 1215 Jefferson Davis Highway, Suite 1204, Arlington, VA 22202-4302, and to the Office of Management and Budget, Paperwork Reduction Project (0704-0188), Washington, DC 20503.				
1. AGENCY USE ONLY (Leave blank)	2. REPORT DATE 19 Oct. 1993	3. REPORT TYPE AND DATES COVERED Final		
4. TITLE AND SUBTITLE PROCESSING AND PROPERTIES OF HIGH TEMPERATURE METAL/FIBER-REINFORCED- THERMOPLASTIC LAMINATES		5. FUNDING NUMBERS		
6. AUTHOR(S) Jeffrey Cook				
7. PERFORMING ORGANIZATION NAME(S) AND ADDRESS(ES) Air Vehicle and Crew Systems Technology Department (Code 6063) NAVAL AIR WARFARE CENTER AIRCRAFT DIVISION WARMINSTER P.O. Box 5152 Warminster, PA 18974-0591		8. PERFORMING ORGANIZATION REPORT NUMBER NAWCADWAR-93079-60		
9. SPONSORING / MONITORING AGENCY NAME(S) AND ADDRESS(ES) Air Vehicle and Crew Systems Technology Department 6.2 Aircraft Materials Block NAVAL AIR WARFARE CENTER AIRCRAFT DIVISION WARMINSTER P.O. Box 5152 Warminster, PA 18974-0591		10. SPONSORING / MONITORING AGENCY REPORT NUMBER		
11. SUPPLEMENTARY NOTES This report was submitted as a Master's thesis at Lehigh University in December, 1992, in partial fulfillment of the requirements for the author's Master's of Science degree in Materials Science and Engineering.				
12a. DISTRIBUTION / AVAILABILITY STATEMENT Approved for Public Release; Distribution is Unlimited		12b. DISTRIBUTION CODE		
13. ABSTRACT (Maximum 200 words) Equations for predicting the theoretical stresses and mechanical properties of fiber/metal laminates were derived. These were applied to a model high temperature laminate system based on 8009 aluminum and glass fiber reinforced U-25 thermoplastic polyimide. The effects of aluminum surface treatment on bond strength were investigated; chemical surface treatments gave superior bond strength compared to mechanical treatments. Adequate bond strength was obtained using simplified and environmentally safe surface preparation techniques. The tensile yield and ultimate strength, elastic modulus, fracture behavior, dynamic mechanical behavior, chemical resistance, and fatigue resistance of the laminate were investigated. Most properties were found to correlate well with the theoretical predictions. The laminate showed excellent strength retention at temperatures above 200°C. Fatigue resistance as-processed was found to be comparable to monolithic 8009. Post-stretching the laminate was shown to increase both fatigue life and yield strength substantially.				
14. SUBJECT TERMS Theoretical Stresses, Mechanical Properties, Fiber/Metal Laminates, Bond Strength			15. NUMBER OF PAGES	
			16. PRICE CODE	
17. SECURITY CLASSIFICATION OF REPORT UNCLASSIFIED	18. SECURITY CLASSIFICATION OF THIS PAGE UNCLASSIFIED	19. SECURITY CLASSIFICATION OF ABSTRACT UNCLASSIFIED	20. LIMITATION OF ABSTRACT SAR	

1.
ABSTRACT (Continued)

Dynamic mechanical properties were found to be superior to monolithic 2024 and 8009 aluminum, and marginally better than ARALL-4, as well. The relatively high dynamic loss modulus suggests that the laminate would be useful for applications involving acoustic fatigue. Chemical resistance of the laminate was found to be excellent against most U.S. Navy environments. The potential usefulness of future high temperature laminates was well demonstrated by this study.

PREFACE

This report was submitted as a Master's thesis at Lehigh University in December, 1992, in partial fulfillment of the requirements for the author's Master's of Science degree in Materials Science and Engineering.

Accession For	
NTIS GRA&I	<input checked="" type="checkbox"/>
DTIC TAB	<input type="checkbox"/>
Unannounced	<input type="checkbox"/>
Justification	
By	
Distribution/	
Availability Codes	
Dist	Avail and/or Special
A-1	

ACKNOWLEDGEMENTS

This research was funded under the Naval Air Warfare Center's 6.2 Aircraft Materials Block, and was conducted at the NAWC using the materials processing and testing facilities of the Aerospace Materials Division. The author would like to acknowledge the contributions of the following individuals:

Dr. D. Thomas, Lehigh University, for his suggestions and advice;

Ethyl Corporation, for supplying glass-reinforced U-25 prepreg at no cost;

Pete Sabatini, for anodizing dozens of aluminum sheets on very short notice;

Dickson Alley, for his assistance in laying up and autoclaving several dozen laminate panels despite a severe nitrogen shortage;

Walt Worden, for teaching me how to set up and use the milling machine and Krouse fatigue machines, and for his assistance and suggestions in machining specimens;

Gabe Pilla, for his assistance in setting up and troubleshooting the MTS hydraulic test system on the hundred or so occasions when it ceased functioning;

and, most of all,

Fuyu Lin Cook, for acting as my liaison at Lehigh and for giving me the encouragement and support to complete my Master's degree.

TABLE OF CONTENTS

ACKNOWLEDGEMENTS.....	iii
LIST OF TABLES.....	ix
LIST OF FIGURES.....	x
ABSTRACT.....	1
1.0. BACKGROUND: Fiber/Metal Laminates.....	2
1.1. Laminate Development.....	2
1.2. ARALL and Other Laminate Systems.....	3
1.3. Fabrication and Properties.....	4
1.4. Applications for ARALL and Glare.....	5
1.5. Drawbacks of ARALL and Glare.....	6
2.0. INTRODUCTION.....	7
2.1. Fabrication of Laminates.....	7
2.1.1. Adhesion.....	7
2.1.2. Lamina Surface Preparation.....	9
2.1.3. Lay-up and Processing.....	10
2.1.4. Residual Stress.....	11
2.1.5. Post-Processing Treatments.....	13
2.2. Properties of Laminates.....	14
2.2.1. Strength.....	14
2.2.2. Modulus.....	17
2.2.3. Density.....	18
2.2.4. Fatigue.....	18

2.2.5.	Toughness.....	23
2.2.6.	Impact Tolerance.....	24
2.2.7.	Dynamic Properties.....	27
2.2.8.	Thermal Resistance.....	29
2.2.9.	Environmental Resistance.....	32
2.3.	High Temperature Laminates.....	33
2.3.1.	The Need for High Temperature Laminates.....	34
2.3.2.	Issues for High Temperature Laminates.....	35
2.3.3.	Materials for High Temperature Laminates.....	41
2.3.4.	Special Problems of High Temperature Laminates....	47
2.4.	Previous and Ongoing Work in High Temperature Laminates...	49
2.4.1.	Drexel University.....	49
2.4.2.	Delft University.....	51
2.4.3.	Lockheed.....	51
2.4.4.	Naval Air Warfare Center, Warminster.....	51
3.0.	CURRENT RESEARCH: Processing and Properties of High Temperature Metal/Fiber-Reinforced-Thermoplastic Laminates.....	54
3.1.	Objectives.....	54
3.2.	Materials.....	54
4.0.	EXPERIMENTAL PROCEDURES.....	57
4.1.	Theoretical Predictions.....	57
4.2.	Laminate Fabrication.....	57
4.2.1.	Surface Treatments.....	57
4.2.2.	Processing.....	58
4.2.3.	Specimen Preparation.....	59

4.3.	Tests Performed.....	59
4.3.1.	Single Lap Shear Tests.....	59
4.3.2.	Floating Roller Peel Tests.....	60
4.3.3.	Tensile Tests.....	61
4.3.4.	Axial Fatigue Tests.....	62
4.3.5.	Dynamic Mechanical Tests.....	63
4.3.6.	Chemical Resistance Tests.....	64
5.0.	RESULTS.....	65
5.1.	Theoretical Predictions.....	65
5.1.1.	Residual Stress.....	65
5.1.2.	Yield Strength.....	66
5.1.3.	Ultimate Strength.....	66
5.1.4.	Modulus.....	66
5.1.5.	Density.....	66
5.2.	Laminate Processing.....	67
5.2.1.	Surface Treatments.....	67
5.2.2.	Processing.....	67
5.2.3.	Specimen Preparation.....	68
5.3.	Tests Performed.....	69
5.3.1.	Lap Shear Tests.....	69
5.3.2.	Roller Peel Tests.....	70
5.3.3.	Tensile Tests.....	72
5.3.4.	Axial Fatigue Tests.....	74
5.3.5.	Dynamic Mechanical Tests.....	75
5.3.6.	Chemical Resistance Tests.....	77

6.0. DISCUSSION.....	78
6.1. Lap Shear Tests.....	78
6.2. Roller Peel Tests.....	80
6.2.1. 2024/U25.....	80
6.2.2. 8009/U25.....	84
6.3. Tensile Tests.....	85
6.3.1. 8009.....	85
6.3.2. U-25 Composite.....	87
6.3.3. 8009/U25 Laminates.....	89
6.3.4. Tensile Fracture Energies.....	96
6.3.5. Summary of Tensile Properties.....	97
6.4. Axial Fatigue.....	99
6.4.1. 2024-T3 Aluminum.....	99
6.4.2. 8009 Aluminum.....	99
6.4.3. 8009/U25 Laminates.....	100
6.4.4. 8009/U25 Laminates: Residual Strength.....	104
6.4.5. 8009/U25 Laminates: Post-Stretched Fatigue.....	107
6.5. Dynamic Mechanical Tests.....	109
6.6. Chemical Resistance Tests.....	110
7.0. SUMMARY.....	112
7.1. 8009/U25 Laminates.....	112
7.2. Implications for Future High Temperature Laminates.....	112
8.0. CONCLUSIONS.....	115
REFERENCES.....	116

TABLES.....	125
FIGURES.....	141
APPENDICES.....	198
VITA.....	205

LIST OF TABLES

TABLE I. ARALL ^R Variants.....	126
TABLE II. Glare ^R Variants.....	126
TABLE III. Forms of Environmental Attack.....	127
TABLE IV. Candidate Metals for High Temperature Laminates.....	128
TABLE V. Candidate Fibers for High Temperature Laminates.....	129
TABLE VI. Candidate Polymers for High Temperature Laminates.....	130
TABLE VII. Aluminum Surface Treatments.....	131
TABLE VIII. Chemical Environments Tested.....	132
TABLE IX. Tensile Properties of 8009 Aluminum.....	133
TABLE X. Tensile Properties of 8009/U25 Laminates.....	134
TABLE XI. 3-Point Bend Results.....	135
TABLE XII. Fiber Stress as a Function of Delamination Length in 8009/U25 Tensile Specimens upon Aluminum Layer Failure.....	136
TABLE XIII. Tensile Fracture Energies.....	137
TABLE XIV. True Stress Range and Mean Stress in Aluminum during Fatigue, and Associated Fatigue Parameters.....	138
TABLE XV. Residual Strength of Fatigued Laminate Specimens.....	139
TABLE XVI. True Stresses and Fatigue Parameters in Aluminum during Fatigue in Post-Stretched Laminate Specimens.....	140

LIST OF FIGURES

Figure 1. Exploded View of ARALL Laminate.....	142
Figure 2. Tensile Properties of ARALL and Glare Laminates vs. 2024 Aluminum.....	143
Figure 3. Fatigue Properties of ARALL Laminates vs. 2024 Aluminum.....	144
Figure 4. Fokker F-27 Wing Panels made from ARALL.....	145
Figure 5. Atomically Rough Surfaces.....	146
Figure 6. Atomically Smooth Surfaces.....	146
Figure 7. Wetting of Surfaces by a Viscoelastic Polymer.....	147
Figure 8. Stress-Strain Diagram for ARALL-4.....	147
Figure 9. Fatigue Crack Growth Behavior of Conventional Materials...	148
Figure 10. Crack Bridging by Fibers in a Laminate.....	148
Figure 11. Fatigue Crack Growth Behavior of ARALL.....	149
Figure 12. Delamination in Laminates During Fatigue.....	150
Figure 13. Fiber Failure in a Laminate due to Excessive Bond Strength.....	151
Figure 14. The Crack Divider Principle.....	151
Figure 15. Cyclic Stress-Strain Response.....	152
Figure 16. Fatigue Specimens Used for S-N Testing of 8009 Aluminum and 8009/U25 Laminates.....	152
Figure 17. SEM Images of 2024 Surface Treatments.....	153-156
Figure 18. SEM Images of 8009 Surface Treatments.....	157-160
Figure 19. Appearance of a Cured 8009/U25 Laminate Panel.....	161
Figure 20. Optical Cross-Section of an 8009/U25 Laminate.....	161
Figure 21. Appearance of a Cured U-25 Composite Panel.....	162
Figure 22. Optical Cross-Section of a U-25 Composite.....	162

Figure 23. Effects of Surface Treatment on Shear Strength.....	163
Figure 24. Effects of Surface Treatment on Shear Strength.....	163
Figure 25. Macroscopic Photographs of 2024/U25 Shear Failures.....	164
Figure 26. SEM Images of 2024/U25 Shear Failures.....	165-166
Figure 27. ARALL-4 Shear Failures.....	167
Figure 28. Shear Strength of Various Laminates.....	168
Figure 29. Peel Strength of 2024/U25 Laminates.....	169
Figure 30. Wet vs. Dry Peel Strength of 2024/U25 Laminates.....	170
Figure 31. Effects of Surface Treatment on Peel Strength of 2024/U25 Laminates.....	170
Figure 32. Effects of Moisture and Processing on Peel Strength of 2024/U25 Laminates.....	171
Figure 33. Peel Strength of Various Laminates.....	172
Figure 34. SEM Images of 2024/U25 Peel Failures (Correctly Processed).....	173-174
Figure 35 SEM Images of ARALL-4 and Glare Peel Failures (Correctly Processed).....	175
Figure 36. Peel Strength of 8009/U25 Laminates.....	176
Figure 37. Peel Strength of 8009/U25 vs. 2024/U25 Laminates.....	176
Figure 38. SEM Images of 8009/U25 Peel Failures.....	177-178
Figure 39. Tensile Properties of 8009 Aluminum as a Function of 343°C Annealing Time.....	179
Figure 40. Stress-Strain Diagram for 8009/U25 Laminates.....	179
Figure 41. Effects of Surface Treatment on the Fatigue Life of 2024.....	180
Figure 42. S/N curves for 2024 and 8009 Aluminum.....	181
Figure 43. S/N Curves for 8009/U25 Laminates and 8009 Aluminum.....	181
Figure 44. DMA Plot for 2024 Aluminum.....	182
Figure 45. DMA Plot for 8009 Aluminum.....	182

Figure 46. DMA Plot for ARALL-4 Laminate.....	183
Figure 47. DMA Plot for U-25 Composite (Dry Condition).....	184
Figure 48. DMA Plot for U-25 Composite (Wet Condition).....	184
Figure 49. DMA Plot for U-25 Composite (Transverse Direction, Dry)..	185
Figure 50. DMA Plot for 8009/U25 Laminate (Longitudinal Direction, Dry).....	186
Figure 51. DMA Plot for 8009/U25 Laminate (Transverse Direction, Dry).....	186
Figure 52. Typical 3-Point Bend Curves for 8009/U25 Laminates.....	187
Figure 53. Tensile Properties of 8009 Aluminum.....	188
Figure 54. Tensile Properties of 8009/U25 Laminates vs. 8009 Aluminum.....	189
Figure 55. Stress in Crack-Bridging Fibers as a Function of Delaminated Length, Immediately after Failure of the Aluminum Layers.....	190
Figure 56. Residual Stress in 8009/U25 Laminate vs. Temperature.....	190
Figure 57. Load-Displacement Curve for -56°C Tensile Failure of 8009/U25 Laminate.....	191
Figure 58. Stress-Strain Curve for Post-Stretching and Subsequent Tensile Testing of 8009/U25 Laminate.....	191
Figure 59. Tensile Fracture Energies vs. Test Temperature.....	192
Figure 60. Maximum Cyclic Stress in Aluminum Layers: 8009/U25 Laminate vs. 8009 Aluminum.....	193
Figure 61. Mean Cyclic Stress in Aluminum Layers: 8009/U25 Laminate vs. 8009 Aluminum.....	193
Figure 62. Stress Range and R Ratio in Aluminum Layers: 8009/U25 Laminate vs. 8009 Aluminum.....	194
Figure 63. S/N Curves for 8009/U25 Laminate, Corrected for True Stress in the Aluminum Layers.....	194
Figure 64. Example Curves for Residual Stress after Fatigue.....	195
Figure 65. Effects of Post-Stretching on the Maximum Cyclic Stress in the Aluminum Layers.....	195

Figure 66. Effects of Post-Stretching on the Mean Cyclic Stress in the Aluminum Layers.....	196
Figure 67. Effects of Post-Stretching on the Stress Range and R Ratio in the Aluminum Layers.....	196
Figure 68. Effects of Post-Stretching on Fatigue Life: 8009/U25 Laminates.....	197

ABSTRACT

Equations for predicting the theoretical stresses and mechanical properties of fiber/metal laminates were derived. These were applied to a model high temperature laminate system based on 8009 aluminum and glass fiber reinforced U-25 thermoplastic polyimide. The effects of aluminum surface treatment on bond strength were investigated. Chemical surface treatments gave superior bond strength compared to mechanical treatments. Adequate bond strength was obtained using simplified and environmentally safe surface preparation techniques.

The tensile yield and ultimate strength, elastic modulus, fracture behavior, dynamic mechanical behavior, chemical resistance, and fatigue resistance of the laminate were investigated. Most properties were found to correlate well with the theoretical predictions. The laminate showed excellent strength retention at temperatures above 200°C. Fatigue resistance as-processed was found to be comparable to monolithic 8009. Post-stretching the laminate was shown to increase both fatigue life and yield strength substantially.

Dynamic mechanical properties were found to be superior to monolithic 2024 and 8009 aluminum, and marginally better than ARALL-4, as well. The relatively high dynamic loss modulus suggests that the laminate would be useful for applications involving acoustic fatigue. Chemical resistance of the laminate was found to be excellent against most U.S. Navy environments. The potential usefulness of future high temperature laminates was well demonstrated by this study.

1.0. BACKGROUND: Fiber/Metal Laminates

Fiber/metal laminates are a relatively new development which seek to combine the beneficial properties of metals and fiber-reinforced composites. These laminates do not represent a new class of material, but rather a hybrid material system which can be designed for and tailored to a particular application in the same way that a component or structure is designed for its intended application.[1]

The field of hybrid composites is perhaps the broadest of any class of materials, encompassing everything from plywood and reinforced concrete to honeycomb structures. This research focuses only on fiber/metal laminates, which can be defined as a sandwich of reinforcing fibers between thin layers of metal. An adhesive matrix is used to bond the layers together. This construction is shown in Figure 1. Several different fiber/metal laminate systems are currently in production, most notably ARALL^R (Aramid-ALuminum Laminate) and Glare^{R*}. The properties of this and other laminate systems will be described in more detail in a later section. First, however, it is beneficial to examine the history and development of laminates.

1.1. Laminate Development.

Laminates were developed in the early 1980's by a team of researchers at Delft University in the Netherlands, primarily to overcome some of the deficiencies inherent in traditional

*- ARALL, ARALL Laminates, ARALL-4, and Glare are all registered trademarks of Alcoa; hereafter the ^R symbol is omitted for simplicity.

aerospace materials. In particular, aircraft skin materials such as traditional aluminum alloys are very susceptible to fatigue damage.^[2-6] Weight reduction in skins and other fatigue-prone structures is also an important factor.^[5,7,8] Furthermore, organic-matrix composites are limited in such applications by their relatively poor toughness, damage tolerance, and resistance to moisture absorption.^[4-6] The Delft team realized that by combining continuous, low-density, fatigue-resistant fibers and aluminum, these problems could be overcome. This led to the development of ARALL Laminates.

1.2. ARALL and Other Laminate Systems. ARALL, which stands for ARamid-Aluminum Laminate, is a registered trademark of Alcoa, who hold the production rights for this type of fiber/metal laminate.^[9] It consists of alternating layers of aluminum alloy sheet and unidirectional aramid fibers in an epoxy matrix. Four variants of ARALL are available, as shown in Table I. Each variant uses a different type of aluminum alloy, and ARALL-1 and -3 are stretched after curing to yield a more favorable residual stress distribution (since aluminum has a higher thermal expansion coefficient than most fiber materials, the aluminum layers are typically in residual tension cooling, with a residual compressive stress in the fibers). In addition, ARALL-4 uses a higher temperature epoxy, allowing higher use temperatures.

Delft has also developed a second type of laminate, called Glare. This laminate is similar to ARALL, but it uses glass fibers instead of aramid. While aramid fibers offer high strength at low density, they

have several drawbacks. For example, they tend to suffer microbuckling and premature failure when subjected to compressive loads.^[10] In addition, there is a considerable bias against the use of aramid or kevlar in aircraft (and particularly naval aircraft) due to its relatively high moisture absorption.^[11-14] The use of glass fibers alleviates these shortcomings. Glare, like ARALL, is available in four variants. Two of these, as shown in Table II, are unidirectional while the other two are cross-ply, having fibers in both the 0° and 90° directions.

ARALL and Glare are both currently being produced by Alcoa and marketed by Structural Laminates, an international company formed by Alcoa and Akzo Fibers and Polymers for the purpose of marketing fiber/metal laminates. The laminates are available in a variety of different thicknesses; the most common of these is designated 3/2 ply. This denotes three layers of aluminum (each sheet being 0.012 inch thick) and two layers of fibers in epoxy (layer thickness about 0.008 inch). Other configurations include 2/1, 4/3, 5/4, and so on.

1.3. Fabrication and Properties. ARALL and Glare Laminates are fabricated using traditional composite techniques. The aluminum layers are first cleaned, anodized, and primed to promote a strong bonding with the epoxy.^[15-19] Initially, a chromic acid anodizing procedure was used, but due to the toxicity of the compounds involved, this was later changed to phosphoric acid. The aluminum and fiber/epoxy layers are then laid up in the desired configuration, and cured in an autoclave

using the standard cure cycle for the epoxy.

The resulting laminates can be handled and machined just like aluminum sheet, [1,3,16,20-22] with some exceptions. For instance, shearing a laminate results in an uneven edge with damage to the aluminum layers near the edge. [20,23] Bend radius in the unidirectional laminates is very good parallel to the fiber direction, but is limited by fiber extension perpendicular to the fibers. [20,24-26]

The mechanical properties of ARALL and Glare Laminates have been thoroughly characterized by a number of different researchers. Results for ARALL can be found in virtually all of the references listed at the end of this thesis; those for Glare are published in references 8, 27, 28, 29, and 30. The results are too extensive to be included in this work, except to say that strength and modulus are comparable to conventional aluminum (Figure 2), density is lower, and fatigue resistance under certain conditions is several orders of magnitude better (Figure 3). The reasons for the excellent fatigue resistance will be discussed in more detail in a subsequent section.

1.4. Applications for ARALL and Glare.

ARALL was originally intended for use in fatigue-loaded wing and fuselage skins in civil aircraft. [1,2,7,16,17,21,31-34] Its first application (Figure 4) was in Fokker F27 lower wing skin panels, [5,9,16,18,21,31,34-37] and subsequently for fuselage crack stoppers in the Airbus A320. [5,16,21] ARALL is also to be used for lower wing panels and fuselage crack stoppers in the Fokker F50 and

F100^[9,38,39], in the deHavilland Canada DHC-8,^[39,40] and in floor panels for the Boeing 777.^[41] The first major military application for ARALL is in the Douglas C-17. A number of major C-17 components were identified as potential ARALL applications,^[5,26,34,39,42,43] the first being the rear cargo door, which was first flown in May, 1992.^[44] Other military applications being studied include various fatigue-prone components in the A-7, A-10, F-5, F-111, and C-130.^[26,39,45]

Glare laminates are intended for use in fuselage skin panels,^[8,30] where their superior fatigue resistance and damage tolerance will allow the use of unstiffened fuselage structures, thus allowing a substantial decrease in weight.^[44-50]

1.5. Drawbacks of ARALL and GLARE. A major drawback of both ARALL and Glare Laminates is the limited range of use temperatures. While ARALL-4, the high-temperature version of ARALL, has demonstrated excellent mechanical properties down to -54°C, it is limited by both its 2024 aluminum and its AF-191 epoxy adhesive to an upper use temperature of about 150°C.^[51,52] ARALL and Glare, therefore, can only be used in applications where conventional aluminum alloys or composites are used. This restriction becomes very significant in military aircraft applications, where, due to temperature requirements, fatigue- and stiffness-critical structures are often made from titanium. The use of high-temperature laminates in such components could yield substantial weight savings. Other problems with ARALL, namely fiber microbuckling in compression and moisture absorption, have already been mentioned.

2.0. INTRODUCTION

2.1. Fabrication of Laminates.

In order for a laminate to achieve its full range of properties, the layers must be joined together in a precisely controllable manner. While just the right bond strength can yield desirable properties, an improper or varying bond strength can seriously degrade those properties.

2.1.1. Adhesion. Adhesion between two surfaces arises from short-range attractive forces between atoms in each surface [53]. Atomically rough surfaces, such as those shown in Figure 5a, have a relatively small fraction of their surfaces in contact. Adhesion forces in this case are small, and relatively little normal force is required to separate them. If the surfaces are sufficiently rough, mechanical interlocking can become a factor, especially when shear and normal forces are both applied (Figure 5b). Atomically smooth surfaces, on the other hand, have a much larger fraction of contact area (Figure 6). As this fraction approaches unity, the adhesion strength between the two surfaces approaches the tensile strength of the solid.[53]

This situation becomes more complicated when fiber/metal laminates are considered. It now becomes a case of a viscoelastic fluid (the polymer adhesive) in contact with an atomically rough solid (the metal). In this case, the strength of the bond formed depends upon both the degree to which the polymer wets the metal surface (which is related to

the surface energies of the polymer and metal),^[54] and the ability of the polymer to conform to the rough surface, displacing trapped air and contaminants. With a clean, atomically smooth metal surface and under vacuum, the degree of wetting is the only important factor (Figure 7a). However, to obtain an atomically smooth surface would inflate the cost of the laminate to the point of uselessness. Therefore, one must contend with a rough surface, and with the inevitable incomplete contact (Figure 7b).

There are a number of ways by which wetting of the metal by the polymer can be improved. These include the following:

- 1) Clean the surfaces of the metal and polymer as well as possible, and process the laminate in vacuo to minimize surface contamination.
- 2) Use a polymer with a lower viscosity at the desired processing temperature, or increase the processing temperature (or pressure) to lower (or overcome) the polymer's viscosity.
- 3) Use a polymer with a lower surface energy or which wets the metal better.^[53,54]
- 4) Reduce surface roughness as much as possible.
- 5) Use a coating on the metal which bonds well to both the metal and the polymer, such as a primer.
- 6) Pretreat the outer surface of the polymer in which the fibers are imbedded to make it more chemically active.

Of these possibilities, (2) and (3) may not be practical, due to the limited choice of polymer and metal systems suited to the desired

laminate's properties, or to material or equipment limitations. Option (4) is probably also impractical, since it is unlikely that such large surface areas could cost-effectively be polished to the required level of smoothness. Options (1) , (5), and (6) are used currently in the production of ARALL and Glare Laminates, and have been shown to improve bonding.[15-19]

2.1.2. Lamina Surface Preparation. The aluminum sheet usually used in laminates is typically degreased and cleaned, and then deoxidized to remove the existing oxide layer. The surfaces of the polymer prepreg may also be chemically etched to remove the surface layer of impurities and increase the chemical reactivity of the surfaces.

In addition to these steps, the aluminum layers are normally anodized as well. This involves the immersion of the sheet in an acid bath while an electric current is passed through the bath with the aluminum sheet as the anode. Anodizing causes a thick, porous, strongly adhering oxide layer to form on the aluminum.[55] While this would seem to be detrimental to the formation of a strong metal/polymer bond, in that it greatly increases surface roughness, it in fact greatly strengthens the bond. The rough surface provides an excellent source of mechanical interlocking between metal and polymer, thus greatly increasing the macroscopic bond strength.[54]

Similarly, mechanical roughening of the metal surface, such as by grit blasting or sanding, would be expected to increase overall bond strength as compared to an unroughened (but still atomically rough)

surface.^[54] Both anodizing and various mechanical surface treatments have been found to improve bonding between metals and polymers.^[55-58]

Following the anodizing or roughening procedure, a primer or adhesive may be applied to the metal surface to further improve bonding. Since primers are typically low-viscosity liquids, they can be applied easily and can achieve intimate contact with the metal surface. Upon curing, the primer becomes mechanically strong, and provides a surface to which the polymer can bond chemically.

2.1.3. Lay-up and Processing. Following the preparation of the metal and polymer surfaces, the layers are stacked or laid up as with traditional composites. Care must be taken not to contaminate the bonding surfaces during this process, or else the quality of the bond will be degraded. Processing of the laminate can be performed in either a laminating press or an autoclave, depending on the size of the panel to be fabricated and the sensitivity of the material system to processing conditions.

If an autoclave process is used, the laminate lay-ups must be assembled on the autoclave table and "bagged" using various polymer sheets and blanket materials. The bag is sealed with sealant strips to allow a vacuum to be maintained on the laminate lay-ups while external gas pressure is applied. The combination of internal vacuum and external pressure insures that air or gas will not be trapped in the laminate, and that the pressure applied to the lay-ups is uniformly distributed. The autoclave also allows the use of an inert atmosphere

to protect the materials from oxidation if high processing temperatures are required. However, autoclave processing requires large, expensive equipment, and consumes a great deal of time, bagging material, pressurizing gas, and cooling water, and is therefore a complicated and expensive technique.

A laminating press is much less complicated. The laminate lay-up is placed between two heated platens, which are then closed and pressure applied hydraulically. This technique is not only much simpler than autoclaving, but is much less costly and time consuming. In addition, it allows the utilization of much higher pressures than are possible with an autoclave, which are typically limited to 200 or 250 psi. The disadvantages include difficulty in evacuating the laminate lay-up of air and gases, the need to fabricate the laminate panels one or two at a time (unless an unusually large press is available), and the fact that the degree of control available may be insufficient to follow the polymer supplier's recommended pressure/temperature cycle.

2.1.4. Residual Stress. The curing or laminating process takes place at an elevated temperature. At some point during post-cure cooling, the polymer will become stiff or glassy. If a thermosetting polymer is used, such as an epoxy, it will become stiff upon curing. If a thermoplastic is used, it will become glassy below its glass transition temperature, T_g . Once this occurs, the fibers imbedded in the polymer and the metal layers are bonded rigidly together. Therefore, as the laminate continues to cool, the different coefficients of thermal

expansion (CTEs) of the fibers and metal will result in residual stresses in both fibers and metal layers in the fiber direction.[59,60]

Since most fiber materials have a lower CTE than most metals,[61] the residual stresses are usually compressive in the fibers and tensile in the metal layers. The latter is very undesirable, as it serves to lower the effective yield strength and decrease the fatigue resistance of the laminate. These effects will be discussed in greater detail in section 2.2.

Residual stress can be calculated based on the CTEs of the components and the assumption that the fibers and metal layers are rigidly bonded by the polymer matrix, with no matrix shear. The equations for residual stress $\sigma_{res.}$ in the metal and fibers, therefore, are as follows:[62,63]

$$\sigma_{res.m} = \Delta e [E_m E_f V_f / (E_m V_m + E_f V_f)] \quad (1)$$

$$\sigma_{res.f} = -\Delta e [E_f E_m V_m / (E_m V_m + E_f V_f)] \quad (2)$$

where m and f stand for metal and fibers respectively, E is the elastic modulus, and V is the volume fraction of each component in the laminate. The contribution of the polymer matrix can be neglected in such calculations, as its contribution is generally very small compared to that of the other components, except for its ability to accommodate part of the residual stress through shear deformation.[63] The factor Δe is the difference in thermal strain between the fibers and matrix if they were not bonded together:[59,60]

$$\Delta e = \alpha_m \Delta T - \alpha_f \Delta T \quad (3)$$

where α is the CTE of the metal or fibers and ΔT is the difference

between the cure temperature (for a thermoset) or T_g (for a thermoplastic) and the testing temperature.

Note that the denominator in equations (1) and (2), $E_m V_m + E_f V_f$, is equal to the nominal modulus of the laminate, hereafter denoted by E_L (see Equation (14), Section 2.2.2). Also notice that the ratio

$$\sigma_{\text{res.m}} / \sigma_{\text{res.f}} = E_m E_f V_f / -E_m E_f V_m = -V_f / V_m, \quad (4)$$

which is independent of the moduli of the metal and fibers due to the mutual constraining effect of the rigid bond between them. Note that these and all subsequent equations refer to properties in the longitudinal (fiber) direction only; the transverse properties are dominated by the metal layers, and are only affected by the longitudinal fibers through poisson effects.

2.1.5. Post-Processing Treatments. As noted above, it is undesirable to have a residual tensile stress in the metal layers. One post-processing treatment which has been used with ARALL and Glare laminates to overcome this problem is post-stretching.^[64] This involves introducing a small (0.4 or 0.5 %) permanent plastic strain into the laminate panel, which reverses the residual stress state in the laminate because the metal deforms plastically while the fibers only deform in an elastic manner. Thus the metal layers now contain a residual compressive stress, which can greatly improve yield strength and fatigue resistance. The latter has been demonstrated through comparisons of the fatigue behavior of stretched and unstretched versions of ARALL and Glare.^[24]

Other post-processing treatments can be used on laminates as well, such as various forming processes and post-curing. Formability of laminates, as mentioned previously, is typically good in the transverse direction, but is very limited in the fiber direction in part by the inability of epoxy matrices to shear to allow relative motion between the fibers and the metal layers. Post-curing involves reheating the laminate to allow further chemical or physical changes to occur in the polymer.

2.2. Properties of Laminates.

Most laminate systems currently available or envisioned utilize unidirectional fibers for reinforcement. As a result, the properties of these laminates are directional. The degree of anisotropy is much less than in unidirectional composites, however, due to the contribution of the aluminum layers to the transverse properties. Most of the properties described in the following sections refer to those in the longitudinal direction since, as mentioned before, the transverse properties are dominated by the metal layers.

2.2.1. Strength. Laminates contain a ductile component, the metal, and a brittle (i.e. non-yielding) component, the fibers. If the fibers have a sufficiently high failure strain, the laminate will undergo yielding when the yield point of the metal is reached, followed by a second stage of elastic deformation as the fibers continue to elongate. This behavior can be seen in Figure 8, which shows a typical stress-strain

plot for ARALL-4. In most laminates, failure is expected to occur upon fiber failure, as opposed to failure of the metal layers, since the elongation-to-failure of the metal is usually the greater.

The strength of laminates, like that of traditional composites, can be predicted by a rule of mixtures (ROM) approach.^[62,63] In its simplest form, the ROM equation for yield strength, σ_{yL} , is:

$$\sigma_{yL} = (\sigma_{ym} - \sigma_{res.m}) V_m + \sigma^*_f V_f \quad (5)$$

where σ_{ym} is the yield strength of the metal, $\sigma_{res.m}$ is the residual stress in the metal layers after processing, V_m is the volume fraction of metal in the laminate, σ^*_f is the stress contribution of the fibers at the laminate's yield point, and V_f is the volume fraction of fibers. Since

$$\sigma^*_f = (\sigma_f - \sigma_{res.f}), \quad (6)$$

where σ_f is the true fiber stress at the laminate yield point, and since the fibers and the metal layers are assumed to be bonded rigidly together, it can easily be shown that

$$\sigma^*_f = (\sigma_{ym} - \sigma_{res.m}) (E_f/E_m) \quad (7)$$

where E_f and E_m are the elastic moduli of fibers and metal, respectively. Notice that, as stated previously, the residual tensile stress in the metal layers reduces the yield strength of the laminate. The residual stress in the fibers affects the yield strength of the laminate only indirectly, in that it is associated with the residual tension in the metal. The ultimate tensile strength σ_{uL} can be predicted in a similar manner:^[62,63]

$$\sigma_{uL} = (\sigma_{ym} - \sigma_{res.m}) V_m + (\sigma_{uf} - \sigma_{res.f}) V_f \quad (8)$$

The yield strength of the metal is still used in this equation because the metal is assumed to exhibit ideal elastic-plastic behavior.

Note that the residual compressive stress in the fibers (remembering that in these equations tension is positive and compression negative) counteracts the residual tension in the metal. In fact, if Equation (4) is substituted into Equation (8), the residual stress terms cancel out, leaving:

$$\sigma_{uL} = \sigma_{ym}V_m + \sigma_{uf}V_f \quad (9)$$

It is advantageous that the residual stress terms in Equation (8) cancel out, because once yielding occurs in the metal layers, the original residual stress calculations are no longer valid. The initial residual compression in the fibers does, however, increase the failure strain of the laminate if laminate failure is controlled by the failure of the fibers. Conversely, if laminate failure is controlled by fracturing of the metal layers, the residual tension in the metal will slightly decrease the failure strain.

It can also be seen that post-stretching a laminate will increase its yield strength and fatigue resistance, but will not affect its tensile strength, and will decrease its elongation at failure.

Finally, it can be seen from the above that from a known nominal stress σ_L , the stress in either the metal layers or the fibers can be calculated using the general equation

$$\sigma_L = (\sigma_m - \sigma_{res.m}) V_m + (\sigma_f - \sigma_{res.f}) V_f \quad (10)$$

By assuming strain is equal in all layers as in Equation (7) it can be shown that

$$(\sigma_m - \sigma_{res.m})/E_m = (\sigma_f - \sigma_{res.f})/E_f \quad (11)$$

Thus the stress in the metal layers is

$$\sigma_m = \sigma_{res.m} + \sigma_L / [V_m + (E_f/E_m)V_f] \quad (12)$$

and that in the fibers is

$$\sigma_f = \sigma_{res.f} + \sigma_L / [V_f + (E_m/E_f)V_m] \quad (13)$$

2.2.2. Modulus. Like strength, the elastic modulus of a laminate, E_L , can be predicted by the ROM technique. The modulus in the first segment in Figure 8, where both the metal and the fibers are deforming elastically, is

$$E_L = E_m V_m + E_f V_f. \quad (14)$$

If a laminate is required to have a modulus equal to or greater than that of the metal component, then the ratio of the moduli of the components must be

$$E_f/E_m \geq (1-V_m)/V_f \quad (15)$$

Thus if the metal volume fraction is 60% and the fiber loading in the polymer/fiber layer is 50%, then the fiber's modulus must be $(1-0.60)/0.15$ or at least 2.67 times that of the metal, otherwise the modulus of the laminate will be less than that of the metal used in the laminate.

In the second segment in Figure 8, where the metal is deforming plastically and the fibers are deforming elastically, the modulus is given by the equation

$$E_L' = E_f V_f. \quad (16)$$

Again, this assumes that the load carried by the aluminum layers during plastic deformation is constant.

2.2.3. Density. The density of laminates is also determined by ROM. When predicting strength or modulus, the contribution of the polymer matrix is generally neglected because its contribution is negligible compared to those of the fibers and the metal layers. This is not the case for the density, of course, where the contribution of the polymer is quite significant. Thus the macroscopic density ρ_L of a laminate is:

$$\rho_L = \rho_m V_m + \rho_f V_f + \rho_p V_p \quad (17)$$

Since in most potential laminate systems, the fibers and especially the polymer matrix are significantly less dense than the metal layers, the density of the laminate, i.e. the weight of a sheet of fixed thickness, is less than for the monolithic metal. This is a major advantage of laminates, especially when it is considered that the strength in the fiber direction is generally comparable to that of the metal, and fatigue resistance can be greatly enhanced. The concept of specific properties, the numerical value of a property divided by the density of the material, is very important in evaluating the properties of laminates, since weight is a universal concern in every aircraft design.

2.2.4. Fatigue. The property for which laminates are best known is their fatigue resistance. As was mentioned previously, the ARALL family of laminates was developed specifically for this property. In monolithic metals, fatigue occurs in three stages: initiation of a

fatigue crack, stable crack propagation, and failure (unstable crack propagation).^[65,66] The duration of the initiation stage is very difficult to predict at any stress level, as there is a large amount of statistical scatter. In general, however, it can be said that the initiation life decreases with both increasing stress and increasing surface or edge roughness.^[66] Thus at low stress, initiation of a crack takes longer, and the fatigue life of the specimen is dominated by this stage.

At a low enough stress, initiation may not occur at all within a reasonable number of cycles, say 10^7 cycles. It can then be said that the material does not suffer fatigue damage at that stress level, i.e. it has unlimited fatigue life at that stress. By reducing the specimen's surface roughness by polishing, this stress, the fatigue limit, can be increased substantially. Surface roughness represents countless tiny stress concentrations, as well as potential pre-initiated cracks, so it is no surprise that it has a strong influence on fatigue.

In metals, once a crack of viable size (i.e. beyond the "short crack" regime) has formed, failure of the specimen is inevitable if the load or stress level remains fixed. For a flat specimen, the stress concentration ΔK at the tip of an edge crack of length a is usually of the form:^[66]

$$\Delta K = Y\Delta\sigma/\pi a \quad (18)$$

where Y is a geometrical factor. For metals, the rate of crack growth, da/dN , always increases with increasing ΔK (as shown in Figure 9). Therefore, as the crack grows, ΔK increases, and so the crack grows at

an increasing rate until failure occurs.

Metal/fiber laminates can be designed to resist both the initiation and the propagation of fatigue cracks. Resistance to crack initiation can be built into the laminate in two ways. The first is to use a high modulus fiber and a high volume fraction of fibers. From Equations (10) through (13), it can be seen that as either E_f or V_f increases, more of the load on the laminate is supported by the fibers and less by the metal layers. With sufficiently high values of E_f and V_f , the stress in the metal layers becomes less than the nominal stress on the laminate, thus increasing the apparent resistance of the laminate to crack initiation as compared to the monolithic metal.

The second means of increasing the laminate's resistance to initiation, also apparent from Equations (10) through (13), is to post-stretch the laminate to leave the metal layers in residual compression. Again, this results in a lower true stress in the metal for a given laminate stress than without post-stretching.

Designing a laminate to resist the growth of fatigue cracks which have already initiated is a more complicated task. When a crack develops in one of the metal layers, that layer experiences a decrease in stiffness. As a result, some of the load initially supported by that layer is transferred to the adjacent fibers, which retain their original stiffness (Figure 10). Thus the maximum stress in the metal is reduced. If the crack continues to grow, more of the metal layer's load is taken up by the fibers, further reducing the stress in the metal. This process is known as load shedding, and the fibers are said to bridge the

advancing crack . This concept is used to advantage in a wide variety of composite systems, including conventional composites and toughened ceramics.[66]

If the laminate can be designed so that the rate of reduction of the stress in the metal due to load shedding is greater than the rate of increase in \sqrt{a} , then the maximum stress concentration factor K_{\max} (and also ΔK) will decrease as the crack grows. As a result of the decrease in ΔK , the crack growth rate da/dN will decrease with increasing crack length. Thus the crack will grow at an ever-decreasing rate, and will eventually cease growing at all.[19,31,42] This is called crack arrest, and for obvious reasons it is a highly desirable condition in any load-bearing material or structure. This behavior can be seen in Figure 11, which shows a plot of da/dN for ARALL versus the stress intensity range ΔK applied to the laminate (which of course differs from the ΔK experienced by the metal layers).

The effectiveness of the load shedding/crack bridging mechanism depends strongly on the strength of the fiber/metal bond formed by the polymer matrix . In general, a strong bond is desirable. Delamination is known to occur in composites and laminates during fatigue crack growth.[67-73] In the case of laminates, prior to crack initiation the instantaneous stresses in the different layers are given by Equations (12) and (13). There is a Mode II shear stress in the polymer layer between the fibers and metal due to the different stresses in the latter two. When a crack forms in the metal, the magnitude of this shear stress increases as load is shed from the metal to the adjacent

fibers.[68,69] The increased cyclic shear stress causes delamination to occur in the polymer layer. The amount of delamination which occurs, and thus the fatigue resistance of the laminate, depends on the bond strengths at both the fiber/polymer and the metal/polymer interfaces.[71,73]

A strong bond results in only a small amount of delamination, as shown in Figure 12a. With such a small length of debonded fiber, a higher fiber stress will result in only a very small amount of stretch in the debonded section of the fiber. This corresponds to a very small amount of crack opening in the adjacent metal layer. Thus the load shedding process is very efficient, the growth rate of the crack drops off quickly, and crack arrest is achieved at a relatively small crack length.

A weak fiber/metal bond, on the other hand, results in a larger area of delamination (Figure 12b). The greater length of debonded fiber can stretch much more for a given stress increase than in the previous case, and this greater stretch translates to more crack opening in the adjacent metal layer. Thus the metal load is shed inefficiently onto the fibers, and crack growth rates may either increase with crack length or decrease too slowly to arrest the crack before the metal layers fail. The fiber layers would still be intact and able to carry axial loads, so even this situation is better than in a monolithic metal, but clearly for good fatigue resistance a strong bond is desirable.

The bond should not be too strong, though, otherwise no delamination will occur during crack formation. If this is the case,

the fibers adjacent to the crack will experience an unblunted stress concentration from the crack tip, and fiber failure due to overloading may occur as the crack advances through the metal (Figure 13). Although this situation represents very efficient load shedding, the fibers are unable to bridge the advancing crack, and little benefit is gained. Therefore a small- but not excessive- amount of delamination is desirable.

Additional resistance to crack growth arises from the fact that the laminate is a layered structure, which prevents cracks which initiate in one layer from growing through the whole laminate (Figure 14).^[66] Because of this crack divider arrangement, cracks must initiate independently in each layer- and in the case of the fiber layers, in each fiber. This further slows the growth of cracks.

In summary, in order to exploit the potential fatigue resistant properties of laminates, one should: (1) Use a high volume fraction of a high-modulus fiber; (2) Post-stretch the laminate to obtain a residual compressive stress in the metal layers; and (3) insure that the polymer/metal bond is strong, but not too strong.

2.2.5. Toughness. The toughness of a material is usually determined by calculating the energy absorbed by a Charpy or Izod specimen during an impact of fixed initial energy. This is impractical with a laminate due to their typically small thickness; however, the energy required to fracture a tensile specimen can give a good indication of the material's toughness. This energy can be estimated by determining the area under

the tensile stress-strain curve. It can be readily seen that if a material is able to deform to a large degree, the energy required for fracture- and thus the toughness of the material- will be high. For laminates with a stress-strain curve like that in Figure 8, it can be shown that the energy absorbed during deformation up to the point of failure, G_d , is

$$G_d = \sigma_Y^2/2E_L + (\sigma_Y^2 - \sigma_U^2)/2E_L' \quad (19)$$

where σ_Y and σ_U are the yield and ultimate strengths of the laminate. The derivative of this with respect to σ_Y is

$$d(G_d)/d(\sigma_Y) = \sigma_Y/E_L - \sigma_Y/E_L', \quad (20)$$

and since $E_L > E_L'$, it can be seen that increasing the yield strength of the laminate by post-stretching decreases the energy required to deform the laminate to failure. This is as expected, since the post-stretch represents an irreversible addition of strain energy toward eventual failure.

At the point of failure, the elastic energy stored in the metal and fibers is released. Neglecting the effects of necking in the metal, this elastic energy G_e is given by

$$G_e = V_f \sigma_{uf}^2/2E_f + V_m \sigma_{um}^2/2E_m \quad (21)$$

where σ_{uf} and σ_{um} are the ultimate strength of the fibers and the metal. This value is constant regardless of residual stress state, and most laminates tend to delaminate extensively upon tensile failure as a result of the elastic energy released anyway.^[28]

2.2.6. Impact Tolerance. A material's ability to withstand impact

loading is determined by the material's toughness and its ability to resist fast crack propagation. The importance of the latter is demonstrated by many materials which possess good toughness and ductile behavior at low strain rates (e.g. during tensile testing), but poor toughness and brittle fracture during high strain rate impact tests. Metals deform at low strain rates by dislocation motion. However, at higher strain rates, the time available for dislocations to move and reduce the stress intensity at the crack tip becomes less. At sufficiently high strain rates, therefore, the material will display brittle behavior, and impact resistance will be very low.

Impact resistance in composite materials is enhanced by the presence of interfaces. In metal-matrix composites, there are particle/matrix or fiber/matrix interfaces. In organic composites and fiber/metal laminates, there are both fiber/matrix interfaces and interlaminar interfaces. As in fatigue crack propagation, when an advancing crack due to an impact encounters an interface which is weak relative to the component materials, delamination occurs at the interface. The creation of internal surface area absorbs some of the crack's energy, as well as blunting the crack tip. Thus an impact which might propagate to failure in a monolithic metal can be absorbed by a laminate, and still leave the fibers intact to bridge any through-component of the crack.

The impact resistance of ARALL laminates has been studied, and has been found to be very good.[3,5,16-18,24,27,32,36,74-76] Residual strength after impact has also been shown to be superior to monolithic

metals. Delamination in the aramid/epoxy layers distributes the impact over a larger area in each successive aluminum layer. Thicker versions of ARALL, containing many layers of aluminum and aramid/epoxy, are being developed for use as ballistic armor.[5]

A major issue which must be considered along with impact tolerance is the inspectability and repairability of impact damage. In metals, impact damage may take the form of cracks, dents, or holes. These are easily identified in most cases, and the damage generally does not go far beyond the visible limits of the feature. In composites, on the other hand, an impact may cause some initial deformation of the surface, but the surface often returns to its normal appearance after the impact. Thus the panel or component may look undamaged, yet may contain serious damage in the form of delamination, matrix cracking, and fiber breakage. The extent, and often the very existence, of such damage can only be ascertained by using ultrasonic or X-ray scanning techniques, which necessitates the removal of the part from the aircraft.

It is highly desirable from cost, time, safety, and supportability standpoints to be able to assess impact damage visually in the field. Furthermore, it should be possible to cut out the damaged area and repair it with some sort of patch so that the aircraft can resume its mission as quickly as possible. While this is a simple procedure with metals, field repair of composites remains difficult despite the enormous cost and effort applied toward this goal. Inspectability and repairability of impact-damaged composites remains one of the strongest arguments against their use in aircraft structures, despite their great

potential for weight reduction.

Laminates are frequently condemned along with traditional composites when the question of impact damage arises. However, there is little question that laminates are vastly superior to composites in both the inspectability and repairability of impact damage. Any impact which might cause internal damage in a laminate is also certain to leave a dent, hole, or crack in the surface metal layer which is as easy to locate visually as it would be in a monolithic metal. There would be some delamination beneath the surface which would extend beyond the visible damage, but this damage has been shown to be of relatively small size and regular shape.^[75]

Furthermore, a laminate part can be patched in the same way as a metal part, and in fact riveted repairs in ARALL have been found to be stronger than those in conventional aluminum.^[50] If the delaminated section is not completely removed in the repair, there is a small loss in stiffness, but strength is essentially unaffected due to the contribution of the metal layers to the integrity of the part.

2.2.7. Dynamic Properties. Traditional non-polymeric materials are characterized primarily by linear elastic or elastic-plastic behavior. Ideally, linear elastic properties imply a number of different types of behavior, including the following:^[77] (1) Strain is proportional to stress, the ratio σ/ϵ being equal to the elastic modulus E ; (2) the stress-strain relationship is independent of time; and (3) the stress response to an applied cyclic strain is perfectly in phase with the

cyclic strain. This last property, shown schematically in Figure 15a, means that any sort of pressure waves, such as sound waves or mechanically produced vibrations, are transmitted through the material with essentially no loss of energy. This can be a source of numerous problems in aircraft, where engine noise and vibration can cause fatigue cracking in any of a number of structural components. In addition, engine noise is a major source of crew and passenger fatigue and environmental damage in both civil and military aircraft.

Non-crystalline polymeric materials, on the other hand, are characterized by viscoelastic behavior. This means that they display a combination of elastic and viscous characteristics. This includes the following properties:^[77] (1) strain and stress are not directly related, but rather are approximately related by the so-called "three-parameter solid" relationship:^[77]

$$\sigma/\mu + (d\sigma/dt)/E = E\epsilon/\mu + (d\epsilon/dt)(1+E_2/E); \quad (22)$$

(2) the stress-strain relationship is highly time-dependent (as is apparent from the above equation); and (3) The stress response to a cyclic strain (or vice-versa) is out of phase with the strain.

This last item is shown schematically in Figure 15b. The amount of the phase shift, δ , depends on a number of factors, including the material, degree of crosslinking or crystallinity, temperature, and the frequency of the cyclic stress or strain. The phase-shifted stress-strain relationship response is described mathematically by a complex modulus, where the real (in-phase or elastic) component is called the storage modulus, and the imaginary (out of phase, viscous) component is

called the loss modulus. The ratio of the loss to the storage modulus is equal to $\tan \delta$.

A purely viscous response results in complete absorption of strain energy, while as mentioned previously, a purely elastic response results in zero energy absorption. $\tan \delta$ represents the amount of viscous character which the material possesses. The value of $\tan \delta$ under any particular conditions is therefore directly related to the material's ability to absorb vibrational or elastic strain energy. For this reason, non-crystalline polymers have better sound- and vibration-attenuating properties than metals or other crystalline materials. Unfortunately, they suffer from low strength, modulus, and chemical and erosion resistance compared with other materials.

By incorporating a polymer into a fiber/metal laminate, a degree of viscous behavior is introduced into the laminate as well. This is the source of ARALL's favorable damping qualities.[3,17,18,22,24,32,74,76,78] In addition, any high temperature laminates which utilize a non-crystalline polymer matrix would be expected to have better damping characteristics than monolithic metals. The degree of damping which is possible, and the range of service conditions for which it exists, will determine the sort of applications for which the laminate might be useful.

2.2.8. Thermal Resistance. The thermal properties of a material include several factors which are critical in aircraft design. One of these is burn-through resistance, which is the resistance of the

material to penetration by an impinging flame of known characteristics. This property is one of the critical considerations in the design of aircraft firewalls and other engine-bay components. The firewall is required to withstand a flame of a certain temperature for a certain length of time, to insure that if an engine should explode or catch fire, the other engine or surrounding structures will not be damaged by excessive heat before the fire can be extinguished or before an emergency landing can be made. The better the material's resistance to burn through is, the thinner and lighter it can be for the same task. At some level of thinness, stress would become the critical property rather than burn-through resistance.

Laminates such as ARALL have been shown to possess excellent burn-through resistance.^[9,74] When exposed to a high temperature flame, the outer layer of aluminum melts away relatively quickly, but the underlying polymer and fibers absorb a great deal of thermal energy by charring. In fact, in 3/2 ply ARALL so much energy is absorbed in this process that the damage is confined to the top layer of aluminum and the first aramid/epoxy layer even after monolithic aluminum of the same thickness as the ARALL has suffered complete burn-through.

Another important thermal property is lightning-strike resistance. The thickness of the lower wing skins on most aircraft is dictated by the magnitude of the tensile fatigue stresses to which they are subjected. However, in many aircraft the thickness of the upper wing skins is dictated not by stress, but by lightning strike resistance. Since the wings usually serve as fuel tanks, the skin must be thick

enough that a lightning strike will not penetrate it and ignite the fuel inside. As a result, the upper wing skins are often substantially thicker than they need to be based on the stresses on them. Clearly, weight savings could be achieved by using a material with improved lightning strike resistance.

The lightning strike resistance of ARALL has been found to be excellent compared to that of monolithic aluminum.[9,16,18,24,32,74,76] As with burn-through, damage is confined to the outer layers of the laminate by both charring of the fibers and epoxy, and due to the thermal and electrical insulation provided by the aramid/epoxy layers.

A third important thermal property is thermal management, or more specifically, the ability of a material to transport heat in the desired manner. In combat aircraft, for instance, it is undesirable for the outside of the aircraft to get hot through conduction of engine heat; to do so would make the aircraft an easier target for heat-seeking missiles. Conversely, there are numerous internal parts in aircraft which must be protected from outside heat or cold, such as avionics, landing gear, or passengers. In either case, a material with low thermal conductivity across its thickness would be beneficial. The polymer layers in laminates provide such a thermal barrier. Furthermore, by using a thermally conductive fiber in the side which is exposed to heating, heat from a concentrated source could be distributed efficiently over a large area.

2.2.9. **Environmental Resistance.** In most material applications, the material's resistance to attack from or degradation due to the environment in which it works is a major concern. Depending on the application and the material, environmental attack can take many different forms. Certain materials are susceptible to certain forms of attack, but not to others, as is demonstrated by the partial list in Table III.

The environmental factors which will affect composite materials, including laminates, depends on (1) the environment, (2) the materials used in the composite, and (3) how the component materials are arranged in the composite. By careful selection of both materials and configuration, a composite which is most suited to its intended environment can be designed.

Laminates were designed primarily with mechanical properties in mind, particularly fatigue resistance and strength. However, when compared to organic composites, their configuration is also beneficial in terms of environmental resistance. Aside from their contribution to the mechanical properties previously described, the outer layers of metal serve to protect the underlying fibers and polymer from most of the environmental effects which would otherwise occur. They act as a barrier to moisture, solvents, oxygen, and ultraviolet radiation; they also protect the softer components from erosion by airborne particles and hot gases.

For the most part, therefore, the environmental resistance of laminates is similar to that of the metal used in the laminate. The

major difference occurs at the edges of the laminates, where the polymer/fiber layers are exposed. The edges are the only means by which moisture and solvents can enter the laminate, aside from cracks or holes in the metal layers themselves. Moisture or solvents can diffuse inward through the edges, where their main effect is to corrode or weaken fiber/polymer and polymer/metal interfaces.[11-15,67,70,79] This can have a detrimental effect on the stiffness, fatigue resistance, and other properties of the laminate. The rate of moisture or solvent absorption is very small compared to that in conventional composites, however, because the area available for entry is very much smaller in laminates.

Environmental attack at the edges can be reduced by sealing them with some sort of material which acts as a moisture and chemical barrier, such as silicone-based sealants. This technique has been shown to reduce the weakening of aluminum/epoxy interfaces in ARALL-4.[80]

2.3. High Temperature Laminates.

The currently available fiber/metal laminate systems, ARALL and Glare, are limited to use temperatures of 250-300°F. Temperature limits in laminates are based on two factors: the temperature capabilities of its components and residual stresses. In ARALL and Glare, the limit is based on the upper use temperatures for the aluminum, the epoxy, and the primer used to promote bonding between them. If high temperature materials were used to produce a high temperature laminate, it is possible that the residual stresses due to the high processing

temperature might be too high for the metal/polymer bond strength, and delamination could occur.

Even if the bond strength were sufficiently high compared to the residual stresses, temperature cycling could lead to fatigue and subsequent delamination or fatigue cracking, even if no load were applied. Clearly, the development of laminates for high temperature applications involves some potential problems which are not encountered in ARALL or Glare.

2.3.1. **The Need for High Temperature Laminates.** To date, ARALL and Glare have found applications, actual and potential, in a number of different types of aircraft. Most of these applications have been in components where acoustic or mechanical fatigue are major concerns. The development of high temperature laminates would allow such benefits to be extended to components exposed to elevated temperatures. The fatigue, acoustic damping, and burn-through properties of such laminates could result in substantial weight reductions compared to titanium in firewalls and engine shrouds. They could also replace titanium or steel in exhaust-heated structures, missile casings, and a wide range of fuselage skins and panels in future supersonic or hypersonic vehicles. The use of high temperature laminates for entire fuselage sections in future high-speed transports could reduce structural weight by thousands of pounds, while increasing fatigue resistance and damage tolerance, and reducing interior noise levels and temperature fluctuations.

Current U.S. Navy interest in high temperature laminates is

focused on firewalls and other engine-heated structures, aerodynamically heated skins, and reduction of noise and thermal signatures in future naval aircraft. Navy research into high temperature laminates is aimed at achieving physical and mechanical properties which will allow their use in the applications above, while minimizing the cost, complexity, and environmental impact of fabricating them. In performing this research, it is necessary to address a number of important issues.

2.3.2. **Issues for High Temperature Laminates.** The important issues associated with the development of high temperature laminates for use in future U.S. Navy aircraft include the following:

(1) **Chemical Stability.** The polymer(s) used in making the laminate should be stable at room temperature, so that they can be handled at room temperature during surface treatment and laminate lay-up. It is also highly preferable if the fiber/polymer prepreg can be stored at room temperature for long periods of time. Most currently available composite resins are chemically active polymer precursors, and become useless within several hours or days if not stored in a freezer. Even in the freezer, many resins have shelf lives of only three to six months. This is clearly a major complicating factor, which adds considerably to the cost and difficulty of working with such materials.

(2) **Processing.** One polymer property which is highly desirable from a processing standpoint is a low volatile content. Many polymer resins contain a large percentage of volatile compounds, such as solvents to hold the polymer precursors, which evaporate during the cure

cycle. In addition, many resins release water vapor or other volatiles as part of the chemical reactions which occur during curing. All of these volatiles must be removed from the composite before the cure cycle is complete, otherwise they will accumulate within the polymer to form voids, which have a detrimental effect on many of the material's properties. This problem is especially severe in laminates, in which the polymer is sandwiched between two sheets of metal. Thus most of the surface area available for the outward diffusion of volatiles is lost. Gases must be squeezed out through the edges of the laminate panel, otherwise large voids and unbonded areas will result. It would therefore be of great benefit to use a polymer which produces very little or no volatiles during processing.

It is also desirable for the laminate to have a processing temperature which is not too much above the maximum use temperature of the laminate. A laminate which must be cured at over 300°C but contains a polymer with a glass transition temperature of 150°C would be of questionable value, because special and expensive high-temperature materials and equipment would be required to withstand the processing conditions, yet the laminate's operating conditions would be well within the capability of traditional low-temperature materials.

Laminate processing can also be simplified by developing simple surface treatments. The number of steps involved, the number of different chemicals, and the complexity of the equipment needed should all be minimized. Ideally, the polymer should be bonded directly to the metal, without primers or adhesives, with a surface treatment consisting

of a cleaning step and no more than one additional treatment. This would save time and money, and would not only eliminate the use of unstable chemicals, but also the need for strict time constraints between processing steps.

(3) **Environmental Impact.** The question of how technology affects the environment is quickly becoming an issue of the greatest importance. As environmental concerns grow stronger and more visible outside of the defense industry, there will be increasing pressure for science, research and development, and military establishments to deal with these concerns and eliminate environmentally unsound practices. Thus it seems wise to make the development of environmentally sound materials and processes a major goal of any Materials project.

Many of the currently available high-temperature polymer resins contain highly toxic compounds such as MDA (methylene dianiline), which is a known carcinogen/mutagen. Large amounts of these compounds are present in most of the high temperature composites currently in use, including AFR-700 and PMR-15. Considerable effort is being expended on the development of high temperature resins which do not contain such hazardous chemicals.

Processing high temperature composites can produce a considerable amount of ash and soot, from both the polymer and the bagging materials. Since they cannot be reused, the bagging materials themselves represent a tremendous amount of waste material, including a great deal of plastic. Polyimide films and tape are usually used for bagging high temperature composites. Reducing the amount of waste produced by

composites or laminate processing will probably require the development of reusable bagging materials and non-consumable sealing tapes.

In laminate processing, the chemicals used in surface preparation are also an environmental concern. As was mentioned previously, chromic acid anodizing has in general been discarded in favor of phosphoric acid anodizing. While this is a positive step, it is only a partial solution to the toxicity problem. The elimination of primers and adhesives, which also usually contain highly toxic chemicals, would also greatly reduce the environmental impact of laminate technology.

(4) **Cost.** With the end of the cold war and the inevitable severe reductions in defense spending, it would be foolish to continue developing more and more exotic and expensive materials for structural applications; for no one will be able to afford to use them. The current prices of both high temperature aluminum alloy sheet and high temperature composite prepregs are hovering between \$500 and \$1000 per pound, an astronomical figure when one is considering a component or structure weighing hundreds or thousands of pounds.

Unless these costs are drastically reduced in the future, developing a high temperature laminate with a reasonable price tag requires either the intelligent use of existing materials such as titanium, or the development of low-cost alternative materials. A low-cost, high temperature resin has been successfully developed by at least one research organization. [80-85]

(5) **Machinability/Formability.** As was mentioned previously, the machinability of ARALL and Glare Laminates is excellent, and except for

shearing and bending, they can be handled just like metals. It is obviously desirable to retain these good workshop properties in high temperature laminates as well. If special equipment or techniques are necessary for machining, the cost of part fabrication will increase, and field repairs will become more complicated and time consuming. Good formability can be achieved in high temperature laminates by using a polymer which softens at elevated temperatures, thus allowing the necessary shear between the fibers and the metal layers.

(6) **Repairability.** The good inspectability of damage and easy repairability demonstrated by ARALL and Glare should also be retained in any high temperature laminate which is developed. It is unlikely that a high temperature laminate can be field repaired by adhesive bonding methods, since it will be exposed to high temperatures, thermal stresses, and probably high levels of acoustic and mechanical vibrations as well. Therefore, its bearing and fatigue properties should be good to allow for riveted repairs. Bond strength should be uniform throughout the laminate panels, so that the extent of delamination due to impact damage is minimal and predictable.

(7) **Environmental Resistance.** The U.S. Navy has the dubious distinction of maintaining the most hostile environment ever created around an aircraft: the carrier deck. Aircraft on board carriers are constantly inundated by salt spray, which is highly corrosive to metal surfaces. The moisture which carries this salt also attacks metals, as well as being absorbed by polymers and weakening bonded interfaces. The older carriers also spew corrosive stack gases most of the time. These

gases include sulfur dioxide, which combines with moisture in the air to form sulfuric acid, which is deposited as a sort of acid rain on the aircraft on deck.

There are numerous chemical hazards associated with the aircraft, as well. For instance, powerful solvents including aromatic hydrocarbons and chloro-fluorocarbons (CFCs) are used extensively for cleaning, degreasing, and stripping aircraft surfaces and components. Aviation fuel, oil, or hydraulic fluids may leak from replenishment ports or damaged areas. Finally, the corrosive effects of all of these environmental hazards are exacerbated by the fact that carriers frequently operate in tropical waters, where temperatures and humidity are high.

Any material which is to be used in naval aircraft must be either resistant to or capable of being protected from all of these environmental influences. Laminates, with their outer layers of metal, can be primed and painted just like conventional skin materials. Furthermore, since the metal layers protect the underlying fibers and polymer, the only major additional concern is the machined edges of the laminate panels and any holes or openings in the panel. These will have to be protected against environmental attack by some sort of sealant. Silicone-based sealants are the most likely candidate, since they are chemically inert and retain their elastomeric qualities under a wide range of operating conditions, and are readily available and easy to use.

(8) **Mechanical Properties.** The required properties of the laminate are determined by the design properties of the component for which the laminate is intended. Laminate properties are a function of (1) the properties of the materials used in the laminate, (2) the configuration of the laminate, i.e. the manner in which the component materials are arranged, (3) the strength of the fiber/polymer and metal/polymer interfaces, and (4) the type of post-curing process used. All of these must be carefully considered if the desired properties are to be achieved.

2.3.3. Materials for High Temperature Laminates. Different aircraft components can have very different property requirements. For instance, lower wing skins usually require high strength and fatigue resistance; Engine shrouds, on the other hand, may not need much strength, but do need good acoustic damping, impact, and burn-through properties. Similarly, laminates with very different properties may be required for different applications. The proper selection of materials is an important part of designing a laminate. The first question to be answered is: What is the range of service temperatures to which the laminate will be subjected?

For ambient or cryogenic temperatures, materials must be selected which will not become brittle at low temperatures. Attention must also be given to the residual stresses due to processing; these increase linearly with decreasing temperature (see Section 2.1.4), and at stratospheric temperatures (-40°C) they may be great enough to fracture

the metal/polymer bond, especially if the polymer is brittle at that temperature. For high temperature laminates, there are a number of candidate materials currently or soon to be available. These are summarized in the following paragraphs, for laminates with service temperatures between 200° and 350°C.

(1) **Metals.** Conventional aluminum alloys can not be used for temperatures above about 150°C. There are, however, several high temperature aluminum (HTA) alloys under development.^[86] These can be used at temperatures up to a maximum of about 350°C. Conventional titanium alloys are easily obtainable, and relatively cheap compared to current HTAs. These can be used up to perhaps 400°C. Steels are also potential laminate materials, but are of course very heavy. Some of the alloys which are candidates for high temperature laminates are summarized in Table IV. It can be seen from the table that the alloy properties are always a tradeoff; the selection of an alloy for use in the laminate is made based on the most critical properties. It is certainly possible to make high temperature fiber/metal laminates using ceramics instead of metals, and in fact such a laminate has been studied;^[87] however, such a laminate would obviously have a completely different range of applications than those envisioned for fiber/metal laminates.

The "Temp." column in Table IV represents the maximum continuous use temperature based on either microstructural stability or mechanical strength, whichever is the limiting property. "Envir" refers to the environmental resistance of the alloy. Cost refers to thin sheet

products; most metals are much more expensive in this form than in cast or wrought forms.

(2) **Fibers.** As with the metal, the selection of a fiber for the laminate must be based on the desired laminate properties. It is also important to consider such factors as the chemical or thermal compatibility of the fibers and metal, and also the interrelatedness of the properties of these two components.

A laminate consisting of a high temperature aluminum and graphite fibers is a good example of the former. Such a laminate would be very desirable from a mechanical property standpoint, yielding a laminate with very high stiffness for a very low density. However, the laminate would be subject to potentially severe galvanic corrosion, which always occurs when graphite and aluminum come into contact. For such a laminate to be viable, some means would have to be devised to prevent any contact whatsoever between the fibers and the aluminum. In addition, based on calculations using Equations (1), (2), and (3), this laminate would have an extremely high residual stress and would experience very high cyclic stresses at the fiber/metal bond when exposed to temperature fluctuations.

As an example of the interrelatedness of the fiber and metal components, consider a fatigue-resistant laminate using titanium with glass fibers. The modulus of glass is only about one-third that of the titanium; from Equations (11), (12), and (13), it is clear that the fibers would carry very little load, and the net stress on the titanium layers would be substantially higher than the nominal stress on the

laminate. The result would be low yield strength and poor fatigue properties compared to monolithic titanium.

Table V summarizes the properties of some potential fibers for high temperature laminates. The category "Compatibility with Metals" refers primarily to coefficient of thermal expansion and chemical compatibility. It is clear from this table that glass and carbon fibers are very attractive candidates for laminates when strength, weight, and cost are major factors.

(3) **Polymer Matrix.** The most serious limiting factor in the development of high temperature laminates is undoubtedly the availability of polymers which can operate at the desired service temperature.

The first question is whether to use a thermosetting polymer or a thermoplastic. Most of the important issues detailed in Section 2.3.2 suggest^[88] that a thermoplastic is preferable for high temperature laminates. To begin with, thermoplastics are relatively inert chemically, in that they do not undergo rapid chemical changes at moderate temperatures. Therefore, the need for refrigeration prior to use is not as critical, and they do not suffer from the uselessly short shelf-lives often found in high temperature thermoset resins. Another major advantage of thermoplastics is that they usually have a very low volatile content, so entrapment of evolved gases is not a problem. Thermosets, on the other hand, frequently evolve such a large volume of volatiles that the laminate would more resemble a laminated foam than a sheet product. Due to their low volatile content, thermoplastics also

have less environmental impact in the laminate processing stage.

The chemical stability and low volatile content of thermoplastics is also a disadvantage, in that the temperatures necessary for them to become fluid and bond to the metal layers is often well above the glass transition temperature (T_g) of the polymer. For instance, unpublished research by this author on laminates of 8009 aluminum with glass-fiber-reinforced PEEK showed that the PEEK softened and caused the laminate's properties to degrade substantially above 150°C, even though the processing temperature of the PEEK/graphite prepreg was over 300°C. In this respect, thermosets, which can typically be used near or above their original cure temperature, are better.

Thermoplastics have the advantage of softening at sufficiently high temperatures, which means that thermoplastic-based laminates have a greater potential for secondary forming and repairability than those based on thermosets. Moisture absorption is also lower in thermoplastics. In terms of mechanical behavior, thermoplastics typically have greater toughness and impact resistance than thermosets.

The important properties of most of the currently available high temperature polymers which are candidates for high temperature laminates are summarized in Table VI.

In many cases, the distinction between thermosets and thermoplastics becomes fuzzy for these high temperature polymers; some of them can possess the characteristics of either one, depending on the cure and post-cure cycle used. Many of those listed as "thermosets" might better be described as "addition-type" polymers, and many under

"thermoplastics" as "condensation-type" polymers.

The majority of the polymers in Table VI are polyimides. The only exceptions are PT, which is a cyanate ester which cures to form a phenolic triazine (hence the name),^[89,90] crystalline PEEK (polyetheretherketone), and Radel C, a polyaryl sulfone. The polyimides include a wide variety of chemical compositions, many of which are proprietary. PMR-15 was the first of the 300°C polymer resins, and was the most widely used high-temperature resin until 1991. In the past, PMR-15 was extremely difficult to process, in part due to its high toxic volatile content. This problem has been alleviated to some extent through refinement of the polymer chemistry. In the late 1980's, TRW developed AFR-700 as a solution to the shortcomings of PMR-15.^[91-94] This resin has demonstrated much better processability and superior mechanical properties; however, there is still a toxicity problem (MDA is a major volatile component), and because the resin precursors are very expensive, the resin is also very expensive, roughly \$600 to \$1000 per pound. The cost problem is compounded by the fact that AFR-700 is produced as a batch process, and its sole commercial producer, Dexter, requires a relatively large minimum order (by research standards). Furthermore, production and availability are restricted by the Air Force due to the highly secret nature of AFR-700 and its applications.

IARC-RP46 is a modification of the PMR-15 chemistry. The methylenedianiline in the latter is replaced by an oxydianiline (ODA), which was not supposed to be as toxic as MDA, but which is now suspected of being just as toxic ^[95]. RP-46 is also reported to have better

processing characteristics and greater toughness than PMR-15.[81-85] Its cost is about one tenth that of PMR-15 and AFR-700, and availability in research quantities from Structural Polymer Systems is currently excellent.

Allied-Signal's PT resin reportedly possesses excellent processing characteristics, including low viscosity in the uncured state.[90]

In general, the mechanical properties of the polymer matrix will not affect the properties of the laminate in which it is to be used. Toughness is an exception, since matrix cracking and debonding can seriously affect the laminate's fatigue properties. In terms of the polymer's physical compatibility, it must obviously bond with the desired strength to the fibers, as well as to the metal. The bond with the fiber can be strengthened or weakened by coating the fibers, while that with the metal can be altered by using a polymeric primer or adhesive. To date the most promising high temperature primer for laminate fabrication has been American Cyanamid's BR-35, which is a fluorinated polyimide as are many of the high temperature polymers in Table VI.

2.3.4. Special Problems of High Temperature Laminates. Many of the problems associated with the development of high temperature laminates have already been discussed. These include materials compatibility, toxicity and environmental concerns, and processability. From a development point of view, the greatest obstacle by far is the cost and

availability of high temperature materials. Many of them are not available in the desired form or thickness, or in the desired fiber/polymer matrix combinations, et cetera. Many are prohibitively expensive, such as IARC-TPI, which is only available in 10-pound lots at \$300 per pound;^[96] or AFR-700, which is only available in large orders, and for which "there is no such thing as scrap".^[97]

Currently, materials and configurations for laminates must be selected based on the solution of these problems, rather than on the desired laminate properties. For instance, in terms of weight savings, it would be desirable to replace a conventional metal component with a laminate using a lighter metal. This may be possible in some cases; for instance, a laminate using an HTA could be used as a replacement for Titanium, even though the latter has vastly superior fatigue properties and much greater modulus than the monolithic HTA. This substitute can be made by using a high modulus carbon fiber and by carefully controlling the interface properties to obtain good fatigue properties.

However, as noted previously, HTAs are currently extremely expensive in thin sheet, and there would be severe problems with galvanic corrosion, residual stresses, and thermal fatigue. In the end it would probably prove very expensive to overcome these problems and produce a successful laminate using these materials. The most cost-effective solution, as well as the one with the greatest chance of success, is to use a laminate based on titanium and a lower-modulus carbon fiber. The weight savings would not be as great as the aluminum-based laminate, but the cost and development time would be far less.

2.4. Previous and Ongoing Work in High Temperature Laminates.

The vast majority of the research performed on fiber/metal laminates to date has been on ARALL. The aramid ARALL family has been very well characterized, and serves as a solid baseline material for future laminates research. While some laminates research has shifted focus to Glare or other variations of ARALL, a great deal of research is still being conducted on aramid-based ARALL from a component design standpoint.

Because of the impending commercial success of ARALL and Glare, little attention has been given thus far to the development of high temperature and thermoplastic-based laminates. However, their potential has been recognized by several research organizations in the last four years. Their experiments are described below.

2.4.1. Drexel University. Drexel, under Dr. Michael Koczak, has investigated several thermoplastic-based laminate systems. [62,63,98-101] These were not high temperature laminates, but they addressed some of the important issues in the fabrication of thermoplastic-based laminates, and demonstrated the feasibility of their fabrication. The laminate systems studied by Drexel were as follows:

(1) 2024-T3 or T-8 aluminum and Kevlar 49 in J-2 epoxy, with AF-163 or AF-191 adhesive. J-2 is a thermoplastic copolyamide from DuPont based on bis(para-amino cyclohexane)methane, while the aluminum, the fibers, and the adhesives are the same as those used in various ARALL configurations.

(2) 2024-T3 and AS4 graphite fibers in amorphous PEEK, with AF-163 adhesive. In both of these systems, the adhesive was used because the temperature limits on the 2024 aluminum required processing to be carried out well below the ideal processing temperatures for the thermoplastics.

(3) 2024-T3 and 7075-T6 with AS4 graphite or E-glass fibers in a polyphenylene sulfide (PPS) matrix. American Cyanamid's FM-73 adhesive was used to promote bonding.

One important observation made during these experiments was that the need for a thick but non-load-bearing adhesive layer resulted in substantial degradation of the apparent strength and modulus of the laminate. The conclusion drawn from this is that the adhesive layer should be eliminated, i.e. the polymer should be bonded directly to the metal layers.^[63] For this to be accomplished, however, higher processing temperatures must be used. This means that a metal capable of higher temperature operation must be used. This is already a requirement for high temperature laminates; thus the advantages of a thermoplastic matrix can only be realized in a high temperature laminate.

Currently, Drexel is working on the development of high temperature thermoplastic laminates. This effort, sponsored by the Naval Air Warfare Center (NAWC), Warminster, is aimed at the development of a laminate capable of continuous operation in damping applications at 315°C. Several candidate systems will be evaluated.

2.4.2. Delft University. Delft University, under Dr. L.B. Vogelesang, was responsible for the invention and early development of ARALL and Glare. More recently, they have studied potential laminate systems based on titanium with glass or carbon fibers in an epoxy matrix, and with carbon fibers in PEEK. Delft is a subcontractor to the Drexel/NAWC contract.

2.4.3. Lockheed. Lockheed Missiles & Space Company, Palo Alto, has been studying the possibility of high temperature laminates based on both thermoplastics and thermosets, and using various rapidly solidified or mechanically alloyed aluminum alloys. Experimental work thus far has concentrated on the latter, using Inco's AL-905XL Al-Li alloy. [102,103] While this alloy is more microstructurally stable at elevated temperatures than other Al-Li alloys, it is not an HTA, having very low strength at high temperatures. [104]

2.4.4. Naval Air Warfare Center, Aircraft Division, Warminster. Formerly the Naval Air Development Center. Several potential high temperature systems have been evaluated under the Macrolaminates effort, part of an ongoing Hybrid Materials (HYMATS) program. These are as follows:

(1) 8009 aluminum with T650-42 carbon fibers in an Amoco Radel-X matrix. Fabrication was accomplished using traditional autoclave procedures, and no adhesive was used. Two primers were evaluated, BR-35 and BR-36, both from American Cyanamid. BR-35 was chosen due to its

superior performance after exposure to the high processing temperatures. Lap shear, roller peel, and ambient and elevated temperature tensile tests were performed on this system. While it was found to possess excellent strength up to at least 150°C, the bond strength was insufficient, and extensive delamination occurred during machining of the specimens.

(2) IARC-TPI resin. Only a very small sample of the unreinforced resin ($T_g=250^\circ\text{C}$) was obtainable, so only lap shear tests could be conducted. These tests revealed very good bond strength, comparable to that measured for ARALL-4. Cohesive failure of the resin occurred when BR-35 primer was used, indicating that the bond strength was greater than the cohesive strength of the resin. This system would probably have proven highly successful in a full-scale fiber/metal laminate with 8009 aluminum, but unfortunately the rights to the resin were sold to a Japanese company which does not give away samples and has a minimum order of ten pounds for the glass- or carbon-fiber reinforced resin. Due to the high cost, about \$300 per pound, work on this system had to be terminated.

(3) 8009 aluminum with S-2 glass fibers in amorphous PEEK. This was an attempt to demonstrate the feasibility of fabricating a direct-bonded thermoplastic-based laminate. The standard autoclave cure cycle for the ICI prepreg was used. The 8009 aluminum was prepared by chromic acid anodization prior to processing, and laminates were fabricated both with and without BR-35 primer. Lap shear tests showed that the PEEK/8009 bond strength was excellent with or without the primer. The

bond strength without primer was about 30% higher than that for ARALL-4, and about 80% higher with the primer.

Tensile tests showed excellent modulus and strength retention up to 150°C, with only a slight decrease at 180°C. Fatigue tests showed that, despite the presence of the glass fibers, the fatigue resistance of the laminate was only comparable to that of monolithic 2024. This was due in part to the fact that there was absolutely no sign of delamination after fatigue. The three aluminum layers cracked almost simultaneously, and only one or two millimeters separated the three cracks in the loading direction. This indicated that the bond between the PEEK and the aluminum was, in fact, too strong. The fatigue tests were conducted on laminate panels which used the ER-35 primer; had they been repeated on specimens without the primer, the fatigue resistance would probably have improved. This theory has not yet been tested.

Experiments with this system proved that a fiber reinforced thermoplastic could be directly bonded to a high temperature aluminum without the use of adhesives or primers, and that the resulting laminate could possess desirable properties. These results led to the research currently underway at NAWC and Drexel, for the development of laminates based on both thermoplastics and thermosets, for U.S. Naval aircraft applications with operating temperatures of 300°C or higher.

3.0. CURRENT RESEARCH: Processing and Properties of High-Temperature Metal/Fiber-Reinforced Thermoplastic Laminates

3.1. Objectives.

The main objective of this research is to demonstrate the feasibility of direct-bonded, thermoplastic-based high temperature fiber/metal laminates. This objective includes several major tasks, including the following:

- (1) To determine the effects of various aluminum surface treatments on the metal/polymer bond strength.
- (2) To characterize the physical and mechanical properties of the laminate, and compare the observed properties with theoretical predictions.
- (3) To draw conclusions and make recommendations concerning further high-temperature laminate development.

3.2. Materials.

The high cost or unavailability of most candidate materials for high temperature laminates has already been described. This proved to be the critical factor in choosing materials for this project. The materials selected are as follows:

- (1) Metal. Because of its low density and its compatibility with the other components selected, a high temperature aluminum (HTA) was chosen as the metal component. The only HTA which could be obtained at all in sheet form was Allied-Signal's 8009 alloy, formerly FVS-0812.

This is an alloy containing roughly 8.5 weight % iron, 1.3 % vanadium, and 1.7 % silicon.^[86,105,106] Though it is still in a pre-production stage at this time, Allied-Signal is in the process of establishing a stockpile of standard mill products.

Approximately 4.46 square meters (48 square feet) of the alloy were obtained in the form of rolled strip 14.6 m (48 ft) long, 30.5 cm (12 in) wide, and 0.305 mm (0.012 in) thick. The amount of material required was based on the fabrication of 3/2 ply panels large enough to yield the desired number of specimens. The 0.3 mm thickness was chosen because this is the thickness of the aluminum layers in ARALL and Glare Laminates.

(2) Polymer. The polymer selected was Ethyl Corporation's Eymyd U-25, a fluorinated thermoplastic polyimide with an advertised T_g of 233°C.^[107] While it is not a true "high temperature" polymer (the original goal was a laminate with a use temperature of 300°C or higher), it is representative of higher temperature thermoplastic polyimides such as those listed in Table VI. It was chosen for reasons of availability; no other high temperature polymers could be obtained in fiber-prepreg form until very recently. The U-25 sample, in the form of unidirectional tape 30.5 cm (12 in) wide, was supplied at no cost by Ethyl. Unfortunately, since that time, Ethyl has discontinued its production of U-25 and all other experimental composite materials, due to their inability to find a purchaser for those operations. As a result, U-25 is no longer available. However, as it is fairly representative of all thermoplastic polyimides, it remains a useful

model system for study.

(3) **Fibers.** The fibers selected were S2 glass. Glass fibers and two different carbon fibers were available in the U-25 matrix; glass was chosen because of its chemical and mechanical compatibility with the 8009 aluminum alloy selected for the laminate.

4.0. EXPERIMENTAL PROCEDURES

4.1. Theoretical Predictions.

Based on the equations discussed in Sections 2.1 and 2.2, the residual stress, yield strength, ultimate strength, and density were predicted for the 8009/U25 laminate. These were compared to the experimentally measured properties. These equations were also used to determine the true stress state in the fibers and aluminum layers under certain test conditions. Other equations were derived as needed to explain various phenomena noted from the tests. For all laminate specimens, a nominal thickness of 1.47 mm (0.058 inches) was assumed.

4.2. Laminate Fabrication.

Traditional, but simplified, composite processing techniques were used in fabricating the 8009/U25 laminates. The important steps in this process were as follows:

4.2.1. Surface Treatments. The surfaces of the aluminum alloys were treated to promote good bonding with the polymer. In order to determine how various surface conditions affected bond strength, a number of different mechanical and chemical surface treatments were tested. These are listed in Table VII. Simple one-step surface treatments were used in most cases, since one of the goals of the project was to demonstrate a simplified fabrication technique to produce a laminate with good bond strength and properties. The phosphoric acid anodizing was performed

according to ASTM D3933 standards.

Most of the surface treatments listed in Table VII are self-explanatory. The aluminum sheets were cleaned and deoxidized prior to the surface treatment. No surface treatments were used on the polymer prepreg. Samples of the surface treatments on both 2024 and 8009 were sputter-coated with gold and stub mounted for Scanning Electron Microscope (SEM) evaluation. An Amray-1000A was used, at an accelerating voltage of 20kV.

4.2.2. Processing. The laminate panels were processed in a Baron BAC-35 autoclave using the standard U-25 cure cycle and standard high temperature bagging techniques. 3/2 panels were assembled by hand and transferred to the autoclave table, then bagged and a vacuum drawn. Once all leaks were eliminated, the chamber was closed and the process begun. The control system monitored time, temperature, and pressure throughout the cycle, and plotted these parameters upon completion. This allowed any deviations from the recommended cure cycle to be identified. Samples of the cured laminate were mounted in diallyl pthalate, then ground and polished using suspended diamond media for observation in an optical microscope.

The U-25/glass composite panel, for tensile testing of the polymer and fiber components without the metal layers, was laid up by hand and cured in a Stanat 50-ton laminating press. The U-25 cure cycle was followed as closely as possible.

4.2.3. Specimen Preparation. Specimens were rough-cut from the laminate panels by bandsaw. They were then machined to their final shape using vertical or horizontal milling machines, Tensilkut machine, and vertical drill press. The edges of the tensile specimens were filed smooth outside the gage section, but sanded with 180-grit silicon carbide paper in the gage sections. The edges of the fatigue specimens were sanded smooth over their full length, and then polished with 1000-grit SiC paper. The edges of most of the remaining specimens were filed smooth, the file being drawn along the length of the specimen to avoid causing edge delamination. Finished specimens were stored in a dessicator until tested.

4.3. Tests Performed.

The tests which were used to characterize the properties of the 8009/U25 laminates were based on those used for ARALL and Glare Laminates. It has become standard practice to use traditional sheet metal testing techniques for evaluating such laminate properties as tensile strength, modulus, fatigue, and notch and bearing strength. Impact and interlaminar properties, such as shear and peel strength, are tested using standard composite testing procedures. A complete evaluation is beyond the scope of this project; therefore, only selected properties were investigated. The tests performed were as follows:

4.3.1. Single Lap Shear Tests. Lap shear tests were performed according to ASTM D1002. 2024 aluminum and the U-25/glass prepreg were

used for the tests. The surface treatments used for these tests are described in Section 4.2.1. These tests were performed on an MTS 810 closed-loop servo-hydraulic testing system, in load control mode. A loading rate of 100N/s (1300 lbs/min) was used for all tests. The purpose of the lap shear tests was to determine the effects of aluminum surface treatment on the shear strength of the polymer/metal bond. Tests were run in the dry (as processed) condition, and after one week's exposure to 140°F, 100% relative humidity conditions (henceforth referred to as "wet" condition) to determine the effect of moisture exposure on bond strength. Wet tests were performed immediately after removal of the specimens from the humidity chamber.

4.3.2. Floating Roller Peel Tests. These tests were performed according to ASTM D3167. The MTS system described above was used to run the tests. Stroke control mode was used, with a stroke rate of 150 mm (6 inches) per minute. Load versus stroke measurements were recorded every 0.5 seconds via an MTS 459.10 Testlink Connector Interface and ITT XIRA microcomputer, using a test data acquisition program in Basic. Following the tests, the data acquired in this manner was imported into a Lotus spreadsheet file. The average peel strength of each specimen was determined by discarding the first and last inch of peel data, and then averaging the remaining load vs. stroke data points.

The purpose of these tests was to determine the effects of aluminum surface treatment and moisture exposure on the adhesive strength of the polymer/metal bond. The first series of peel tests was

performed using bare and clad 2024 aluminum. Specimens were tested in both dry and wet conditions. The tests were then repeated using 8009 alloy, using the surface treatments which appeared most promising in the lap shear and peel tests with 2024. The 8009 peel tests were performed to determine whether tests using 2024 were valid for the high temperature alloy as well.

4.3.3. Tensile Tests. Tensile tests were performed according to ASTM E-8 using the MTS system described above. An MTS 418.91 digital microprofiler was used to generate the loading sequence. Tests were run in stroke control mode at an extension rate of 0.002 inches per second. A one-inch MTS extensometer was used to measure strain. Load, strain, and stroke measurements were recorded at 0.25 second intervals via the microcomputer data acquisition program described above. The data for each test was analyzed using Lotus, and values for yield and ultimate stress, fracture strain, and primary and secondary modulus were determined.

Specimens tested include 8009 aluminum sheet in the as received condition, after 2 hours at 343°C (650°F, the processing temperature for U-25), and after 24 hours at 343°C; conventional 5-ply unidirectional U-25/ glass composites; and 3/2 ply laminate specimens in the longitudinal direction. The laminate specimens, 20.3 cm (8 in) long with a 6.4 cm (2.5 in) reduced section, were made from panels with phosphoric-acid anodized aluminum only. A nominal thickness of 1.47 mm (0.058 in) was assumed for all laminate specimens. Transverse specimens were not

tested due to (1) difficulty in machining these specimens, (2) the limited amount of material available, and (3) the fact that transverse strength is controlled by the aluminum layers, and is affected very little by the fibers or residual stresses.

Tensile tests were run at ambient temperature, -56° , 150° , 204° , and 250°C . All tests were run in the dry condition, as the strength and modulus using U-25/glass were not expected to be affected by moisture. Three of each type of specimen were tested at each temperature.

4.3.4. Axial Fatigue Tests. Fatigue tests were performed on 1500-lb. and 5000-lb. Krouse direct-stress fatigue machines. These machines automatically maintain a constant maximum and minimum load, i.e. the stress on the specimen increases as cracks form and grow. The machines were set to a load which corresponded to the desired initial nominal stress. The number of cycles to failure were recorded for each stress level. 2024 aluminum specimens were tested with different surface treatments to determine the effects of the surface treatment on the fatigue life of otherwise identical specimens. 8009 alloy specimens were tested in the as-received, untreated condition. 8009/U25 laminates were tested using untreated and phosphoric acid anodized aluminum sheet. The edges of the anodized laminate specimens were sanded and polished by hand to remove all roughness from the aluminum layers. Failure in the laminate specimens was defined as the complete fracture of all aluminum layers. Tests were terminated after 10^7 cycles if no failure occurred.

The specimens used for the fatigue tests are shown in Figure 16.

Larger specimens were used for testing the aluminum sheet because of minimum stress limitations in the test machines. Smaller specimens were used for the laminate specimens due to the limited amount of material available. Three or more tests were run for each material/surface treatment combination. Following the failure of the laminate specimens, residual strength tests were performed to determine whether any fiber damage occurred as a result of the fatigue test. The MTS system was used for these tests, which were performed at 0.002 inch per second under stroke control.

4.3.5. Dynamic Mechanical Tests. These tests were performed according to ASTM D4065 using a DuPont 982 Dynamic Mechanical Analyzer operating in resonant frequency mode, and controlled by a 1090B Thermal Analyzer. A nitrogen atmosphere was used for the tests, which were conducted between ambient temperature and 360°C at a heating rate of 10°C per minute. A nominal initial frequency of 30 Hz was used for the specimens, which were 7.62 cm (3 in) long and 1.27 cm (0.5 in) wide. The thickness varied depending on the material. Tests were run on 2024-T3 and 8009 sheet, U-25/glass composite, 2/1 ply 8009/U25 laminates, and 3/2 ply ARALL-4. The ARALL-4 was tested to only 220°C in order to avoid degradation of the epoxy and subsequent contamination of the test equipment.

Storage modulus, loss modulus, and $\tan \delta$ were calculated as a function of temperature and plotted by the 1090B analyzer. Specimens were run in both longitudinal and transverse directions, and in dry and

wet conditions. Specimens tested in the wet condition were tested several times in succession to determine the effect of drying of the polymer layer due to exposure to the elevated temperatures. The purpose of these tests was to assess the damping characteristics of the laminate and the possibility of using it in acoustic damping applications.

4.3.6. Chemical Resistance Tests. Laminate specimens approximately 51mm (2 in) long and 11mm (0.45 in) wide were submerged in various liquid environments which were representative of some of the chemical hazards to which naval aircraft might be exposed. The environments used are summarized in Table VIII. Following the exposure, the specimens were tested in three-point bend to determine the effects of the chemical exposure on interlaminar strength. True interlaminar tests, adhering to ASTM standards, could not be performed because the difficulty of machining 8009-based laminates made it impossible to cut specimens of small enough size to conform to ASTM standards. The tests were performed on an Instron 1122 screw-type tension/compression frame at a deflection rate of 0.05 in/min.

5.0. RESULTS

5.1. Theoretical Predictions.

5.1.1. **Residual Stress.** The calculations used to determine the residual stress in the aluminum and fibers are shown in Appendix I. These values were found to be 71.0 MPa (10.3 ksi, tensile) in the aluminum, and -332.5 MPa (-48.2 ksi, compressive) in the fibers. The calculations assume that the polymer bond between the metal and fibers is rigid, i.e. it does not deform under shear, and that the CTE of the polymer does not contribute to the residual stress state. It also assumes that no fiber buckling occurs. Thus the calculated residual stress represents an upper limit. The lower limit in both components is zero, this result being obtained by assuming the CTE mismatch between fibers and metal to be fully relieved by shear deformation or creep in the polymer matrix.

The value for the volume fraction of fibers was determined from the modulus of the laminates as measured in tensile tests, rather than using a theoretical volume fraction. This was done because, as will be explained in a later section, it was not possible to accurately estimate the volume fraction of fibers from micrographs. The volume fraction calculated from the average moduli of the tensile specimens tested at room temperature was 0.135. This calculation is shown as part of Appendix I.

5.1.2. Yield Strength. The theoretical yield strength was calculated according to Equations (5), (6), and (7). Yield strength was predicted for both the maximum and minimum predicted values of residual stress; the calculations are shown in Appendix II. The theoretical yield strength with the maximum theoretical residual stress is 345.9 MPa (50.2 ksi), while that with no residual stress is 401.1 MPa (58.2 ksi). These values were compared to the yield strengths obtained in tensile tests on laminate test specimens.

5.1.3. Ultimate Strength. Theoretical ultimate strength was calculated using Equations (8) and (9), as shown in Appendix III. In this calculation it is assumed that the ultimate strength is achieved at the theoretical ultimate strength of the fibers, i.e. that failure of the laminate in tension is controlled by the fibers. The ultimate strength calculated in this way is 935.0 MPa (135.6 ksi).

5.1.4. Modulus. The equation for theoretical modulus, Equation (14), was used not to determine the modulus from volume fractions and moduli of the components, but rather to determine the apparent volume fraction of fibers from the experimentally measured laminate modulus. This is shown in Appendix I as part of the residual stress calculation.

5.1.5. Density. The theoretical density, based on Equation (17), the density of the components (8009=2.93 g/cc, E-glass=2.62 g/cc, and U-25 resin=1.39 g/cc), and the calculated volume fraction of each component,

is 2.53. This figure uses a metal volume fraction of 0.632, as calculated from the thickness of the sheets (0.3 mm, 0.012 in.) and a nominal laminate thickness of 1.47 mm (0.058 in.), and the calculated fiber volume fraction of 0.135. The remaining 0.233 is assumed to be polymer. While this is not actually true, it allows a first approximation and an upper limit for the laminate's nominal density.

5.2. Laminate Processing.

5.2.1. Surface Treatments. The mechanical surface treatments, especially the blasting treatments, had a considerable shot peening effect, leaving the aluminum sheets considerably bowed when blasted on only one side. To minimize the bowing, both sides of all sheets were treated. The appearance of the 2024 and 8009 surface treatments in SEM are shown in Figures 17 and 18. The treated surfaces of the two alloys were slightly different, in some cases (DA, WA, GB, and SB) because the 8009 is harder than the alclad coating on the 2024, and in some cases (UT, PA) because of differences in surface texture. The ridges in the UT and PA 8009 (Figures 18a and f) are an artifact of the rolling operation used to fabricate the sheet.

5.2.2. Processing. Processing the laminate panels proved to be somewhat difficult. Specifically, it was very difficult to obtain a leak-free vacuum bag which would hold the vacuum until the maximum cure temperature was reached. As a result of this and the fact that the

aluminum layers make it difficult to remove all of the gases from the laminate, most panels contained a substantial amount of trapped gases. The dimensions and appearance of a cured laminate panel is shown in Figure 19. A typical cross section micrograph of the laminate is shown in Figure 20, showing clearly the metal, fibers, polymer, and entrapped gas spaces. The presence of the gas spaces resulted in a very uneven fiber distribution in some areas, which made microscopic measurement of fiber volume fraction impossible. For this reason, the fiber loading was instead calculated from tensile modulus measurements.

The U-25 panels without metal layers suffered some "oozing" of the polymer matrix due to the relatively thick (5-ply) layup and the lack of restraining devices at the edges. The panel, which was 20 by 30 cm before processing, was 40 cm wide after processing, with considerable displacement of the fibers near the edges (Figure 21). About half of the panel was useful for fabricating tensile specimens. Figure 22 shows a cross section of this panel; the fiber volume fraction, from the micrograph and based on the modulus of the tensile specimens, was determined to be about 73%.

5.2.3. Specimen Preparation. Fabrication of laminate specimens was found to be very difficult. The machining properties of 8009 sheet are very poor compared to those of traditional aluminum alloys. The alloy cannot be cut with a dull tool or at high speeds, as it galls, smears, and bends very badly. An extremely sharp tool and relatively low cutting speeds must be used, and large bites must be taken at each cut.

The laminate specimens must be tightly clamped and well supported by thick aluminum side plates in order to avoid delamination and outward bending of the cut edges. A number of specimens were unusable because of delamination, particularly the fatigue specimens with the dry alumina surface treatment and all of the transverse specimens which were attempted. Only a bandsaw was available for the rough cutting of specimens; it is possible that a thin-bladed diamond or composite cutting wheel would greatly improve the machinability of laminates made with 8009.

5.3. Tests Performed.

5.3.1. Lap Shear Tests. The results of lap shear tests using 2024-T3 are shown in Figures 23 to 28. The effects of surface treatment on shear strength in the dry condition are shown in Figure 23. The chemical surface treatments yielded much higher shear strengths than did the mechanical treatments. The strength using the phosphoric acid anodizing treatment (PA) was 12.27 MPa. Dry alumina grit blasting (DA) gave the highest strength of the mechanical treatments, 8.23 MPa.

When the DA treatment was followed by a PA treatment (DAPA) the bond strength increased to 13.86 MPa. Failure occurred cohesively and at fiber/polymer interfaces. The appearance of the failed shear specimens is shown in Figures 25, 26, and 27.

The effects of moisture exposure on the same surface treatments are shown in Figure 24. The exposure caused a moderate drop in the

chemically treated specimens (from 12.27 to 9.86 MPa for the PA specimens), and a somewhat more severe drop in those with mechanical treatments. The specimens with untreated 2024 failed under their own weight after moisture exposure.

The lap shear strength of the 2024/U25 specimens with the CA surface treatment is compared in Figure 28 to that of glass/PEEK, LARC-TPI, and ARALL-4, all with the same anodizing treatment. The U-25 is lower than ARALL-4 by about one third.

5.3.2. Roller Peel Tests. The results of the roller peel tests using 2024 and 8009 are as follows:

(1) 2024/U25. Due to a faulty nitrogen inlet valve, no external pressure was applied to the first set of roller peel panels during the cure cycle. They cured only under vacuum pressure, about six percent of the total pressure required in the standard U-25 cure cycle. These "ruined" specimens, using both clad and bare 2024 and the surface treatments listed in Table VII, were tested in both dry and wet conditions. A second set of panels for peel specimens was fabricated after correcting the faulty valve. These specimens were tested only in the dry condition.

The peel strengths exhibited by the "ruined" specimens are shown in Figures 29 and 30. For all surface treatments in both dry and wet conditions, the peel strength with clad 2024 was two to three times higher than that with bare 2024. The UT, SB, and CP surface treatments gave particularly high peel strength, all three exceeding 425 g/mm in

the dry condition. The DA, GB, and CA treatments gave the lowest strength. Moisture exposure weakened the peel strengths with clad 2024 by between 20% (UT, CP) and 60% (GB, CA), as shown in Figure 30.

The peel strength of the correctly processed specimens, shown in Figures 31 and 32, was somewhat different from that of the "ruined" specimens. The strength of the UT specimens (with clad 2024, Figure 32a) was considerably lower in these specimens, and GB went from the highest peel strength to the lowest (451 to 196 g/mm). The strongest of these specimens with clad 2024 were WA (390 g/mm) and PA (383 g/mm, Figure 32b). With bare 2024, however, PA was the weakest, and all specimens were between 91 and 212 g/mm (Figure 31).

The peel strengths of ARALL-4 and Glare Laminates were measured as well, for comparison. The latter was tested as part of NAWC's participation in Structural Laminates Co.'s 1991 Glare Evaluation Program. The peel strength of the correctly processed specimens with clad 2024 are compared in Figure 33 to that of glass/PEEK laminates (fabricated and tested previously at NAWC- see Section 2.4.4), ARALL-4, and Glare. ARALL has the lowest peel strength in the longitudinal direction, while Glare and the glass/PEEK have the highest.

Figures 34 and 35 show SEM micrographs of the peeled surfaces for the correctly processed specimens with clad 2024, and of the ARALL-4 and Glare specimens as well.

(2) 8009/U25. Figure 36 shows the wet and dry peel strength of UT, DA, and PA surface treatments using 8009 aluminum. PA was the strongest at 312 g/mm. Moisture exposure caused only a moderate drop in

strength. The peel strengths with 8009 compared well with those using 2024 (Figure 37); all were considerably higher than with bare 2024, and just above or below those with clad 2024. SEM micrographs of the peel surfaces are shown in Figure 38.

5.3.3. Tensile Tests. The results of the tensile tests at ambient and elevated temperatures are summarized in Tables IX and X.

(1) **8009 Aluminum.** The results of tensile tests on 8009 are shown in Table IX. The as-received 8009 had an ambient temperature yield strength of 452 MPa (65.6 ksi), an ultimate strength of 472 MPa (68.4 ksi), an elastic modulus of 76.8 GPa (11.1 Msi), and an elongation at fracture of from 9.4% to 14.3%. When the specimens were exposed to 343°C for two hours to simulate the laminate cure cycle, the yield strength increased to 516 MPa (74.8 ksi), the UTS to 551 MPa (79.9 ksi), and the modulus to 82.6 GPa (11.98 Msi), while the elongation at failure decreased to between 2% and 6.3%. Upon further exposure at 343°C, the yield point dropped slightly, while elongation increased to 4.5%. These properties are shown graphically in Figure 39.

At -56°C, the ultimate strength of the 8009 increased in the As Received condition to about 645 MPa (93.6 ksi), and in the "Processed" condition to about 669 MPa (97.0 ksi). Elongations at failure averaged about 2%. Due to the unavailability of an extensometer which could operate in the low temperature conditions, the yield stress, modulus, and elongation could only be estimated. The estimated values appear in Table IX.

At elevated temperatures, the yield strength, ultimate strength, and modulus decreased, as expected. The ultimate strength in the Processed condition dropped to 356 MPa (51.6 ksi) at 204°C (400°F), and to 295 MPa (42.8 ksi) at 250°C (482°F). The strengths for the As Received specimens were slightly lower. The yield and ultimate strengths coincided for the Processed 8009 at these higher temperatures. Moduli decreased with increasing temperature, but to a relatively small degree. Elongation of the Processed specimens remained roughly constant with test temperature, while that of the As Received ones decreased with increasing temperature. Yield strength, modulus, and elongation could not be accurately determined due to the unavailability of a high temperature extensometer and the necessity of using spring-loaded grips instead of hydraulic grips above 150°C.

(2) U-25 Composites. The breaking stress of the U-25 laminates at ambient temperature was found to be around 1440 MPa (210 ksi), with a modulus of about 65 GPa (9.5 Msi). These specimens had no tabs on the ends, so the specimens were clamped in the grips between two sheets of 2024. However, failure still occurred incrementally at the grips. At 150°C, a strength of about 1600 MPa (232 ksi) was measured using thick sheets of aluminum to protect the specimens from crushing in the grips. No other tests were completed at elevated temperatures due to the difficulty in gripping the untabbed specimens in the spring-loaded high temperature grips.

(3) 8009/U25 Laminates. The tensile data for the laminates is shown in Table X. The yield and ultimate strengths of the laminate

specimens at ambient temperature were found to be 365 MPa (53 ksi) and 584 MPa (84.7 ksi), respectively. The average modulus was 64.2 GPa (9.31 Msi), and the elongation at fracture was 3.42%. The stress-strain curve was similar to that for ARALL (Figure 40).

At -56°C, the yield and ultimate strengths increased to 467 MPa (67.7 ksi) and 599 MPa (86.9 ksi) respectively. Modulus increased slightly to 66.5 GPa (9.64 Msi), and elongation decreased to between 1.3 and 2.4%.

The yield and ultimate strength of the laminates varied relatively little with temperatures. The yield strength was about 312 MPa (45.2 ksi) at 204°C, and then decreased more quickly to about 246 MPa (35.7 ksi) at 250°C. The ultimate strength behaved in a similar manner, dropping to 493 MPa (71.5 ksi) at 204°C and to 405 MPa (58.7 ksi) at 250°C. Modulus could not be determined due to the equipment limitations described above and the nonlinearity of the strain-stroke relationship over most of the test range. Elongation also could not be accurately determined, but was roughly 2 to 3%.

5.3.4. Axial Fatigue. The results of axial fatigue tests were as follows:

(1) **2024-T3 Aluminum.** Fatigue tests revealed that all of the surface treatments in Table VII increased the fatigue life of 2024 compared to the untreated sheet. The DA and GB treatments roughly doubled the fatigue life, from 117,400 cycles (UT) to 227,800 (DA) and 261,100 (GB). The other treatments increased the life to a lesser

extent, as can be seen from Figure 41.

(2) **8009 Aluminum.** Tests on the 8009 aluminum revealed a run-out stress between 172 and 207 MPa (25 and 30 ksi). Fatigue life of 8009 was found to be slightly inferior to 2024-T3 (tested previously at NAWC) at higher stress levels, but was better at stresses below about 250 MPa (36 ksi). The S-N curves for 2024 and 8009 are shown in Figure 42.

(3) **8009/U25 Laminates.** Due to the difficulty in machining laminate specimens and obtaining smooth edges, only the PA treated specimens yielded useful fatigue data. The results of fatigue tests on these laminates are shown in Figure 43. The fatigue life of the laminates was found to be inferior to that of monolithic 8009 sheet for a given nominal stress. The difference was greatest at the higher stresses, and less at the lower stresses. Like the 8009 sheet, the laminates showed a run-out stress over 172 MPa (25 ksi).

5.3.5. Dynamic Mechanical Tests. The results of the DMA tests were as follows:

(1) **Aluminum Sheet.** Plots of storage modulus, loss modulus, and $\tan\delta$ are shown for 2024 in Figure 44, and for 8009 in Figure 45. As expected, loss modulus and $\tan\delta$ are very low for both alloys, although the loss modulus for 8009 increases substantially around 190° to 240°C. The storage modulus of both alloys drops rapidly above about 220°C. The value of $\tan\delta$ does not exceed 0.02 in either alloy.

(2) **ARALL-4.** In the dry condition and in the longitudinal direction, ARALL-4 shows a peak in loss modulus and $\tan\delta$ around 25°C

to 120°C, these properties are somewhat lower, though still slightly (Figure 46). Maximum $\tan\delta$ at this temperature is about 0.08. From 60° higher than in 2024. They increase slightly above 120°C, and then sharply at 190°C, where the storage modulus drops off. The dynamic behavior in the wet condition is similar, except that the peak in loss modulus and $\tan\delta$ at 25°C is not present.

(3) U-25 Composites. As with the ARALL, there is a peak in loss modulus and $\tan\delta$ in the dry longitudinal specimens just above 30°C. The peak is much larger in the composite, however, with $\tan\delta \approx 0.1$ (Figure 47). Both properties drop off at higher temperatures, and level off at $\tan\delta \approx 0.04$ or 0.05. They increase sharply again at 220° or 240°C. Beyond this range $\tan\delta$ reaches a maximum value of about 0.28. After moisture exposure, the longitudinal specimens no longer show the peak at low temperatures, and the loss modulus and $\tan\delta$ are considerably lower below 180°C than in the dry condition, with $\tan\delta \leq 0.02$ (Figure 48). Above 180°C, both loss modulus and $\tan\delta$ increase dramatically, the latter to about 0.35.

In the transverse direction, the storage modulus is naturally low, and so too are the loss modulus and $\tan\delta$. Above 220°C, $\tan\delta$ increases sharply to about 0.4. The behavior of the moisture exposed transverse specimens was similar to that of the dry ones. A plot of one of these tests is shown in Figure 49.

(4) 8009/U25 Laminates. In the longitudinal direction, the dry laminate specimens showed a $\tan\delta$ between 0.02 and 0.04 up to 240°C, and a peak of 0.26 at 280°C. Storage modulus decreased sharply, and loss

specimens behaved in a similar manner. It was found that when several modulus increased, above 240°C. This is shown in Figure 50. The wet tests were run one after the other under the same conditions using the wet specimens, the storage modulus increased in each test until it reached the value measured for the dry specimens. At the same time, in both wet and dry specimens, the temperature at which the maximum loss modulus and $\tan\delta$ occurred increased after several successive tests by about 20°C.

In the transverse direction, $\tan\delta$ rose from about 0.03 below 240°C to about 0.32 at 280°C (Figure 51). After moisture exposure, the value of $\tan\delta$ was slightly higher at low temperatures, about 0.4 to 0.6.

5.3.6. Chemical Resistance Tests. The results of the three-point bend tests are shown in Table XI. Large variations in maximum load were found from one specimen to the next in some cases, even for the same chemical exposure. The number of specimens available was insufficient to determine accurate average loads. Typical load vs. displacement curves are shown in Figure 52.

6.0. DISCUSSION.

6.1. Lap Shear Tests.

SEM examination of the lap shear failure surfaces indicated that in the specimens with untreated aluminum and all of those with mechanical surface treatments, failure occurred primarily at the polymer/aluminum interface. This indicated that the shear strength of the polymer/aluminum bond was less than the shear strength of the polymer or the polymer/fiber interfaces. Some regions of polymer/fiber failure was found in the DA specimens (Figure 26a), with shear failure of the polymer matrix between the polymer/aluminum and polymer/fiber failure regions.

The CA and PA specimens (Figures 26b and c) revealed failures primarily at or near the polymer/fiber interfaces, with cohesive failure of the polymer matrix between fibers, indicating that the polymer/aluminum bond was stronger than the polymer/fiber bond. The appearance of the failure surfaces did not change significantly after moisture exposure, so it does not appear that exposure to hot/wet conditions weakened the polymer/aluminum bond enough for failure to occur at that interface.

The DAPA failure surfaces (Figure 26d) were dominated by failures at the polymer/fiber interfaces, with cohesive failure of the matrix in between. There were also small regions of polymer/aluminum failure. This was probably due to the fact that the initial DA surface treatment left the surface rough and uneven, so the failure surface (which is also

uneven) intersected the aluminum surface in some spots. The higher shear strength of these specimens therefore results from the introduction of large-scale roughness by the DA treatment without loss of strength in the subsequent anodizing procedure.

Lap shear tests on ARALL-4 resulted in a "furry" failure surface, the fibers being pulled apart and shredded by the shear failure (Figures 27a). It appears that the epoxy/aluminum and epoxy/fiber interfaces are relatively strong, and that the failure occurs through shear failure of the fibers. Tensile fiber failures could not be identified due to the chaotic appearance of the failure (Figure 27b), but it appears that most of the fibers visible have been sheared apart, as suggested by the numerous fine filaments visible in the image.

Figure 28 shows that the lap shear strength of 2024/U25 is lower than that of ARALL-4, 2024/LARC-TPI, and 2024/glass-PEEK. This seems to be due to the low shear strength of the U-25/glass interface compared to the corresponding interfaces in ARALL and PEEK/glass, rather than inferior polymer/metal bond strength. Recall that the tests on LARC-TPI used an unreinforced film; since the shear strength with a film should be higher than that using a fiber reinforced prepreg, the polymer/aluminum shear strength using the U-25 polyimide is probably comparable to that using LARC-TPI, which is also a thermoplastic polyimide. This could not be ascertained due to the unavailability of unreinforced U-25 film.

6.2. Roller Peel Tests.

6.2.1. 2024/U25. Peel tests using 2024/U25 revealed that with most surface treatments, the peel strength was much higher with clad 2024 than with bare 2024 (Figures 29 and 31). In the case of the mechanical surface treatments, this is probably due to the lower hardness and greater capacity for deformation in the pure aluminum coating of the clad surfaces. For the chemical treatments and in the untreated specimens, the strength difference is most likely the result of the greater chemical reactivity of the clad coating. The difference is most severe with the PA surface treatment; this indicated the need to perform peel tests using 8009 as well, to determine whether the clad or the bare 2024 was a more accurate representation of the bonding behavior of 8009.

The effects of processing are shown in Figure 32. For most surface treatments, the peel strength was higher for the correctly processed panels than for the "ruined" ones. This is not surprising, as one would expect a low processing pressure to result in poor or incomplete bonding. However, the untreated and scotch-brite abraded surfaces demonstrated higher peel strengths when incorrectly processed. This occurred because these two surface treatments, unlike the other mechanical treatments, yielded relatively flat surfaces. The high processing pressures in the correctly processed panels resulted in much of the polymer being squeezed out of the panel at the edges, leaving fibers in contact with the aluminum. The peel strength of a fiber in contact with the aluminum is essentially zero, so the macroscopic peel

strength is lower for the higher processing pressure. This did not occur in the other mechanical treatments, because their rough surfaces retained more of the polymer. In the case of the chemical treatments, the higher pressures in the correctly processed panels promoted greater infiltration of the polymer into the porous oxide surface, resulting in higher peel strengths.

The untreated surfaces yielded relatively high peel strengths due to the relative smoothness of the surface. This gave good contact between the polymer and the aluminum, but because of the lack of mechanical interlocking, the shear strength of the resulting bond is low. The peel strengths of the mechanical surface treatments can be justified based on the morphology of the surfaces. The GB treatment, with the large, dish-shaped depressions, has the lowest strength, while the deep, angular depressions of the alumina blasted surfaces give higher peel strengths.

Phosphoric acid anodizing gave higher peel strengths than chromic acid anodizing under both processing conditions, and after moisture exposure, as well (Figure 32b). Chromic acid anodizing with subsequent priming gave even higher peel strengths, and it is reasonable to assume that the PA treatment plus primer would give comparable results. However, one of the goals of this research is to demonstrate direct bonding of the polymer and the aluminum, and the elimination of toxic, chemically unstable primers. As the peel strength of the PA treatment alone was good, the elimination of the primer can be considered successful.

The peel failures in all of the specimens tested occurred at the polymer/aluminum interface, as seen in Figure 34, indicating that the peel strength of the bond is weaker than that of the polymer/fiber interfaces. This represents a potential area for improvement of the bonding procedure, possibly by etching the polymer surface prior to laminate fabrication or through improved cleanliness of the lay-up procedure.

It can readily be seen from the micrographs in Figure 34 that the peel specimens contained a substantial fraction of unbonded surface. These appear as smooth surfaces in the micrographs, with some drawn-out filaments where the polymer was in contact with the aluminum. The amount of unbonded area is quite high, approaching 10% in some cases. These unbonded regions are the result of incomplete removal of trapped gases during the cure cycle. From the smooth appearance of the polymer in the unbonded areas, it appears that air pockets were present from the beginning of the cycle, i.e. the air was not completely evacuated from the layup.

This is primarily due to the difficulty in transporting all of the air to the edges of the panels by the combination of a vacuum inside the bag and external pressure. This difficulty is compounded when the aluminum surface has been mechanically roughened. The panels were cured without a cover plate on top of the layups; as a result, the edges were pinched together by the external pressure, and the top surface of the cured panel was not quite smooth. This may have contributed to the trapped gas problem, as well. The use of a thick (say 3.2mm, 0.125 in)

cover plate on the layups should reduce the amount of unbonded area.

The high level of trapped gas spaces also explains the fact that the actual density of the laminate was found to be 2.28 g/cc (based on the 1.47 mm nominal thickness), about 90% of the "theoretical" value (recall Section 5.1.5). The measured density suggests that the polymer volume fraction is only 0.055. This implies a fiber loading in the cured prepreg of 71%, which agrees well with the 73% measured in the U-25 composite (Section 5.2.2), and an overall porosity volume fraction of 0.178. The latter figure seems excessive, and optical images suggest that the fiber loading in the fully dense prepreg is somewhat less than 71%, i.e. the polymer volume fraction is more than 0.055. This is quite possible, since the exact density of the fibers was not known, the value of 2.62 representing an upper limit.

Figure 33 shows the peel strengths of 2024/U25 with the correct processing pressure and in the dry condition compared to ARALL-4, Glare, and 2024/PEEK/glass. Peel failures in ARALL occur exclusively within the fiber layer, i.e. near the polymer/fiber interfaces. It appears that the failure occurs primarily at the interface, with some shredding of the fibers (Figure 35a). Thus the peel mechanism in ARALL differs from that in 8009/U25.

In both the Glare and the 2024/PEEK/glass, peel failures occur primarily within the polymer matrix, with some failure at polymer/fiber interfaces (Figure 35b). The essentially cohesive nature of these failures indicates that the peel strengths of both the polymer/fiber and the polymer/aluminum bonds are so great that they exceed the cohesive

strength of the matrix. This has been found to be beneficial in Glare, but bad in glass/PEEK laminates due to the deleterious effect it has on the fatigue properties of the latter.

6.2.2. 8009/U25. Based on the peel results obtained with 2024, only the DA and PA surface treatments were chosen for further evaluation, along with UT as a baseline. The DA treatment was chosen for its potential applicability to field repairs. PA was chosen, of course, because it has the best combination of good bond strength and reduced environmental risk. A fourth laminate panel was fabricated using the DAPA surface treatment described previously, but the level of trapped gases was very high and as a result the panel delaminated badly while being cut for specimens.

The bond strength of the other specimens was found to be good, and was not strongly affected by moisture exposure (Figure 36). The peel strengths measured compared favorably to those using clad 2024, as shown in Figure 37; thus in future tests with other polyimide systems, the peel strength with 8009 can probably be well represented by peel tests with clad 2024. For these purposes, the low peel strengths measured for bare 2024 can be neglected.

Micrographs of the peeled surfaces (Figure 38) show that, as with the 2024, failure occurs primarily at the polymer/aluminum interface. With 8009 and the PA surface treatment, however, there is evidence of some failure at the polymer/fiber interfaces (Figure 38c). Again, there is a significant amount of unbonded area. There is also a considerable

amount of "waviness" in the fibers, which was visible to a lesser extent in the 2024/U25 specimens. This waviness probably represents the alleviation of residual stresses by crumpling of the fibers. This was only seen in certain locations, and did not appear to affect the tensile behavior of the laminates.

Based on all of the lap shear and peel test results described above, the best surface treatment for promoting good bond strength is phosphoric acid anodizing. It appears that with reasonable attention to the cleanliness of the surfaces and a one-step etching treatment for the polymer, wholly adequate bond strengths can be achieved using the simplified anodizing procedure and direct-bonding of the thermoplastic to the metal.

6.3. Tensile Tests.

6.3.1. 8009. The tensile data for 8009 (Table IX) is shown graphically in Figure 53. Figure 53a shows the yield and ultimate strengths as a function of test temperature, while Figure 53b shows modulus and elongation versus temperature.

(1) **Ambient Temperature.** The increase in ambient temperature yield strength and decrease in elongation in 8009 upon annealing is shown in Figure 39. This phenomenon has been noted previously in 8009 aluminum, [86,106] and is believed to be due to dynamic strain aging (DSA). DSA in aluminum alloys is characterized by reduced ductility and

increased flow stress, caused by the immobilization of dislocations by solute atoms.[106]

(2) **Low Temperature.** The 8009 aluminum showed a slight increase in yield strength in both the As Received and the "Processed" conditions. This is as expected with fcc metals such as aluminum, which tend to show a moderate increase in yield strength with decreasing temperature. The strain to failure decreases somewhat due to the inability of dislocations to move quickly enough at the low temperature to accommodate the plastic deformation in the forming neck.

An attempt was made to estimate the modulus of the 8009 at -56°C by measuring strain as a function of the stroke of the hydraulic ram at ambient temperature and using this relationship to infer strain from the stroke at the lower temperature. The -56°C modulus calculated in this way for 8009 was 70.5 GPa (10.2 Msi), considerably less than the modulus at ambient temperature, indicating that the technique was not successful for the 8009 specimens.

(3) **Elevated Temperatures.** The As Received and Processed specimens showed similar strength-to-temperature relationships. The strength decreases almost linearly with test temperature, which is in agreement with results published elsewhere.[86,105,106] The major difference between the two was that the As Received material showed some strain hardening at elevated temperatures, and elongation decreased at elevated temperatures, whereas the Processed material showed no strain hardening, and maintained a constant elongation to failure at most temperatures. The reason for this is the dynamic strain hardening,

described above, which takes place in the As Received alloy upon exposure to elevated temperatures. Both the As Received and Processed 8009 showed a minimum in ductility at 150°C. This phenomenon has been found in 8009 by other researchers, as well, [86,106] and again is attributed to dynamic strain aging.

As with the -56°C tests, the lack of an extensometer for extreme temperatures made the estimation of yield strength, modulus, and elongation difficult. This problem was compounded by the fact that the sprung grips which had to be used above 150°C were less stiff than the hydraulic ones used at lower temperatures, and also caused problems with specimen slippage. However, it appears that the light weight of these grips worked in favor of the 8009 sheet specimens, as strain-stress calibrations at ambient temperature yielded a relatively linear relationship, and the property estimates made using this relationship seem very reasonable. The modulus estimates in particular agree well with those determined elsewhere. [106]

6.3.2. U-25 Composite.

(1) **Ambient Temperature.** The composite specimens tested at room temperature broke at less than half of their theoretical strength because they were not adequately protected from the grip clamping forces. The crushing of the specimen in the hydraulic grips resulted in premature fiber breakage at the edge of the grips. Thick tabs are clearly needed to protect the ends of the specimen; they were protected somewhat between 0.063 inch sheet aluminum tabs, which were somewhat

effective, but not enough so.

Even so, useful modulus data was obtained from the tests, allowing the fiber volume fraction to be calculated based on the theoretical modulus of the fibers. The resulting fraction was about 0.74, which agreed well with the 0.73 calculated from optical micrographs. Based on these values, the theoretical strength of the composite is about 3390 MPa (492 ksi).

(2) **Elevated Temperatures.** Tensile tests at 150°C revealed the same need for end tabs as was noted at ambient temperature. However, thicker pieces of aluminum were used to protect the specimens in these tests, and a maximum stress of 1600 MPa (232 ksi) was obtained. This is still well below the theoretical strength of the composite, but the estimated fracture energy (see section 6.3.4) suggests that the full strength of each fiber was reached.^[61] In other words, the fibers reached their breaking strength at different nominal stress levels, rather than all at the same time.

Testing of the composite material at temperatures above 150°C were not completed because, it was found, the spring-loaded grips could not hold on to the specimens, even after the surfaces in the grip section were roughened. These tests will be attempted again after tabs suitable for high temperature testing have been added to the specimens. This will also prevent the premature fiber failure noted in the ambient temperature tests.

6.3.3. 8009/U25 Laminates. The yield and tensile strength of the laminates are shown as a function of test temperature in Figure 54.

(1) Ambient Temperature. The ambient temperature yield strength of the laminates, 365 MPa, was slightly less than the predicted strength assuming the maximum level of residual stress. The linear relationship of theoretical yield strength with residual stress level suggests that the laminates possessed about two thirds of the maximum theoretical residual stress. It is likely that some of the residual stress was accommodated by shear strain within the polymer matrix and by waviness of the fibers as noted previously.

The measured ultimate tensile strength was much lower than the theoretical strength, 584.1 MPa versus 935 MPa. The primary explanation for this difference is in the failure mode of the laminate. As was mentioned previously, the theoretical calculation assumed that failure occurred upon failure of the fibers at their ultimate strength, with the aluminum layers plastically deformed but intact just prior to failure. However, this is not the case. The elongations of the laminate specimens at failure averaged about 3.4%, which was approximately the average elongation of the 8009 aluminum specimens after being exposed to the laminate processing conditions. The failure strain of the fibers, on the other hand, is σ_{uf}/E_f or just over 5%.

It can therefore be concluded that the laminate fails catastrophically in tension upon fracture of the aluminum layers, even though the stress on the fibers is far below their breaking strength. This can be explained by considering a tensile test at the instant of

failure of the aluminum layers. It is assumed that all three aluminum layers fail simultaneously and in the same area on the specimen, and that the effects of necking in the aluminum are negligible. Just prior to the failure, the specimen's modulus and strength is constant along its length (Figure A1, Appendix IV(A)). The gage section can be considered to be in equilibrium along its length. The tests were run at a constant stroke rate, which was very slow compared to the time required for fracture to occur. Therefore, it can be assumed that immediately after failure of the aluminum layers, the total elongation of the specimen is the same as before failure. The specimen would then have a new equilibrium state, with the total strain divided between the intact parts of the specimen and the fibers between the broken aluminum layers (Figure A3, Appendix IV(B)). The length of the latter section depends on how much delamination occurs upon failure of the aluminum layers.

As shown in Appendix IV(A), the length change Δl in the specimen prior to failure of the aluminum layers can be described as the original length l_0 times the sum of the elastic and plastic components of strain:

$$\Delta l = l_0 [\sigma_{YL}/E_L + (\sigma_{UL} - \sigma_{YL})/E'_L] \quad (22)$$

Immediately after fracture, Δl has the same value, but is now divided between the broken and unbroken segments of the specimen:

$$\Delta l = l_1 \left[(\sigma_{YL} + \sigma_1 - \sigma_{UL})/E_L + (\sigma_{UL} - \sigma_{YL})/E'_1 \right] + l_2 (\sigma_2/E_2) \quad (23)$$

This derivation is shown in Appendix IV(B). By using various substitutions and the measured tensile properties of the laminate, the

stress in the fibers at the instant of aluminum failure can be calculated as a function of the length of the delaminated zone surrounding the breaks in the aluminum. These calculations are shown in Appendices IV (A) and (B) and in Table XII, and are plotted graphically in Figure 55.

It can easily be seen in the figure that as the length of the delaminated zone approaches zero, the stress in the fibers bridging the cracks in the aluminum approaches the theoretical strength of the fibers. In reality, glass fibers typically fail at 20% to 40% below their theoretical strength,^[61] and there is also additional stress placed on the fibers by the elastic energy released when the aluminum fails. Thus if the size of the delamination zone is less than some critical value, failure of the aluminum layers will result in catastrophic failure of the specimen, even though the stress in the fibers prior to aluminum failure is much less than their theoretical strength. Note from Table XII that when the length of the delaminated zone is zero, the complicated equation from Appendix IV(B) can be discarded, and the stress in the fibers at the break is simply σ_{UL}/V_f .

(2) Low Temperature. The average yield strength of the laminate at -56°C was found to be about 466 MPa (67.6 ksi), or about 102 MPa (15 ksi) greater than at ambient temperature. This is due to the increased yield strength of the 8009 aluminum at this temperature. The 8009 yield strengths estimated from the load/stroke data does not show much of an increase compared to ambient temperature, however. This suggests that, since the strain/stroke relationship used proved inaccurate for

estimating the modulus for the 8009, it also produced an erroneous yield strength estimate for that alloy.

The expected increase in the laminate's yield strength is offset somewhat by the increased theoretical residual stress, which can be calculated from Equations (1), (2), and (3), and is shown as a function of temperature in Figure 56. In this way, the theoretical maximum residual stress in the aluminum layers at -56°C is found to be 95.5 MPa (13.85 ksi) tension, an increase of 24.5 MPa over that at ambient temperature. By using this value and the measured yield strength of the laminate in Equation (5), an expected yield strength for the 8009 of between 605 and 700 MPa (88 and 102 ksi), depending on the residual stress state, is obtained.

The ultimate strength of the laminate specimens varied considerably, but two of the three broke soon after yielding began. The average strength was 599 MPa (86.9 ksi). The fibers did not fail immediately upon aluminum layer failure at -56°C as they did at ambient temperature (Figure 57). This is because the failure strain of the 8009 is lower at low temperatures, and therefore the stress in the fibers upon failure of the aluminum is lower.

The estimated elastic modulus, 66.5 MPa (9.64 Msi), was slightly higher than that at ambient temperature. From Equation 14, this implies an 8009 modulus of 86.2 MPa (12.5 ksi) at -56°C . This is slightly higher than the modulus of the aluminum at ambient temperature. It therefore appears that the technique of inferring strain from the stroke of the hydraulic ram was reasonably successful for the laminates at

-56°C, even though it was unsuccessful for the 8009 sheet.

(3) **Elevated Temperature.** The yield and tensile strength of the laminate decreased much more slowly with increasing temperature than did the strength of the 8009 sheet. The reason for this is twofold. First, as temperature increases, the residual tension in the aluminum layers decreases (Equations (1), (2), and (3), Figure 56). Thus at higher temperatures, the yield point is reduced to a lesser degree by the residual stress (recall Equation (5)). Second, the modulus of the aluminum decreases more sharply with increasing temperature than that of the glass fibers. Therefore the fibers carry a greater percentage of the load at higher temperatures, increasing the apparent yield stress. The effect of a higher E_f/E_{Al} ratio can be seen by noting the arrowed equation in Appendix II.

The yield strength drops off significantly between 204° and 250°C as the glass transition temperature of the polymer is approached. At all temperatures between ambient and the T_g , tensile failure occurred more or less in a brittle manner immediately upon failure of the fiber layers. At 250°C, fibers failed one or several at a time over about a 30-second interval (corresponding to a 1.3 mm increase in ram extension) following failure of the aluminum layers. Bending and shearing of the fibers relative to one another confirmed that the polymer matrix was above its T_g . The different tensile failure behavior at 250°C was a result of the loss of stiffness in the polymer matrix. Equation (23) and the calculations in Appendix IV(B) are no longer valid at this temperature, because they assume that the polymer matrix is stiff, and

does not suffer any shear deformation. This clearly would not be true at or above the T_g .

The ultimate strength behaves in a similar manner to the yield strength, with a gradual dropoff below 204°C and a more rapid decrease above that temperature. Unfortunately, the contribution of the fibers to the high temperature tensile strength could not be determined because of the delays in testing the U-25 composites.

As was mentioned in Section 5.3.3, the moduli and elongations to failure of the laminates could not be determined at the higher temperatures. It appears that the relatively high loads involved in the laminate tensile tests, while an asset at lower temperatures with the massive hydraulic grips, caused excessive settling and forced changes in the alignment and seating of the load train when the light-weight, sprung grips were used at high temperatures. The result was the highly non-linear strain-stroke relationship noted at the lower loads. Thus the elastic and secondary moduli could not even be estimated at the two highest temperatures. Both moduli are expected to behave in a manner similar to the tensile and yield strength, however.

(4) **Stretched Laminate Specimen.** In addition to the above tensile tests, one additional test was conducted at ambient temperature, in which the specimen was loaded to a nominal stress of about 480 MPa (69.6 ksi) and then unloaded. This stress was about 120 MPa (17.5 ksi) above the specimen's yield point, and represented a total permanent strain (as measured from the stress-strain diagram, Figure 58 of about 1.41%. The residual stress in the aluminum layers was altered according

to the equation:

$$\Delta\sigma_{\text{res.Al}} = E_{\text{Al}} \Delta\epsilon \quad (24)$$

where $\Delta\epsilon$ is the strain of unloading from 480 MPa (-0.00878, as measured from the stress-strain diagram), and $\Delta\sigma_{\text{res.Al}}$ represents the change in stress from the tensile yield stress of the aluminum. Thus the theoretical change in stress in the aluminum is -725 MPa, giving a residual stress when the specimen is unloaded of 516-725 MPa or -209 MPa (-30.3 ksi, compression) in the aluminum. Equation (4) is still valid, so the corresponding residual stress in the fibers would be 978 MPa (142 ksi) tension.

The residual compression in the aluminum layers would be expected to increase the yield strength of the laminate. In fact, using Equations (5) and (7), the new yield strength should be about 563 MPa (81.7 ksi). The actual yield strength after stretching was measured at about 490 MPa (71 ksi); the difference was probably due to the accommodation of part of the residual stress by shear in the polymer matrix and stress relaxation in the aluminum. Based on the predicted and measured yield strengths above, and the theoretical yield strength in the absence of residual stresses (Appendix II(B)), approximately half of the residual stress appears to have been accommodated in this manner. The stress-strain curves for both the initial stretch and the subsequent tensile test are shown in Figure 58.

The ultimate strength of the stretched laminate specimen was not affected by the stretching procedure. Compared to unstretched specimens, the elongation was reduced by the approximate amount of the

initial stretch, from 3.4% to about 2.1%. The elastic modulus increased about 5% after stretching, probably due to some strain hardening in the aluminum.

6.3.4. Tensile Fracture Energies. The work absorbed by the specimens in the tensile tests was determined by graphically integrating the stress-stroke curve to obtain the area under the curve. The stroke was used instead of the strain in order to obtain the total energy for failure rather than just the energy per inch of gage section. The resulting energies were normalized by the cross-sectional area of the specimens. The resulting values have the units of Nm/mm^2 (ft.lbs/in^2), and are summarized in Tables XIII and shown graphically in Figure 59.

At ambient temperature the highest failure energy per unit area belongs to the As Received 8009, followed closely by the 8009/U25 laminates (Table XIII). The failure energy of the "Processed" 8009 is roughly half that of the laminate, though. The higher energy of the laminate is due to the very high fracture energy of the glass fibers, which even with a laminate failure strain of only 3.4% amounts to nearly 6.8 Nm/mm^2 (over 3200 ft.lbs/in^2). The theoretical fracture energy of the U25 composite, based on the theoretical UTS and failure strain, is about 9.55 Nm/mm^2 .

All of the materials showed a decrease in fracture energy at -56°C . Over the temperature range -56°C to 250°C , the fracture energy of the As Received 8009 first increased with temperature, but then decreased at the higher temperatures as dynamic strain aging occurred.

The Processed 8009, which represents a much more stable microstructure, showed a general increase in fracture energy with temperature. This is due to the increased mobility of dislocations at higher temperatures. The fracture energies of the laminate specimens were nearly constant over the entire temperature range, except at -56°C , where the greatly reduced toughness of the Processed 8009 resulted in a substantial reduction in that of the laminate, and at 150°C , where dynamic strain aging resulted in premature fracture in both the laminates and the 8009 sheet.

The failure energy of the U-25 composite at 150°C was found to be 7.31 Nm/mm^2 , which is just over three quarters of the theoretical fracture energy at ambient temperature. As was mentioned above, this suggests that the full strength of the fibers was obtained, especially when it is recalled that fibers typically fail 20-40% below their theoretical strength.[61]

6.3.5. Summary of Tensile Properties.

The tensile behavior described above demonstrates the excellent potential of high temperature laminates from a strength point of view. The variation of strength with temperature is much less pronounced than with the monolithic HTA alloy 8009. This is because of the contribution of the fibers to the tensile properties. The glass fibers do not yield, and the reduction of their theoretical ultimate strength at elevated temperatures does not appear to affect the tensile properties of the laminate, since failure is generally controlled by the aluminum layers.

At the same time, the decrease in fiber modulus with increasing temperature is less than that of the aluminum, so the fibers carry a larger fraction of the load at higher temperatures.

The laminate tensile properties are very promising for another reason, namely the dramatic increase in yield strength with post-stretching. The degree to which post-stretching can be used to improve the yield strength in high temperature laminates is not clear, however, because as temperature is increased, the residual compression in the aluminum which results from the stretching will be increased by the additional thermal expansion-induced compression. While there is little danger of exceeding the compressive yield strength of the aluminum, there is the possibility of shear fatigue or shear failure in the polymer binding the aluminum and fibers together. This possibility would have to be examined experimentally, such as by performing shear fatigue tests, to determine how much post-stretching can be tolerated by the laminate.

In considering high temperature laminates, the applications for which they are intended must be kept in mind, as it is the applications which define the critical properties. Shear strength is usually not the most important property for a laminate. From this point of view, the 8009/U25 laminates have demonstrated good tensile properties which are wholly sufficient to justify further research into thermoplastic-based high temperature laminates.

6.4. Axial Fatigue.

6.4.1. 2024-T3 Aluminum. The fatigue life of 2024 is increased by surface treatment as shown in Figure 41. For the three grit blasting treatments, this is due to the shot-peening effect; the blasting process causes plastic deformation in the surface of the aluminum, which results in a residual compressive stress at the surface [66]. Since most fatigue cracks initiate at the surface, the time required to initiate a crack is increased.

The scotch-brite (SB) surface treatment was less effective, because it does not produce a uniform compressive stress at the surface as do grit or bead blasting. Most of the increase in fatigue life in these specimens was probably due to the removal of pre-existing surface cracks and flaws. The increased fatigue life in the chemically treated specimens may be due partly to the creation of a hard oxide coating on the specimen surface, and partly to the blunting of pre-existing cracks by the chemical dissolution of the surface aluminum.

6.4.2. 8009 Aluminum. Figure 42 shows that the fatigue life of 8009 is less than that of 2024 at high stresses, but greater at lower stresses. At lower stresses, fatigue life is dominated by crack initiation, whereas crack propagation is dominant at higher stresses.[66] The longer life of the 8009 at low stresses suggests that it is more resistant to crack initiation than is 2024-T3, but less resistant to crack propagation once a crack has formed. This may be due in part to

the fact that the 8009 fatigue specimens were tested in the As Received condition, and so were softer and more ductile than the Processed 8009. Fatigue tests have not yet been performed on 8009 in the Processed condition, but it is reasonable to assume that its fatigue resistance will be less than that of the As Received alloy.

6.4.3. 8009/U25 Laminates. From the results of fatigue tests on 2024 with various surface treatments, and from the discussion of laminate fatigue properties in Section 2.2.4, the fatigue life of the laminate should be greater than that of the 8009 sheet at any given stress level. However, Figure 43 suggests that this is not the case. The explanation for this lies in the fact that the stress levels used in the tests and shown in the figure represent nominal stress levels in the laminate, not the true stresses in the metal layers. The true stresses must be considered in order to appreciate the effectiveness of the laminating technique in increasing fatigue resistance, and the potential fatigue properties of this particular laminate.

The true stress in the metal layers is given by Equation (12). The stress in the aluminum would be expected to be higher than the nominal stress in the laminate because of the presence of the polymer matrix, which does not contribute significantly to the strength, and the fact that the fibers have nearly the same modulus as the metal. Neglecting residual stresses for the moment, the metal:laminate stress ratio is $1/[V_{Al} + (E_f/E_{Al})V_f]$. Note that, by rearranging the terms in Equation (12), this ratio is equal in theory and experiment to the ratio

of the moduli of aluminum to laminate. Using the properties determined from the tensile tests, these ratios are found to be equal to 1.285. In other words, assuming no residual stress,

$$\sigma_{Al} = 1.285 \sigma_L. \quad (25)$$

If the residual stress in the aluminum is now considered, the true stress in the aluminum is even higher, since $\sigma_{res.Al}$ is tensile. The maximum theoretical residual stress is 71 MPa, as calculated in Appendix I. Thus the upper limit for the true stress in the aluminum layers is

$$\sigma_{Al} = 1.285 \sigma_L + 71, \quad (26)$$

while the lower limit is represented by Equation (25). Table XIV lists the values of σ_{Al} corresponding to σ_L over a range of fatigue stress levels, along with the associated $\Delta\sigma$ and R-ratio values. This data is shown graphically in Figures 60, 61, and 62.

From the figures and the data in Table XIV, it is clear that the lower-bound true stress in the aluminum (i.e. assuming no residual stress) is substantially higher than the nominal stress, the difference being greater at higher σ_L . The minimum stresses increase proportionally with the maximum stress, namely by a factor of 1.258. The mean stress and stress range increase by the same factor. The R ratio, however, remains 0.1 at all stress levels.

When the maximum theoretical residual stress is considered, the maximum and minimum stresses and the mean stress are all increased by 71 MPa. As a result, the stress range $\Delta\sigma$ is the same as it is for the zero residual stress condition. The R ratio, however, is changed drastically because both σ_{max} and σ_{min} have increased by the same 71 MPa. The

increases in $\Delta\sigma$ and σ_{mean} are greater at high nominal stresses than low, and the R ratio decreases at higher stresses. In other words, the fatigue conditions in the laminate compared to those in the 8009 are relatively worse at higher stresses than at low, and therefore the laminate S-N curve should be flatter than the 8009 curve. As Figure 43 shows, this is in fact the case.

Figure 63 shows the data from Figure 43, plus two additional sets of data representing the "nominal" laminate S-N data corrected for the true stress in the aluminum layers. The middle curve represents the true S-N response of the aluminum assuming no residual stress, while the upper curve assumes the maximum theoretical residual stress. As was noted in Section 6.3.3 for the yield response of the laminate, the actual S-N response of the aluminum in the laminate lies somewhere between the middle and upper curves, depending on how much residual stress is actually present.

For the laminate specimens, the actual values of σ_{max} , σ_{min} , σ_{mean} , and $\Delta\sigma$ are all greater than the nominal values, while the R ratio is higher than the nominal. As a result, the contribution that the fibers make to the fatigue resistance of the laminate can not be determined by comparisons with the 8009 data. Nonetheless, it can easily be seen from Figure 63 that based on the true stress in the 8009, the fatigue response of the aluminum component was greatly improved by incorporating it in a laminate. Despite the fact that the true stresses in the aluminum were much worse than the nominal stresses, the fatigue life of the laminate was reasonably good compared to the monolithic

8009. This suggests the possibility of achieving superior fatigue properties in the laminate by somehow reducing the true stresses in the aluminum relative to the nominal stresses. This can be done in two ways.

The first way is to design the laminate so that more of the load is carried by the fibers. This can be done in a number of ways, such as (1) increasing the fiber volume fraction; (2) increasing the total thickness of the polymer/fiber layers relative to that of the aluminum; or (3) replacing the glass fibers with higher modulus fibers, such as carbon. These changes must be done with care, however, as all will likely increase the residual tension in the aluminum (see Equations (1) and (4)), which would shift the S-N curve downward.

The second way to improve the fatigue resistance is to reduce the residual stress in the aluminum layers by post stretching. Again, this must be done carefully, as reducing the residual stress also increases the R ratio, again decreasing the apparent fatigue resistance. These two techniques can be used in combination to achieve the greatest possible fatigue resistance. Some optimum condition must be found where the sum of all the positive and negative effects are maximized. If the relationships between the stress conditions and R ratio and the fatigue life are known for the metal, then the optimum conditions for the laminate can be determined. Otherwise, the fatigue life of the laminate must be determined experimentally as a function of fiber modulus and volume fraction and residual stress state.

If the laminate is intended for a fatigue-critical application,

the above problems can be avoided to some extent by using a compliant polymer or a film layer in between the polymer/fiber and metal layers. This would allow most of the residual stresses to be accommodated by shear deformation of the polymer, thus allowing the use of a high volume fraction of high modulus fibers without excessive residual stresses or the need for post-stretching. Securely fixing the layers together at their ends would present a problem, however.

6.4.4. 8009/U25 Laminates: Residual Strength. Following the fatigue failure of the aluminum layers, the laminate specimens were tested in tension to determine the residual strength of the unbroken fiber layers. Ideally, the failure of the aluminum layers would not cause any fiber damage, and the residual strength would approach the theoretical strength of the fibers. However, as the data in Table XV shows, this was not the case. The tensile failure loads show no relationship to the stress levels in the initial fatigue tests. Rather, the residual strength varies widely at all fatigue stress levels.

The calculated stress in the fibers at the maximum load varies from 0 to 28.2% of the theoretical strength of the fiber layers. As can be seen in Figure 64, the failure energies- the area under the curves- also varies greatly. In addition, the maximum load is followed by a number of peaks at progressively lower loads. These observations suggest two things.

First, the latter fact indicates that the fibers are not uniformly loaded; rather, there is a range of loads on the individual fibers or on

clusters of fibers, and each fiber or cluster fails as it reaches its own particular failure stress. This explanation is supported by observations made for tensile tests on the U-25 composites, and by the micrographs in Figure 38, which show that some of the fibers appear straight while others are obviously not. Under stress, the fibers which were initially arched or twisted may only have a small load on them while the initially straight ones may be near their failure stress. A higher degree of anisotropy in fiber loading would result in a lower maximum load to failure, but a more extended failure, i.e. a greater total elongation to the last fiber failure.

The second thing which can be inferred from the residual strength data is that the fatigued specimens have widely varying amounts of fiber damage at the termination of the fatigue test. The source of the damage may have been overloading of some fiber clusters due to the anisotropic stress distribution described above, or it may have resulted from cutting or abrading by the fractured ends of the aluminum layers (the fatigue machines shut off automatically when all three aluminum layers were broken, but due to the momentum of the motor and crank assembly, the machine took about 200 cycles to come to a stop). The fracture energies (i.e. the areas under the residual strength curves) were not calculated, but is probably reasonable to assume that the specimens with the highest residual strength were relatively free of fiber damage. The specimen with a residual strength of zero, obviously, suffered complete fiber damage.

It was mentioned in Section 2.2.4 that the length of the

delaminated region around a fatigue crack was very important to the ability of the fibers to bridge the cracks in the adjacent aluminum layers. An estimation of the size of the delaminated zone can be made from the load-displacement plot. At the point of the first fiber failures, the theoretical strain ϵ_{uf} on those fibers is σ_{uf}/E_f . From the load-displacement curves, the approximate change in length of the fibers within the delaminated zone, Δl , at the maximum load P is equal to P divided by the stiffness S (in N/m or lbs/in). It can be seen that the delaminated length l of the fibers at the instant of fracture is given by:

$$l = \Delta l / \epsilon_{uf} = PE / \sigma S \quad (27)$$

By using the Δl value for the first fiber failure and that for the final failure, the minimum and maximum delamination lengths can be estimated. This was done for all of the fatigue specimens tested for residual strength (see Figure 64, for example). The results are listed in Table XV. The minimum values ranged from 16.5 to 34.3 mm, while the maximum delamination lengths were from 29.5 to 60.7 mm. If the average delamination size for each specimen is assumed to be approximately the average of the minimum and maximum values, the resulting average delamination sizes vary from 25 to 46 mm, with a slight increasing trend with increasing fatigue stress. This suggests that while the amount of fiber damage suffered during the fatigue tests varied, the size of the delamination zone is sensitive to the fatigue stress level.

It should be noted that the delamination lengths calculated from residual strength tests are not those present in the laminate during

fatigue crack growth, but after the relatively severe stress conditions encountered during failure of the aluminum layers and run-down of the fatigue machine. It can be assumed that the size of the delamination during fatigue is substantially smaller than the values in Table XV. The fact that the specimens did not delaminate completely upon failure of the aluminum layers is encouraging, indicating that the polymer/metal bond strength is sufficient for fatigue applications. The bond could be made stronger, however, without causing fiber overloading due to insufficient delamination (a situation encountered in earlier experiments with 8009/PEEK-Glass laminates).

6.4.5. 8009/U25 Laminates: Post-Stretched Fatigue. In order to determine the effects of post-stretching on the fatigue properties of the laminate, some laminate pieces were stretched in the MTS hydraulic test system prior to being machined into fatigue specimens. From the stress-strain plots of tensile specimens, it was estimated that a strain under load of about 0.010 would approximately reverse the residual stress state in the laminate. The specimens were therefore stretched to this value of strain, and were then unloaded. The average stress required to reach 0.010 strain was about 390 MPa. Upon unloading, the residual strain in all specimens was 0.0035. Using Equation (24), $\Delta\epsilon$ was 0.0066, and the resulting $\Delta\sigma_{Al}$ was 545 MPa. The residual stress in the aluminum was thus 516-545 or -29 MPa (-4.2 ksi, compressive). This represents a change in the residual stress in the aluminum of -100 MPa (-14.5 ksi).

The resulting true stresses in the aluminum layers under various fatigue loads are shown in Table XVI and in Figures 65, 66, and 67. From these figures, and by comparing the data in Table XVI to that in Table XIV, the effect of post-stretching can clearly be appreciated. The maximum, minimum, and mean loads are all reduced by 100 MPa; the load range remains the same. However, as shown in the Table and in Figure 67, the R ratio is reduced to well below the nominal 0.1. The true aluminum R ratio is the lowest, -0.151, at the lowest stress levels, and increases to 0.020 at higher stresses. Thus below a maximum stress of about 220 MPa, the aluminum layers are actually experiencing tension/compression fatigue cycling.

Recall that without post-stretching, the R ratio in the aluminum was higher than the nominal 0.1 due to the residual tension in the aluminum. After post-stretching, the R ratio is reduced because the residual stress in the aluminum layers is compressive. The lower R ratio represents more severe fatigue conditions than without post-stretching; however, the mean and maximum stresses are much lower. The latter condition was expected to have the greater influence on fatigue life, and in fact this was found to be the case.

Due to the limited number of specimens available for post-stretched fatigue testing, tests were run only at 207 MPa (30ksi) nominal maximum stress. Figure 68 shows the data from Figure 43 with the "207 MPa Post-Stretched" data added. The improvement in fatigue life is immediately apparent. By the use of a crude post-stretching treatment, the fatigue crack initiation life of the laminate at the same

nominal stress was increased by a factor of at least 50. The fatigue curves are relatively flat, however, and so the 10^7 cycle run-out stress increased only about 34 MPa (5 ksi), compared to the estimated 100 MPa decrease in true stress in the aluminum. In other words, the actual effect of the post-stretching was only about one third the expected effect. This can probably be attributed to uneven stretching due to the crudely controlled post-stretching procedure employed. Even so, the improvement is substantial. By using a carefully controlled stretching procedure such as that perfected for ARALL,^[108,109] there is no reason why a comparable or better level of fatigue resistance can not be guaranteed in standard production runs of the high temperature laminate.

6.5. Dynamic Mechanical Tests.

As expected, the $\tan\delta$ values measured for the U-25 composites and the 8009/U25 laminates were higher than those for 2024 and 8009 aluminum. The presence of a non-crystalline polymer in the laminate guarantees that $\tan\delta$ will be greater. The amount of polymer present is relatively small, and its elastic modulus is very low compared to the aluminum and fibers. Therefore, the effect of the polymer in the longitudinal direction, where isostrain conditions prevail, is relatively small. On the other hand, if the laminate could be tested in the thickness direction, the effect of the polymer and thus the value of $\tan\delta$ would be much greater due to the isostress conditions which would prevail in that direction. In the transverse direction, $\tan\delta$ values would be intermediate between those in the other two directions because

of the isostress conditions existing between the polymers and fibers.

This suggests that while the laminate would have superior vibration damping characteristics compared to monolithic aluminum, its damping ability would be the greatest for vibrations passing through its thickness direction, e.g. sound waves. Applications such as engine shrouds and firewalls therefore seem ideal for the laminate from a damping point of view.

The large peak in $\tan\delta$ in the composite and laminate specimens is the α -transition peak, i.e. the glass transition peak. The $\tan\delta$ peaks vary from 220° to 280°C, depending on the test conditions; most were from 240° to 275°C, somewhat higher than U-25's advertised 233° transition temperature. It is not known whether the difference is due to test frequency effects or some chemical or processing factor. It was clearly seen, however, that successive tests on the same specimen caused an increase in the T_g of about 20°C. This is most likely due to the occurrence of some cross-linking in the ideally linear polymer with repeated heating.[95]

It was also noted that the storage modulus of the laminates decreased upon moisture exposure, and then increased gradually with repeated heating until they returned to their original level. This is probably a result of the absorption of a small amount of moisture by the polymer matrix; this would decrease the stiffness of the polymer, allowing matrix shear which would reduce the elastic contribution of the glass fibers. Upon heating, the moisture is driven off, and the stiffness of the polymer is restored to its original level.

6.6. Chemical Resistance Tests.

Due to the large variation in bend strength of the As Processed laminate specimens, no accurate assessment can be made of the effects of chemical environments on the laminate. Methanol and jet fuel had no discernable effect on bend strength; methyl ethyl ketone appears to have had a slight effect, as did the paint stripper. The latter was an Exxon product containing "solvent G", and was based on aromatic hydrocarbons with a flashpoint of 150°F. It is worth noting that all paint strippers used by the U.S. Navy are screened to eliminate those which attack polyimides.[110] The apparently good bond strength retention after salt fog + SO₂ exposure is encouraging, especially considering the relatively severe pitting and corrosion in the outer aluminum layers.

Overall, the chemical resistance of the laminate is excellent. Sealing the edges would still be advisable, however, as one can never be certain what types of environmental attack might be encountered over years of service. Of special concern would be the effects of long-term environmental exposure accompanying cyclic loading of the laminate, which could cause delamination at the edges of the laminate sheet. Sealing the edges would help prevent this from occurring, resulting in a level of environmental resistance essentially equal to that of the metal layers in the laminate.

7.0. SUMMARY

7.1. 8009/U25 Laminates.

The major problem encountered with this laminate system is the relatively high level of trapped gases in the cured panels. The resulting porosity is unquestionably detrimental to the lap shear strength and peel strength of the polymer/aluminum bond, and probably detracts from the fatigue resistance of the laminate as well. This problem can probably be alleviated by using a thick cover plate to insure that the aluminum sheets in the laminate remain perfectly flat during processing, and that the edges do not pinch together.

In general, the bond strength achieved was acceptable, especially considering the simple surface preparations used and the relatively dirty manner in which the panels were handled prior to curing. The bond strength can probably be improved slightly by improving the cleanliness of the precure handling.

The mechanical properties of the laminate were generally very good. The fatigue resistance and strength were not as good as those for ARALL, but the 8009/U25 properties are stable to higher temperatures. Post-stretching was found to improve the yield strength and fatigue resistance of the laminate.

7.2. Implications for Future High Temperature Laminates.

Based on the results obtained in this research, it appears that high temperature laminates (HTLs) based on polyimides (particularly the

thermoplastic variety) hold considerable promise for future U.S. Naval aircraft applications. While the laminate system studied has an upper use temperature of only about 210°C or slightly higher, it is believed that it provides a good representation of the processing characteristics and potential properties of future laminate systems with higher use temperatures.

The elimination of volatiles and trapped gases will probably be the biggest obstacle to the development of laminates for higher temperature applications, especially if thermosetting polymers are used (recall from Table VI that among the currently envisioned polymer systems the thermosets have the highest use temperatures). It appears that future high temperature laminates can be fabricated using simplified and environmentally safe surface preparation techniques. This will help reduce fabrication costs and improve the repairability characteristics of the laminates.

The laminate system studied here has several limitations. One is the poor machinability of the 8009 aluminum. Another is the relatively low yield strength and modulus which results from the use of glass fibers. These properties could be increased dramatically in future HTLs by using carbon fibers. Potential properties can be predicted using the equations appearing in previous sections and in the Appendices. The use of carbon fibers will introduce several other problems, however. For instance, there is the possibility of galvanic corrosion if high temperature aluminum is retained. In addition, the difference in CTE is substantially larger for aluminum/carbon than for aluminum/glass, and

the result will be greatly increased residual tensile stresses in the aluminum. Calculations reveal that these stresses may be high enough to cause fiber buckling or shear failure at the polymer/metal interface even before a post-stretching operation can be performed. The residual stresses will be even higher if higher processing temperatures are required for curing.

Because of the problems described above, it is likely that future laminates for applications requiring high strength and stiffness will probably be based on titanium sheet rather than aluminum. This will allow the use of very high modulus carbon fibers without excessive residual stresses. The higher density of the titanium will be offset to some degree by the low density of the fibers. Overall density will be significantly lower than that of monolithic titanium, and specific properties will be better.

Aluminum/glass HTIs will prove useful for many applications, especially where intermediate strength levels, light weight, and good damping characteristics are required. Their damage tolerance, burn-through and lightning-strike resistance, and fatigue resistance are also superior to monolithic metals. There is a wide variety of potentially useful metal/polymer/fiber combinations, and the selection of these components will depend primarily on the applications for which the laminate is intended. The metal/fiber laminate concept has been well proven at low temperatures by ARALL and Glare, and this research has proven that high temperature laminates are promising as well.

8.0. CONCLUSIONS

The conclusions drawn from this research are as follows:

- 1) Adequate metal/polymer bond strength was obtained using simplified and environmentally safe aluminum surface preparation techniques. This can probably be improved by improving the cleanliness of the procedure.
- 2) The bond strength between 8009 aluminum and the polymer prepreg can be reasonably represented using clad 2024.
- 3) The lack of a cover plate during processing resulted in high levels of trapped gases in the cured laminate panels.
- 4) Good tensile and fatigue properties were obtained with the 8009/U25 laminate system.
- 5) Post-stretching can substantially increase both the yield strength and fatigue resistance of high temperature fiber/metal laminates.
- 6) The methods and equations used to predict the mechanical properties of the laminate were generally very accurate.
- 7) The techniques described herein provide a useful basis for the development of laminate systems for use at temperatures over 300°C.

REFERENCES:

- 1- "New ARALL Development Offers Promising Potential for Aircraft Design". Aircraft Engineering, Sept. 1985, pp.11-12.
- 2- Marissen, R. "Fatigue Crack Growth Predictions in Aramid Reinforced Aluminum Laminates (ARALL)". AIAA/ICAS, Report No. 86-2.6.2. (1986), pp.801-807.
- 3- Vogelesang, L.B., Chen, D., Roebroeks, G.H.J.J., and Vlot, A. "ARALL Laminates Past, Present, and Future". Paper presented at the ARALL Laminates User's Conference, Seven Springs, PA, Oct.26, 1987.
- 4- Vogelesang, L.B., Gunnink, J.W., and Schijve, J. ARALL Laminate Research Project- Review 1978-1987 by Posters. Report by Delft University, Delft, The Netherlands, 1987.
- 5- Vogelesang, L.B., Gunnink, J.W., Chen, D., Roebroeks, G.H.J.J., and Vlot, A. New Developments in ARALL Laminates. Report by Delft University, Delft, The Netherlands, 1988.
- 6- Pindera, M.J., Williams, T.O., and Macheret, Y. "Time Dependent Response of Aramid-Epoxy-Aluminum Sheet, ARALL, Laminates". Polymer Composites, Vol.10, No.5 (Oct. 1989), pp.328-335.
- 7- "Aluminum-Resin Laminate Offers Strength, Weight-Saving for Aircraft Construction". Light Metal Age, Aug. 1985, pp.29-30.
- 8- Verbruggen, Marc. "Metal Laminates for Aerospace Applications". Metals and Materials, Aug. 1990, pp.493-5.
- 9- ARALLetter, Ed. M. Gregory, Vol.1, No.1 (Sep. 1987).
- 10- Langston, P.R. "Design and Use of Kevlar in Aircraft Structures". Proceedings, SAE General Aviation Meeting and Exposition, Wichita, KS, April 1985, pp.41-55.
- 11- Verbruggen, M.L.C.E. The Moisture Absorption of ARALL Compared to Carbon and Aramid Reinforced Composites. Delft University Memorandum M-506, May 1984.
- 12- Kipp, T.R. Durability Testing of ARALL-1 and ARALL-2 Laminates. Alcoa Technology Division Report No. US-126b,c, Jul.18, 1986.
- 13- Lee, S., and Kipp, T.R. ARALL Laminates Environmental Durability Test Results. Alcoa Laboratories Technical Report, Oct.25, 1987.

- 14- Kipp, T.R. Effect of Temperature and Humidity on the Adhesion Durability of ARALL-1 and ARALL-2 Laminates. Alcoa Technology Division Report No. US-126F, Jun.8, 1989.
- 15- Verbruggen, M.L.C.E. Bondline Corrosion Properties of ARALL in a Saltspray Environment- Final Results. Delft University Memorandum M-495, Dec. 1983.
- 16- Gunnink, J.W., Verbruggen, M.L.C.E., and Vogelesang, L.B. "ARALL, A Light Weight Structural Material for Impact and Fatigue Sensitive Structures". Vertica, Vol.10, No.2 (1986), pp.241-254.
- 17- Bucci, R.J., Mueller, L.N., Schultz, R.W., and Prohaska, J.L. "ARALL Laminates - Results from a Cooperative Test Program". Proceedings, 32nd International SAMPE Symposium, Apr.6-9, 1987.
- 18- Bucci, R.J., and Mueller, L.N., ARALL Laminates Properties and Design Update. Alcoa Laboratories Report No. 57-87-26, Dec.14, 1987. Presented at the 33rd International SAMPE Symposium and Exposition, Anaheim, CA, Mar.7-10, 1988.
- 19- "New Fokker Materials Concept Points to Lighter, Fatigue-Free Airframes". Aircraft Engineering, Apr. 1988, pp.10-12.
- 20- Holt, R.A., Pajerski, A.V., and Prosser, R.A. Preliminary Investigation into the Forming, Machining, and Joining Characteristics of ARALL. Alcoa Product Engineering Division Report No. 86-52-41, 1986.
- 21- Vogelesang, L.B., and Gunnink, J.W. "ARALL: A Materials Challenge for the Next Generation of Aircraft". Materials and Design, Vol.7, No.6 (Nov/Dec. 1986).
- 22- "Alcoa ARALL Laminate Sheet". Alcoa Aerospace Technical Fact Sheet (Sheet and Plate Division), no date.
- 23- Sinke, J. "Workshop Properties of Fiber/Metal Laminates". Paper presented at AeroMat'92, Anaheim, CA, May 18-21, 1992.
- 24- Bucci, R.J., and Mueller, L.N., "ARALL Laminate Performance Characteristics". Paper presented at the ARALL Laminates User's Conference, Seven Springs, PA, Oct.25-28, 1987.
- 25- Bentley, R.M., and van Gent, P.H. "Formability in Bending of ARALL Laminates". Source Unknown, 1988.
- 26- Miller, Nicholas F. Structural Improvement of Operational Aircraft - Volume IV - ARALL Evaluation. LTV Aircraft Products Group, Final Report, Wright Laboratory Contract No. AFWAL-TR-87-3029, Sept. 1991.

- 27- Vlot, A. Impact Tests on Aluminum 2024-T3, Aramid and Glass Reinforced Aluminum Laminates and Thermoplastic Composites. Delft University Report No. LR-534, Oct. 1987.
- 28- Cook, J., and Donnellan, M.E. Tensile and Interlaminar Properties of Glare Laminates. NADC Report No. NADC-91087-60, Sep.1, 1991.
- 29- Donnellan, M.E., and Cook, J. "Metal/Polymer Reinforced Laminates: Potential Candidates for Space Applications". Proceedings, 23rd International SAMPE Technical Conference, Kiamesha Lake, NY, Oct.21-24, 1991. Vol.23 (1991), pp.777-786.
- 30- "Glare^R". AKZO Technical Information - Aerospace ARALL. No date.
- 31- van Veggel, L.H., Jongebreur, A.A., and Gunnink, J.W. "Damage Tolerance Aspects of an Experimental ARALL F27 Lower Wing Skin Panel". Paper presented at the 14th ICAF Symposium, Ottawa, Jun.10-12, 1987.
- 32- Bucci, R.J., Mueller, L.N., Vogelesang, L.B., and Gunnink, J.W. "ARALL Laminates Properties and Design Update". Paper Presented at the 1987 TMS Fall Meeting, Cincinnati, OH, Oct.14, 1987.
- 33- Gregory, M.A. "ARALL Laminates", ARALL-1, -2, -3, and -4. Preliminary Technical Information, Alcoa Technical Center, Oct.1, 1987.
- 34- Gunnink, J.W. "Design Studies of Primary Aircraft Structures in ARALL Laminates". Paper presented at the ARALL Laminates User's Conference, Seven Springs, PA, Oct.25-28, 1987.
- 35- van Baten, T., and Gunnink, J.W. "Design and Analysis of ARALL Laminate Wing Panels". Paper Presented at Composites '88 Conference.
- 36- Gunnink, J.W. "Damage Tolerance and Supportability Aspects of ARALL Laminate Aircraft Structures". Composite Structures, Vol.10 (1988), pp.83-104.
- 37- Gunnink, J.W. "Design Studies of Primary Aircraft Structures in ARALL Laminates". Journal of Aircraft, Vol.25, No.11 (Nov. 1988), pp.1023-1032.
- 38- ARALLetter, Ed. M. Gregory, Vol.1, No.2 (May 1988).
- 39- ARALLetter, Ed. M. Gregory, Vol.2, No.1 (May 1989).
- 40- Ioannou, M., Kok, L.J., Fielding, T.M., and McNeill, N.J. "Evaluation of New Materials in the Design of Aircraft Structure". Source Unknown; Supplied by Alcoa. No date.

- 41- Personal Communication, Ted Reinhart, Jr.
- 42- Leodolter, W., and Pettit, R.G. Production Implementation of ARALL Laminate Structures. Douglas Paper No. 8164, Presented at the Specialist Conference on ARALL Laminates, Delft University, Oct.25-28, 1988.
- 43- Pettit, R.G. ARALL Applications of Large Transport Aircraft. McDonnell Douglas Corporation Paper No. 91K0007, Presented at AeroMat'91, Long Beach, CA, May 20-24, 1991.
- 44- Pettit, R.G. "Residual Strength Damage Tolerance Philosophy for ARALL Laminates". Paper Presented at AeroMat'92, Anaheim, CA, May 18-21, 1992.
- 45- Orsborn, L.M. "Properties of Fiber/Metal Laminates/ARALL/Glare Derivatives". Paper Presented at AeroMat'92, Anaheim, CA, May 18-21, 1992.
- 46- Berg, G. "Test Flight of T-38 ARALL Dorsal Covers". Paper Presented at AeroMat'92, Anaheim, CA, May 18-21, 1992.
- 47- Gunnink, J.W. (for R. van Oost) "Fiber/Metal Laminates: The Structural Advantages for the '90s". Paper Presented at AeroMat'92, Anaheim, CA, May 18-21, 1992.
- 48- Kok, L.J. "ARALL Laminates in Fuselage Applications". Paper Presented at AeroMat'92, Anaheim, CA, May 18-21, 1992.
- 49- van Veggel, L., and West, J. "Structural Aspects of ARALL Structures". Paper Presented at AeroMat'92, Anaheim, CA, May 18-21, 1992.
- 50- Vogelesang, L.B. "Damage Tolerance Aspects of Glare". Paper Presented at AeroMat'92, Anaheim, CA, May 18-21, 1992.
- 51- Wu, H.F., and Dalton, J.F. Temperature Dependence on the Tensile Properties of ARALL-4 Laminates. Alcoa Technical Center Report No. 57-88-10, May 1988.
- 52- Wu, H.F. "Temperature Dependence of the Tensile Properties of ARALL-4 Laminates". Journal of Materials Science, Vol.25 (1990), pp.1120-1127.
- 53- Adhesion and Bonding, Ed. Norbert M. Bikales. Wiley-Interscience, New York, 1971.
- 54- Kinloch, A.J. Adhesion and Adhesives. Chapman and Hall, New York, 1987.

- 55- Griffen, C.W., and Askins, D.R. "Chrome-Free Surface Preparations for Aluminum Adhesive Bonding". Proceedings, 21st International SAMPE Technical Conference, Sep.25-28, 1989, pp.72-84.
- 56- "Anti-Static Spot Blaster Provides Ideal Bonding Surface". Aircraft Engineering, May 1989, p.19.
- 57- Lucma, G.A. "New Epoxy Adhesives for Bonding to Poorly Prepared Surfaces". Proceedings, 21st International SAMPE Technical Conference, Sep.25-28, 1989, pp.72-84.
- 58- Bergquist, P.R., Petrie, S.P., and Wentworth, S.E. "Evaluating Surface Treatments for Bonding Reinforced Metals". Adhesives Age, Apr. 1991, pp.38-43.
- 59- Agarwal, B.D., and Broutman, L.J. Analysis and Performance of Fiber Composites. Wiley & Sons, New York, 1980.
- 60- Tsai, S.W. Composites Design 1986. Think Composites, Dayton, OH, 1986.
- 61- Engineered Materials Handbook, Volume 1: Composites, Ed. Reinhart, T.J., et al. ASM International, Metals Park, OH, 1987.
- 62- Laubsch, K.L.R. Processing and Mechanical Characterization of Aluminum/Thermoplastic Lamina Hybrid Composites. Master's Thesis, Drexel University, March 1989.
- 63- Khatri, S.C. Processing and Evaluation of Hybrid Lamina Composites. Master's Thesis, Drexel University, March 1989.
- 64- "ARALL-1 Laminates". Alcoa Advertisement, 1987.
- 65- Caddell, R.M. Deformation and Fracture of Solids. Prentice-Hall, Inc., Englewood Cliffs, NJ, 1980.
- 66- Hertzberg, R.W. Deformation and Fracture Mechanics of Engineering Materials. 2nd Edition. Wiley & Sons, New York, 1983.
- 67- Cook, J., and Donnellan, M.E. Flexural Fatigue Behavior of ARALL Laminates. NADC Report No. NADC-90073-60, Aug.1, 1990.
- 68- Roebroeks, G.H.J.J. Observation on Cyclic Delamination in ARALL under Fatigue Loading. Delft University Report No. IR-496, Sep. 1986.
- 69- Roebroeks, G.H.J.J. Mechanistic Aspects of Fatigue Crack Growth in ARALL. Delft University Report No. IR-502, Nov. 1986.

- 70- Lee, S., and Kipp, T.R. The Environmental Resistance of ARALL Laminates. Alcoa Report. Presented at the 20th International SAMPE Technical Conference, Minneapolis, MN, Sep.27-29, 1988.
- 71- Macheret, J., Teply, J.L., and Winter, E.F.M. "Delamination Shape Effects in Aramid-Epoxy-Aluminum (ARALL Laminates with Fatigue Cracks". Polymer Composites, Vol.10, No.5 (Oct. 1989), pp.322-327.
- 72- Ritchie, R.O., Yu, W., and Bucci, R.J. "Fatigue Crack Propagation in ARALL Laminates: Measurement of the Effect of Crack-Tip Shielding from Crack Bridging". Engineering Fracture Mechanics, Vol.32, No.3 (1989), pp.361-377.
- 73- Macheret, J., Bucci, R.J., and Kulak, M. "Metal Plasticity and Specimen Size Effects in Evaluation of ARALL Laminates Notched Panel Residual Strength". Fracture Behaviour and Design of Materials and Structures (Proceedings of the 8th European Conference on Fracture, Torino, Italy, Oct. 1990).
- 74- "Aluminum Laminates: Coming of Age". Light Metal Age, Feb. 1988, pp.10-14.
- 75- Donnellan M.E., and Cook, J. Evaluation of ARALL-4, an Aramid Fiber Reinforced Aluminum Laminate. NADC Report No. NADC-89100-60, Oct. 1989.
- 76- Bucci, R.J., Mueller, L.N., Vogelesang, L.B., and Gunnink, J.W. "ARALL Laminates". Treatise on Materials Science and Technology, Vol. 31 (1989), pp.295-321.
- 77- Ward, I.M. Mechanical Properties of Solid Polymers, Second Edition. Wiley & Sons, New York, 1983.
- 78- Pettit, R.G. Current ARALL Technology. Douglas Paper No. 7925. Presented at the ARALL Laminates Technical Conference, Champion, PA, Oct.25-28, 1987.
- 79- Verbruggen, M.L.C.E. Moisture Absorption of ARALL. Delft University Report No. IR-474, Aug. 1985.
- 80- Hergenrother, P.M. "Composites and Adhesives for High Speed Civil Transports". Proceedings, High Temple Workshop XII, Cocoa Beach, FL, Jan.27-30, 1992, pp.A1-A15.
- 81- Structural Polymer Systems Advanced Materials brochure, no date.
- 82- Gupta, H., Baggert, R., Srinivasan, K., and Pater, R.H. "New Commercial High Performance MDA Free Processable IARCTM RP46 (CPI-2320) Composites". Proceedings, High Temple Workshop XII, Cocoa Beach, FL, Jan.27-30, 1992, Part C.

- 83- Pater, R.H. "LaRCTM RP46: A New 700°F Matrix Resin". Proceedings, High Temple Workshop XII, Cocoa Beach, FL, Jan.27-30, 1992, Part B.
- 84- Srinivasan, K., Johnston, N.J., and Pater, R.H. "Toughness and Damage Tolerance Properties of FMR-15, LaRCTM RP46, and Toughened LaRCTM RP46 Composites". Proceedings, High Temple Workshop XII, Cocoa Beach, FL, Jan.27-30, 1992, Part D.
- 85- Pater, R.H., and Schneider, T. "Microcracking and its Effects on 700°F Properties of FMR-15, LaRCTM RP46, and Toughened LaRCTM RP46 Composites". Proceedings, High Temple Workshop XII, Cocoa Beach, FL, Jan.27-30, 1992, Part E.
- 86- Lee, D.Y., and Zupon, D.E. "High Temperature Performance of Dispersion Strengthened P/M Aluminum Alloys". Dispersion Strengthened Aluminum Alloys, Ed. Y.W. Kim and W.M. Griffith. The Minerals, Metals, and Materials Society, 1988.
- 87- Hsu, S.E., Chen, J.C., Chang, J.F., Weng, B.J., Hwang, D.G., and Chen, W.Y. "High Temperature Organic and Ceramic Hybrid Composite". Proceedings, 21st International SAMPE Technical Conference, Sep.25-28, 1989, pp.803-811.
- 88- Engineered Materials Handbook, Volume 1: Composites, Ed. Reinhart, T.J., et al. ASM International, Metals Park, OH, 1987, Table 15, p.100.
- 89- Das, Sajal, Prevorsek, D.C., and DeBona, B.T. "PT Resins - A Versatile High Performance Thermoset for Composite Applications". Proceedings, 21st International SAMPE Technical Conference, Sep.25-28, 1989, pp.972-983.
- 90- "PrimasetTM PT Resins". Presented by Allied-Signal to NADC, Spring 1992.
- 91- Brown, A.S. "The Air Force Finds an Ultrahigh-Temperature Resin". Aerospace America, October 1991, pp.56-57.
- 92- McCoy, J.R. "The Chemical Composition, Analysis, and Reactivity of AFR700B Resin". Proceedings, High Temple Workshop XII, Cocoa Beach, FL, Jan.27-30, 1992, pp.G1-G18.
- 93- Rice, B., and Price, W. "Postcure Considerations for AFR700B". Proceedings, High Temple Workshop XII, Cocoa Beach, FL, Jan.27-30, 1992, pp.K1-K19.
- 94- Valia, D.A. "Processing and Properties of AFR700". Proceedings, High Temple Workshop XII, Cocoa Beach, FL, Jan.27-30, 1992, pp.J1-J19.

- 95- Personal Communication, M. DiBerardino (NAWC), October 1992.
- 96- Personal Communication, Mitsui Toatsu Chemicals, Apr.17, 1991.
- 97- Personal Communication, P. Chang (TRW), Spring 1992.
- 98- Laubsch, K.L., and Koczak, M.J. "Processing and Mechanical Characterization of Unidirectional Aluminum/Thermoplastic Lamina Hybrid Composites". Paper presented to NADC September, 1988.
- 99- Laubsch, K.L. "Processing and Blunt-Notched Tensile Response of Aluminum/Reinforced Thermoplastic Lamina Hybrid Composites". Proceedings, 21st International SAMPE Technical Conference, Sep.25-28, 1989, pp.892-902.
- 100- Laubsch, K.L. "Elevated Temperature Tensile Response of Aluminum-Thermoplastic Hybrid Laminates". Paper Presented at AeroMat'91, Long Beach, CA, May 20-23, 1991.
- 101- Khatri, S., and Koczak, M.J. "Elevated Temperature Response of Hybrid Laminate Composites". Paper Presented at AeroMat'92, Anaheim, CA, May 18-21, 1992.
- 102- Yaney, D.L. "Advanced Light-Weight, High-Temperature Al-Polymer Laminates for Aerospace Applications. Paper Presented at AeroMat'91, Long Beach, CA, May 20-23, 1991.
- 103- Yaney, D.L. "Aluminum Polymer Laminates for Space Applications". Paper Presented at AeroMat'92, Anaheim, CA, May 18-21, 1992.
- 104- Personal Communication, Dr. E.W. Lee (NAWC), November, 1992.
- 105- Jata, K.V., Walsh, J.A. "Influence of Temperature and Frequency on Fatigue Behavior of a High Temperature Aluminum Alloy Al-8.5Fe-1.3V-1.7Si". Low Density, High Temperature Powder Metallurgy Alloys, Ed. W.E. Frazier, M.J. Koczak, and P.W. Lee. The Minerals, Metals, and Materials Society, 1991, pp.225-240.
- 106- Porr, W.C.Jr., Leng, Y., and Gangloff, R.P. "Elevated Temperature Fracture Toughness of P/M Al-Fe-V-Si". Low Density, High Temperature Powder Metallurgy Alloys, Ed. W.E. Frazier, M.J. Koczak, and P.W. Lee. The Minerals, Metals, and Materials Society, 1991, pp.129-155.
- 107- "Eymyd Prepreg U-25". Ethyl Corporation brochure, 1990.
- 108- Verbruggen, M.L.C.E. The Influence of Prestrain Level on the Crack Propagation of ARALL under a Mode I Condition. Delft University Memorandum No. M-480, July 1983.

- 109- Verbruggen, M.L.C.E., and Reumeran, R. Prestrain Process of ARALL. Delft University Memorandum M-523, September, 1984.
- 110- Personal Communication, D. Gauntt (NAWC), October, 1992.
- 111- Metals and Ceramics Information Center/Battelle Columbus Division, Aerospace Structural Metals Handbook. Columbus, OH, 1987.
- 112- Personal Communication, Gil London (NAWC), October, 1992.

TABLES

TABLE I.

ARALL^R Variants. [18, 64]

Variant	Alloy	Cure Temp.	Stretched
ARALL-1	7075-T6	121°C	Yes
ARALL-2	2024-T3	121°C	No
ARALL-3	7475-T76	121°C	Yes
ARALL-4	2024-T8	176°C	No

TABLE II.

Glare^R Variants. [30]

Variant	Alloy	Fiber Direction	Stretched
Glare-1	7075-T6	0°	Yes
Glare-2	2024-T3	0°	No
Glare-3	2024-T3	0° (50%) 90° (50%)	No
Glare-4	2024-T3	0° (70%) 90° (30%)	No

TABLE III.

Forms of Environmental Attack

Metals:	Oxidation Liquid Corrosion Radiation Effects	Environment Assisted Cracking (stress corrosion, corrosion fatigue, liquid/gaseous embrittlement)
Ceramics*:	Oxidation/Reduction Liquid Corrosion Radiation Effects	Environment Assisted Cracking Thermal Shock Erosion
Polymers:	Oxidation Moisture Absorption Radiation Effects Solvents	Environment Assisted Cracking Thermal Instability Ultraviolet Light Degradation Erosion
Composite Materials:	All of the above Thermal Fatigue	Galvanic Corrosion Bondline Corrosion

*- includes ceramics, intermetallics, and covalent materials.

TABLE IV.

Candidate Metals for High Temperature Laminates. [86,105,106,111,112]

Metal	Temp. (°C)	Strength & Modulus	Fatigue/ Toughness	Envir.	Cost	Dens.
<u>Aluminum:</u>						
8009	370	good	fair	good	poor	2.9
CU78	350	good	fair	good	poor	3.0
Ti	350	good	fair	excellent	poor	2.8
<u>Titanium:</u>						
Pure	N.A.	poor	excellent	excellent	good	4.5
6Al-4V(q)	400	excellent	good	excellent	good	4.5
(aged)	400	good	excellent	excellent	good	4.5
6Al-6V-2Sn	400	excellent	good	good	?	4.6
<u>Steel:</u>						
low alloy	350	excellent	good	good	ex.	7.5
Ni-steels	800	excellent	excellent	excellent	good	8.5
<u>Others:</u>						
Be-Al*	315	excellent	good/fair	good	poor	2-2.2

* - Beryllium alloys have a severe toxicity problem which is also a major issue in their use.

TABLE V.

Candidate Fibers for High Temperature Laminates. [61]

Fiber	Strength	Modulus	Compatability with Metals	Elongation	Cost	Dens.
<u>Glass:</u>						
S Glass	excellent	poor	good	excellent	ex.	2.5
Astroquartz	excellent	poor	good	excellent	poor	2.2
<u>Carbon:</u>						
Low Modulus (AS-4, IM-6, T700, etc)						
	excellent	good	fair	good	good	1.8
High Modulus (P-75, P-100, etc.)						
	good	excellent	fair	poor	good	2.0
<u>Alumina:</u>						
FP	good	good	excellent	poor	poor	3.9
Nextel 440	good	good	excellent	fair	poor	3.1
<u>Silicon Carbide:</u>						
SCS-2, -6	excellent	excellent	good	poor	poor	3.0
Nicalon	good	good	excellent	good	poor	2.5
<u>Boron</u>	excellent	excellent	excellent	poor	poor	2.5

TABLE VI.

Candidate Polymers for High Temperature
Laminates. [61,80,81,90,95,107]

Polymer	Temperature Capability	Toughness	Toxicity	Volatile Content	Cost/ Avail.
<u>Thermosets:</u>					
PMR-15	340°C	fair	poor	moderate	poor
AFR-700	>370°C	fair	poor	moderate	poor
Bismaleimides	230-290°C	poor	good	low	good
LARC-RP46	>370°C	fair	fair/poor	moderate	ex.
PT	>370°C	poor	excellent	low	good
<u>Thermoplastics:</u>					
U-25	245°C	good	good	low	poor
LARC-TPI	250°C	good	good	low	poor
New TPI	?	good	good	low	poor
LARC-CPI	?	good	good	low	poor
Avamid-K	240-280°C	excellent	poor	moderate	poor
Avamid-N	350°C	good	poor	moderate	poor
PEEK (cryst.)	>300°C	excellent	excellent	low	good
Radel C	260°C	excellent	good	low	fair
Torlon	275°C	excellent	good	low	good

TABLE VII.

Aluminum Surface Treatments.

Surface Treatment	Lap Shear	Roller Peel		Tensile	Fatigue
		2024	8009		
Untreated (Cleaned)	yes	yes	yes	no	yes
Untreated (Dirty)	no	yes	no	no	no
Dry Alumina Grit Blasted	yes	yes	yes	no	yes
Wet Alumina Grit Blasted	yes	yes	no	no	no
Glass Bead Blast	yes	yes	no	no	no
Scotch-Brite Abraded ($\pm 45^\circ$)	yes	yes	no	no	no
Chromic Acid Anodized	yes	yes	no	no	no
Chromic plus BR-35 Primed	yes	yes	no	no	no
Phosphoric Acid Anod.	yes	yes	yes	yes	yes

TABLE VIII.
Chemical Environments Tested.

Environment	Conditions	Duration of Exposure
As Processed	_____	_____
Methanol	100%, ambient temp.	1 week
Methyl Ethyl Ketone	100%, ambient temp.	1 week
Jet Fuel (JP-5)	100%, ambient temp.	1 week
Aircraft Paint Stripper	100%, ambient temp.	1 week
Salt Fog + SO ₂ *	95°F, 95-98% R.H.	6 days

* - SO₂ gas was injected for 1 hour every 6 hours, at a rate of 1 cm³ per minute per ft³ of box volume.

TABLE IX.

Tensile Properties of 8009 Aluminum

Test Temp. (°C)	Condition	Yield Strength σ_{yL} (MPa)	Ultimate Strength σ_{uL} (MPa)	Elastic Modulus E_L (GPa)	Failure Strain (%)
-56	As Received	557	645	86.2*	2.4
	343°C x 2 hrs	566	669	86.2*	1.6
20	As Received	452	472	76.8	12.1
	343°C x 2 hrs	516	551	82.6	3.9
	343°C x 24hrs	476	553	83.8	4.5
150	As Received	340	373	—	3.4
	343°C x 2 hrs	410	421	—	1.8
204	As Received	315	328	70	≈6
	343°C x 2 hrs	356	356	79	≈3-4
250	As Received	266	281	66	≈5-6
	343°C x 2 hrs	295	295	74	≈4-5

* - Estimated from 8009/U25 laminate stroke/strain data at -56 and 20°C.

TABLE I.

Tensile Properties of 8009/U25 Laminates

Test Temp. (°C)	Yield Strength σ_{YL} (MPa)	Ultimate Strength σ_{uL} (MPa)	Elastic Modulus E_L (GPa)	Secondary Modulus E'_L (GPa)	Strain to Failure (%)
-56	467	599	66.5*	≈ 12	1.7
20	364	584	64.3	8.2	3.4
150	362	536	—	—	≈ 2
204	312	493	—	—	$\approx 2-2.5$
250	246	405	—	—	$\approx 2-2.5$
20°C (Theoretical)					
Max σ_{res}	346	935	64.3	12.0	3.4
No σ_{res}	401	935	64.3	12.0	3.4
20°C: Post-Stretching					
Initial	358	—	63.6	7.4	—
Stretched ($\epsilon=1.41\%$)	490	567	66.8	6.9	2.1

* - Estimated from stroke/strain data at 20°C.

TABLE XI.

3-Point Bend Results.

Specimen	Environment	Max. Load (lbs)
B-1	As Processed	76
B-2	As Processed	56
B-3	As Processed	56
B-4	As Processed	91
B-5	100% Methanol, 1 week	56
B-6	100% Methanol, 1 week	61
B-7	100% MEK, 1 week	50
B-8	100% MEK, 1 week	49
B-9	100% JP-5, 1 week	82
B-10	100% JP-5, 1 week	68
B-11	100% Paint Stripper, 1 week	47
B-12	100% Paint Stripper, 1 week	56
B-13	Salt Fog + SO ₂	80
B-13	Salt Fog + SO ₂	55

TABLE XII.

Fiber Stress as a Function of Delamination Length
in 8009/U25 Tensile Specimens upon Aluminum Layer Failure

$$\sigma_2 = \frac{\Delta l - l_1 \left[(\sigma_{uL} - \sigma_{yL}) (1/E'_1 - 1/E_1) \right]}{(l_1 V_2/E_1) + l_2/E_2}$$

$$l_o = l_1 + l_2$$

$$l_o = \frac{\Delta l}{\sigma_{yL}/E_L + (\sigma_{uL} - \sigma_{yL})/E'_L}$$

$$\begin{array}{llll} \sigma_{yL} = 365 \text{ MPa} & E'_L = 64.3 \text{ GPa} & E_2 = 88.9 \text{ GPa} & \Delta l = 3.46 \text{ mm} \\ \sigma_{uL} = 584 \text{ MPa} & E'_L = 8.2 \text{ GPa} & V_2 = 0.135 & \\ & l_o = 106.8 \text{ mm} & \sigma_1 = \sigma_2 V_f & \end{array}$$

Delaminated Length, l_2 (mm)	Undelaminated Length, l_1 (mm)	Stress in Bridging Fibers σ_2 (MPa)	Stress in Intact Segt. σ_1 (MPa)
0	106.8	4332	584
0.1	106.7	4324	583
1	105.8	4262	575
2	104.8	4197	567
5	101.8	4029	544
10	96.8	3815	515
20	86.8	3530	477
50	56.8	3134	423
100	6.8	2898	391
106.8	0	2880	—

Theoretical Strength of Fibers = 4585 MPa

TABLE XIII.

Tensile Fracture Energies

Test Temp. (°C)	Material/Condition	Fracture Energy (Nm)	Frac. Energy per Unit Area (Nm/mm ²)
-56	8009 As Received	3.96	1.17
	343°C x 2 hrs	1.33	0.39
	8009/U25	15.44	0.80
20	8009 As Received	6.20	1.89
	343°C x 2 hrs	3.23	0.99
	343°C x 24hrs	3.04	0.93
	U-25 Actual (poorly gripped)	8.12	1.72
	Theoretical	45.13	9.55
	8009/U25 As Processed	32.19	1.51
	Stretched (Net)	26.90	1.30
	Stretched (Total)	36.86	1.78
150	8009 As Received	4.12	1.25
	343°C x 2 hrs	1.79	0.55
	8009/U25	15.98	0.98
204	8009 As Received	6.18	1.88
	343°C x 2 hrs	3.88	1.18
	8009/U25	25.02	1.51
250	8009 As Received	4.26	1.29
	343°C x 2 hrs	4.15	1.26
	8009/U25	31.13	1.48

TABLE XIV.

True Stress Range and Mean Stress in Aluminum during Fatigue,
and Associated Fatigue Parameters

True Stress in Aluminum σ_{Al} (MPa)					
Nominal Stress σ_L (MPa)		No Residual Stress		Max. Resid. Stress	
σ_L (max/min)	σ_{mean}	σ_{Al}	σ_{mean}	σ_{Al}	σ_{mean}
276 / 27.6	151.8	354/35.4	194.9	425/106.4	265.7
241 / 24.1	132.7	310/31.0	170.6	381/102.0	241.5
207 / 20.7	113.8	266/26.6	146.2	337/97.6	217.3
172 / 17.2	94.8	222/22.2	121.8	293/93.2	192.9
138 / 13.8	75.8	177/17.7	97.5	248/88.7	168.4
103 / 10.3	56.9	133/13.3	73.1	204/84.3	144.1

Based on True Stress in Aluminum σ_{Al}						
Based on Nominal Stress σ_L (MPa)			No Residual Stress		Max. Resid. Stress	
σ_L (max)	$\Delta\sigma$	R ratio	$\Delta\sigma$	R ratio	$\Delta\sigma$	R ratio
276	248.2	0.1	319.0	0.1	319.0	0.250
241	217.2	0.1	279.1	0.1	279.1	0.268
207	186.2	0.1	239.2	0.1	239.2	0.290
172	155.1	0.1	199.4	0.1	199.4	0.319
138	124.1	0.1	159.5	0.1	159.5	0.357
103	93.1	0.1	119.6	0.1	119.6	0.413

TABLE XV.

Residual Strength of Fatigued Laminate Specimens

Nominal Fatigue Stress (MPa)	Residual Strength (N)	Δl (mm)		Delam. Length l (mm)		
		First Failure	Final Failure	First Failure	Final Failure	Avg.
276/27.6	3905	1.03	3.12	20.1	60.7	40.4
	2908	0.99	3.05	19.0	59.2	39.1
	471	1.38	2.31	26.8	44.7	35.8
	0	—	—	—	—	—
						(38.4)
241/24.1	3471	0.86	2.74	16.7	53.4	35.0
	1146	0.97	1.78	18.8	34.6	26.7
						(30.9)
207/20.7	3873	1.77	3.00	34.3	58.2	46.2
	2817	0.85	2.54	16.5	49.3	32.9
	2314	1.10	1.68	21.3	32.5	26.9
	2286	1.10	2.82	21.3	54.6	38.0
	1202	1.07	1.89	20.8	36.7	28.8
	1137	1.51	2.08	29.2	40.4	34.8
						(34.6)
172/17.2	736	1.09	1.53	21.2	29.5	25.4

TABLE XVI.

True Stresses and Fatigue Parameters in Aluminum during Fatigue
in Post-Stretched Laminate Specimens

True Stress in Aluminum σ_{Al} (MPa)

Nominal Stress σ_L (MPa)		No Residual Stress		Post-Stretched $\sigma_{resAl} = -29$ MPa	
σ_L (max/min)	σ_{mean}	σ_{Al}	σ_{mean}	σ_{Al}	σ_{mean}
276 / 27.6	151.8	354/35.4	194.9	325/6.4	165.7
241 / 24.1	132.7	310/31.0	170.6	281/2.0	141.5
207 / 20.7	113.8	266/26.6	146.2	237/-2.4	117.3
172 / 17.2	94.8	222/22.2	121.8	193/-6.8	92.9
138 / 13.8	75.8	177/17.7	97.5	148/-11.3	68.4
103 / 10.3	56.9	133/13.3	73.1	104/-15.7	44.1

Based on True Stress in Aluminum σ_{Al}

Based on Nominal Stress σ_L (MPa)			No Residual Stress		Post-Stretched $\sigma_{resAl} = -29$ MPa	
σ_L (max)	$\Delta\sigma$	R ratio	$\Delta\sigma$	R ratio	$\Delta\sigma$	R ratio
276	248.2	0.1	319.0	0.1	319.0	0.020
241	217.2	0.1	279.1	0.1	279.1	0.007
207	186.2	0.1	239.2	0.1	239.2	-0.010
172	155.1	0.1	199.4	0.1	199.4	-0.035
138	124.1	0.1	159.5	0.1	159.5	-0.076
103	93.1	0.1	119.6	0.1	119.6	-0.151

FIGURES

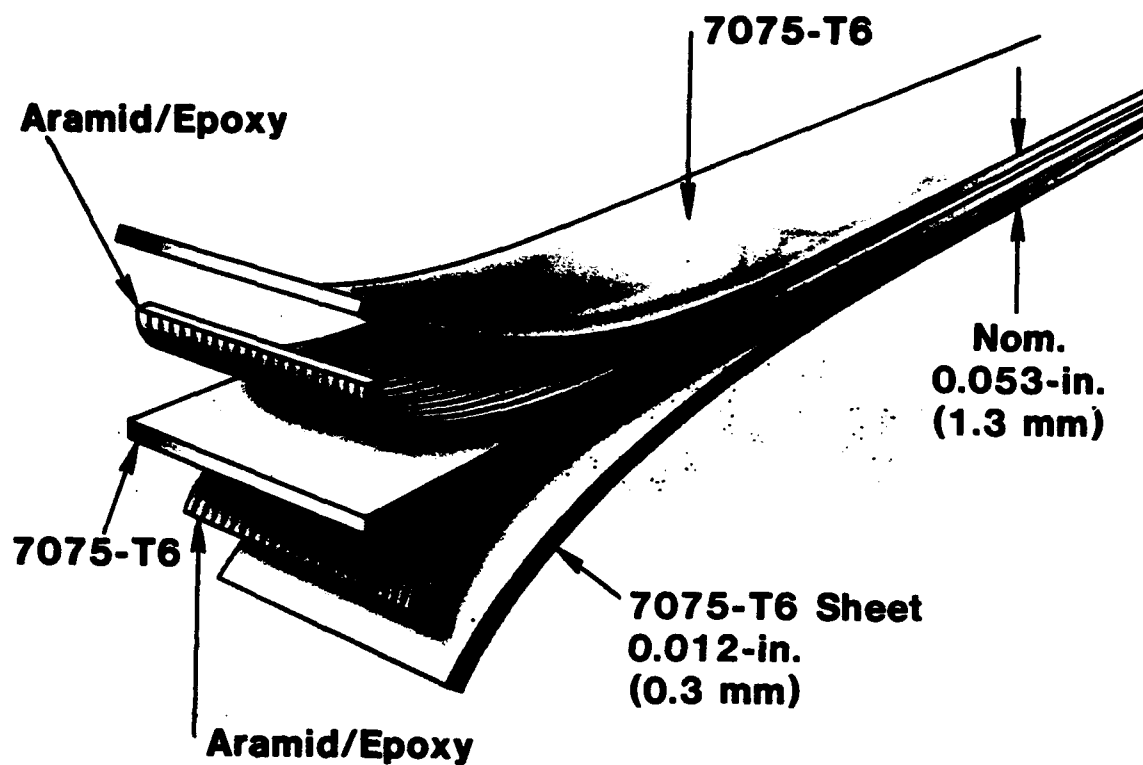


Figure 1. Exploded View of AFRL Laminate. [24]

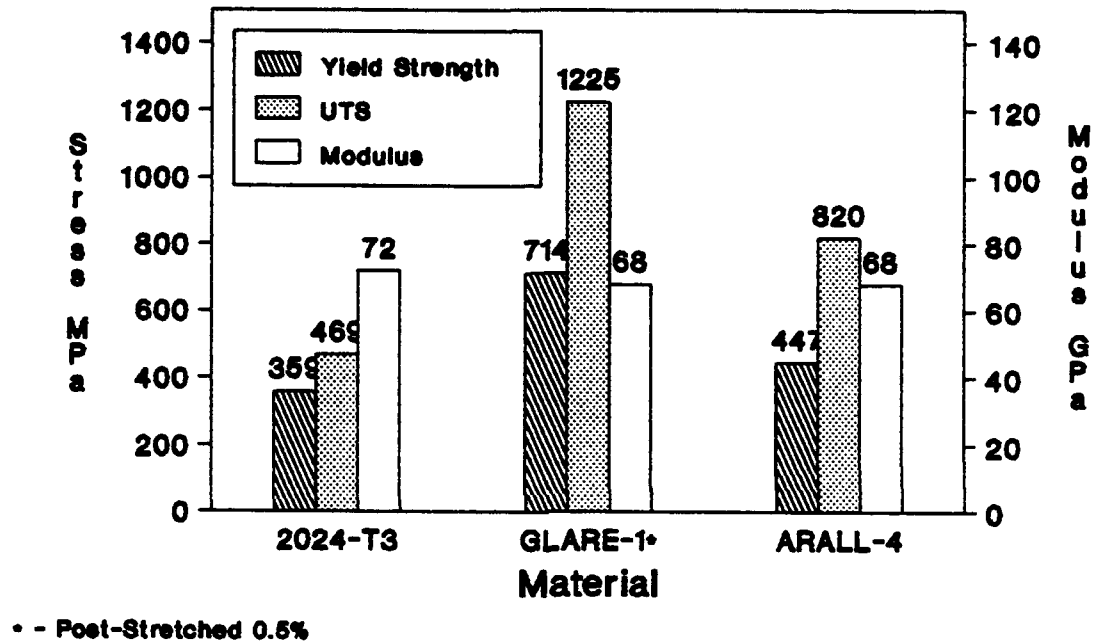


Figure 2. Tensile Properties of ARALL and Glare Laminates vs. 2024 Aluminum. (NAWC)

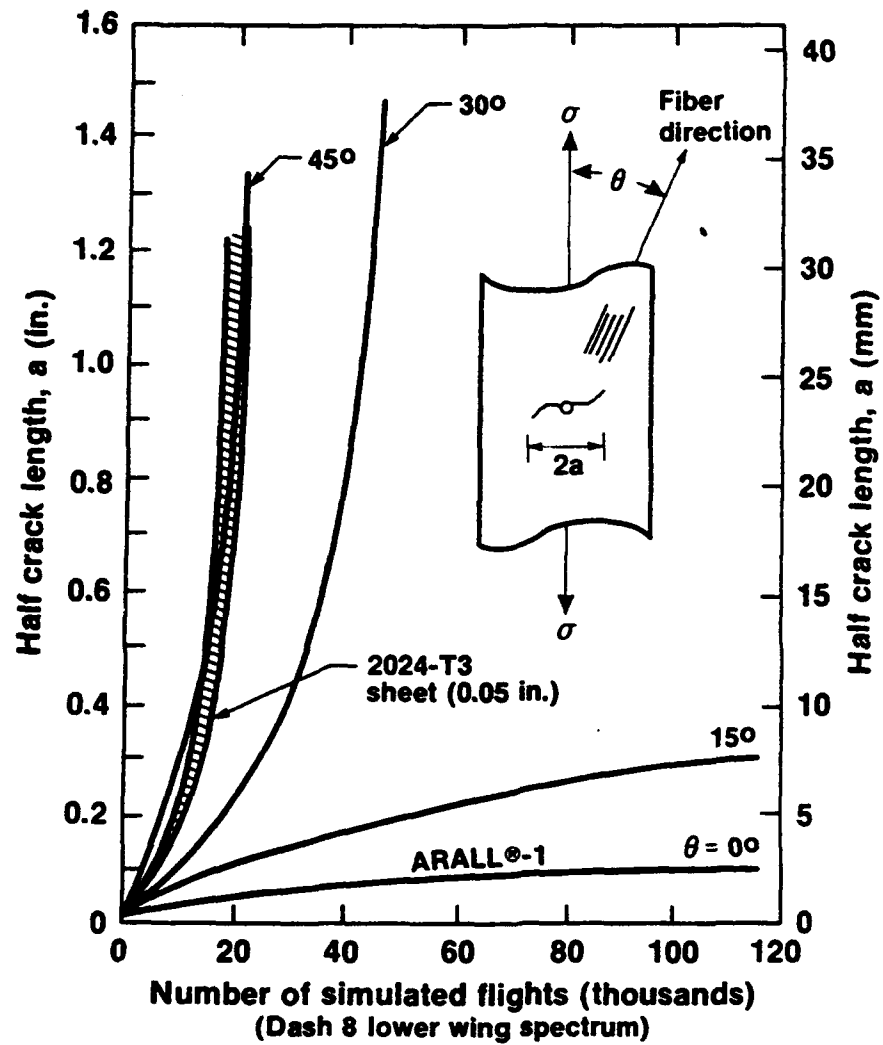


Figure 3. Fatigue Properties of ARALL Laminates vs. 2024 Aluminum. [24]

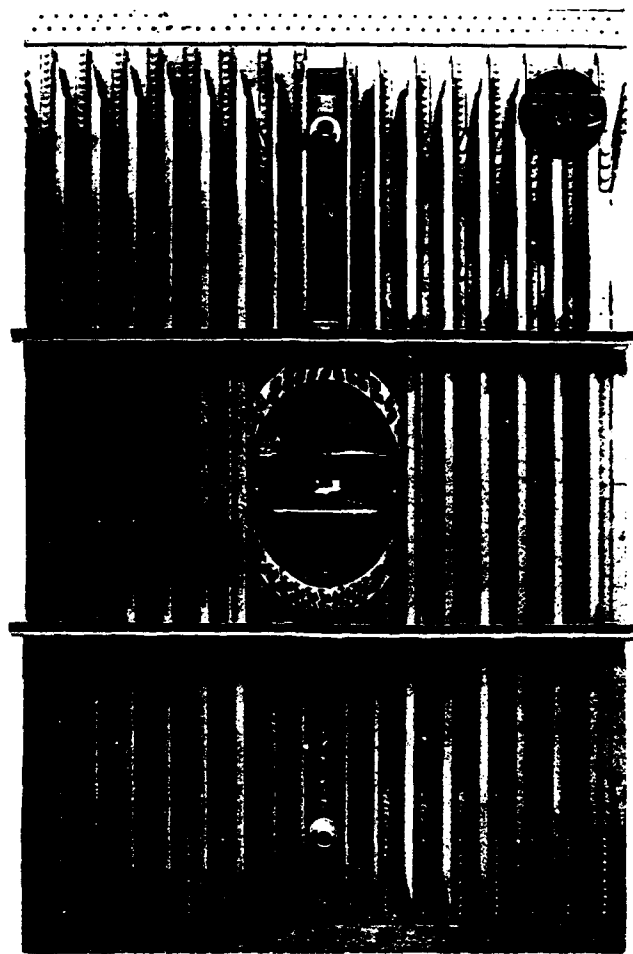


Figure 4. Fokker F-27 Wing Panels made from ARALL. [9]

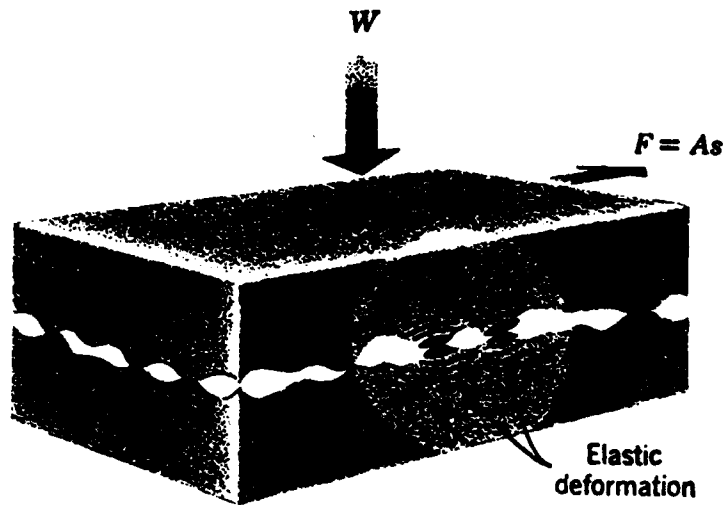


Figure 5. Atomically Rough Surfaces: Small Contact Area, with Mechanical Interlocking in Shear. [53]

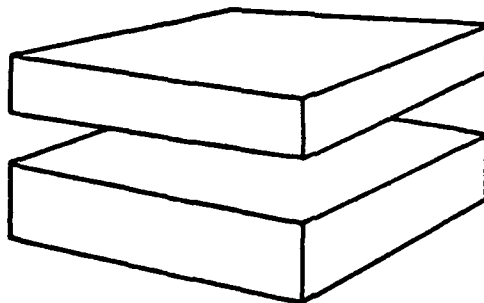


Figure 6. Atomically Smooth Surfaces: Large Contact Area. [53]

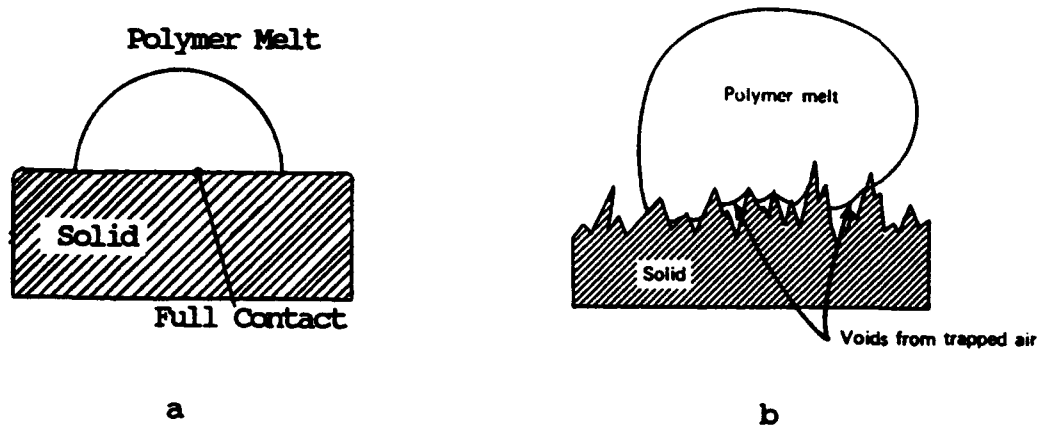


Figure 7. Wetting of Surfaces by a Viscoelastic Polymer:
 (a) Atomically Smooth Surface.^[53]
 (b) Atomically Rough Surface.

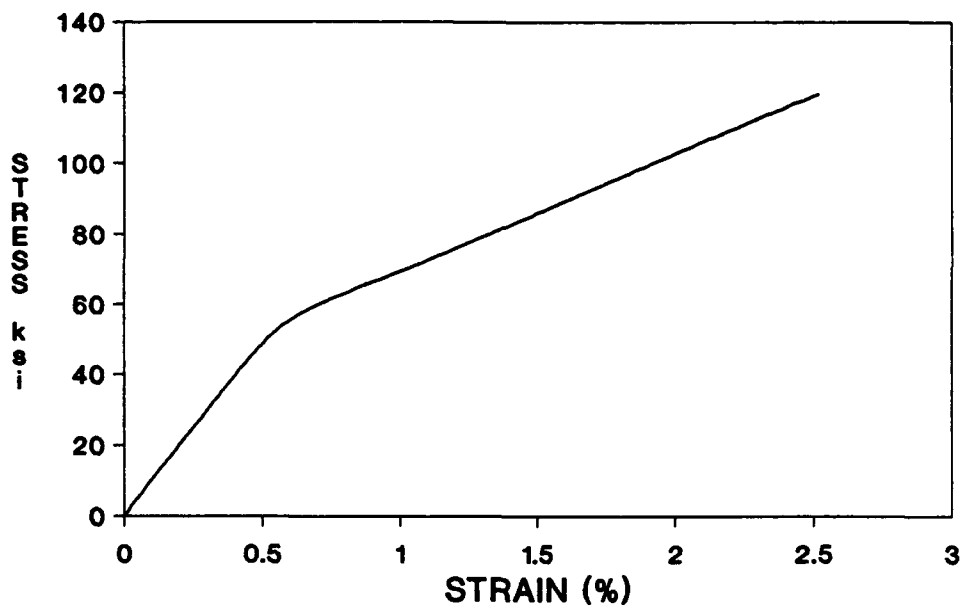


Figure 8. Stress-Strain Diagram for ARALL-4. (NAWC)

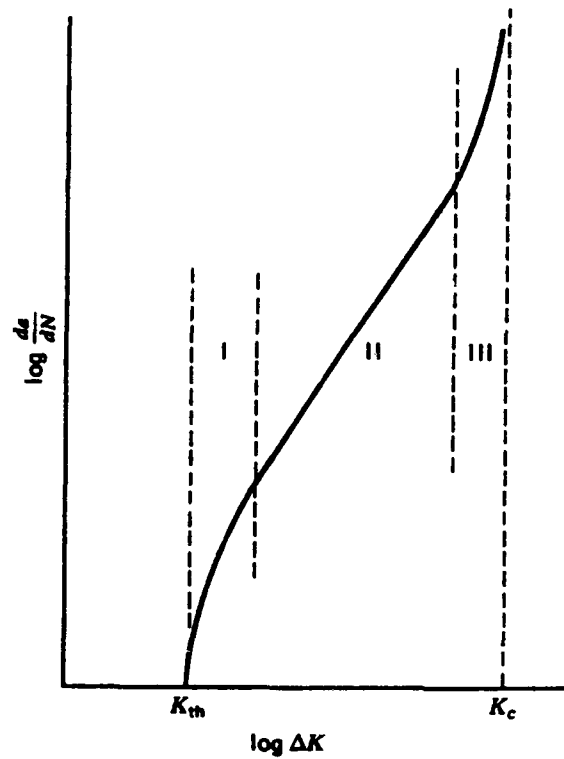


Figure 9. Fatigue Crack Growth Behavior of Conventional Materials.[66]

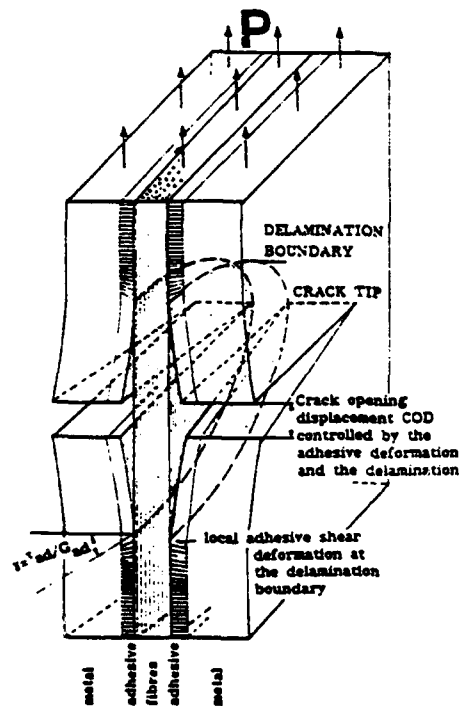


Figure 10. Crack Bridging by Fibers in a Laminate.[2]

Figure 1 Fatigue Crack Growth Behavior, ARALL 1 Laminate vs. 7075-T6 Aluminum Sheet
 da/dN vs. ΔK Behavior

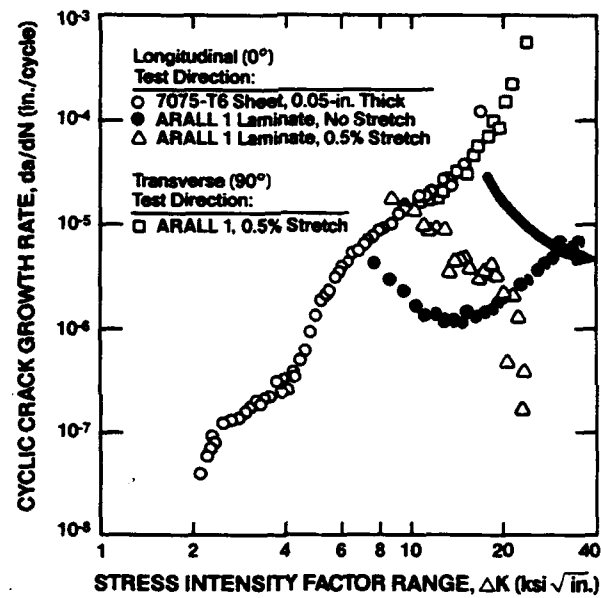


Figure 11. Fatigue Crack Growth Behavior of ARALL. [64]

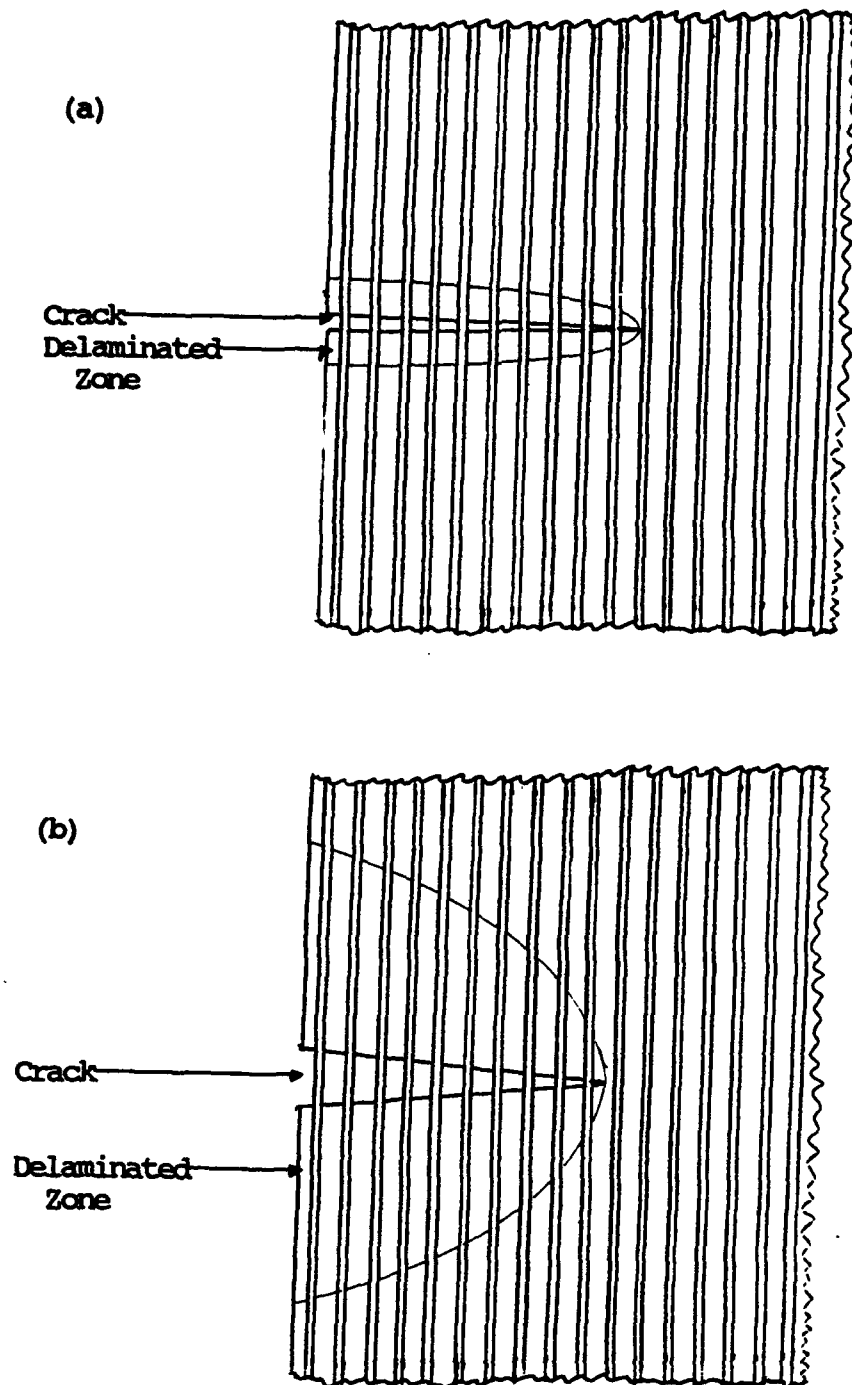


Figure 12. Delamination in Laminates During Fatigue:
 (a) Strong Interlaminar Bond.
 (b) Weak Interlaminar Bond.

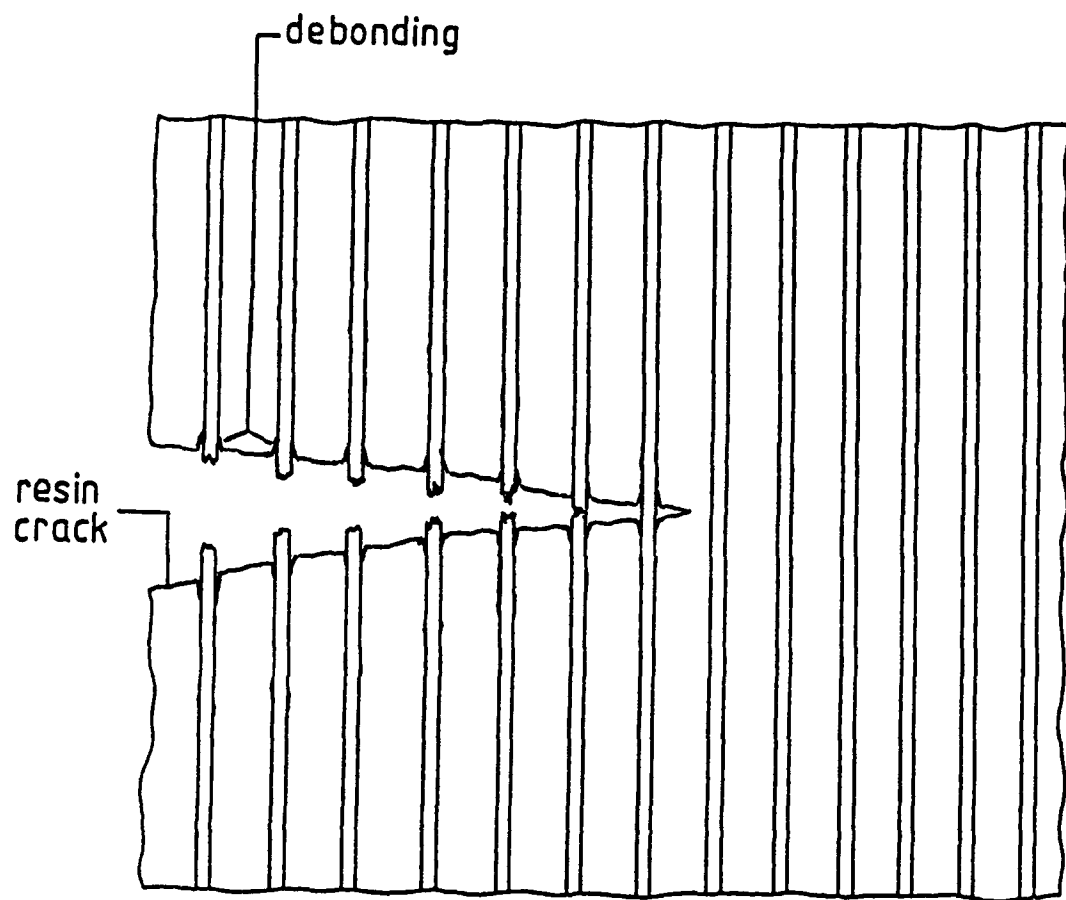


Figure 13. Fiber Failure in a Laminate due to Excessive Bond Strength.
(Adapted from Ref. 3)

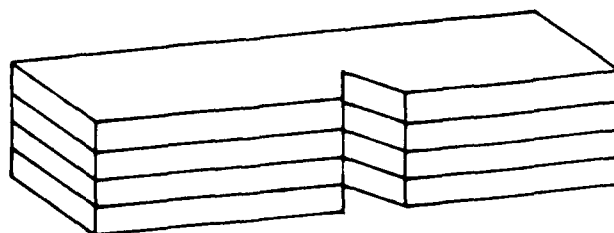


Figure 14. The Crack Divider Principle.^[66]

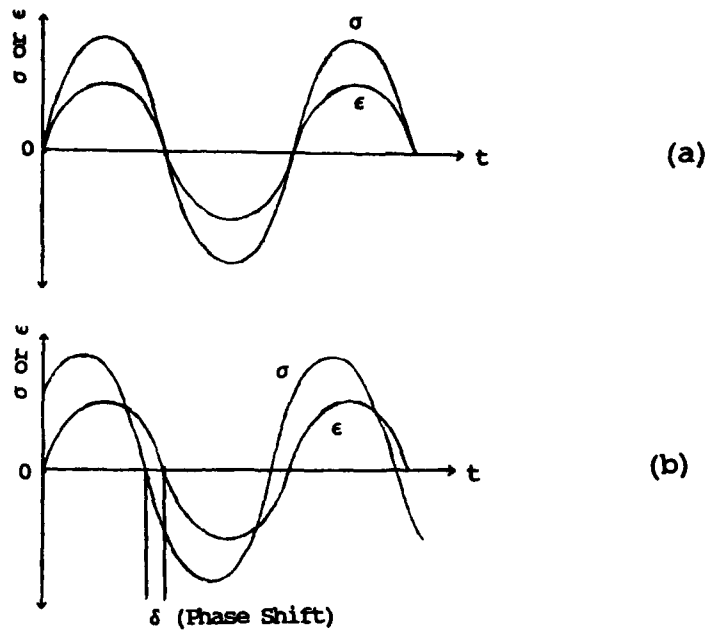


Figure 15. Cyclic Stress-Strain Response:
 (a) Perfectly Elastic Material.
 (b) Viscoelastic Material.

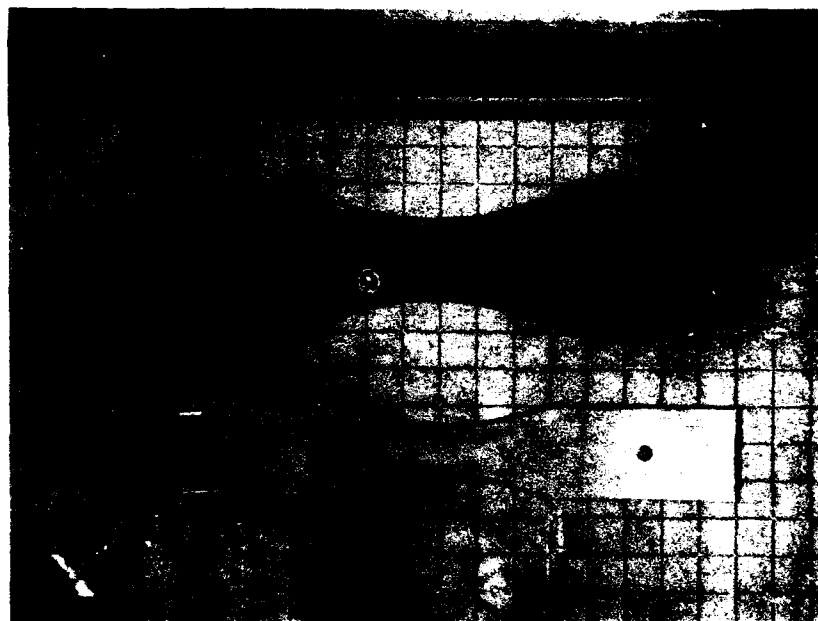
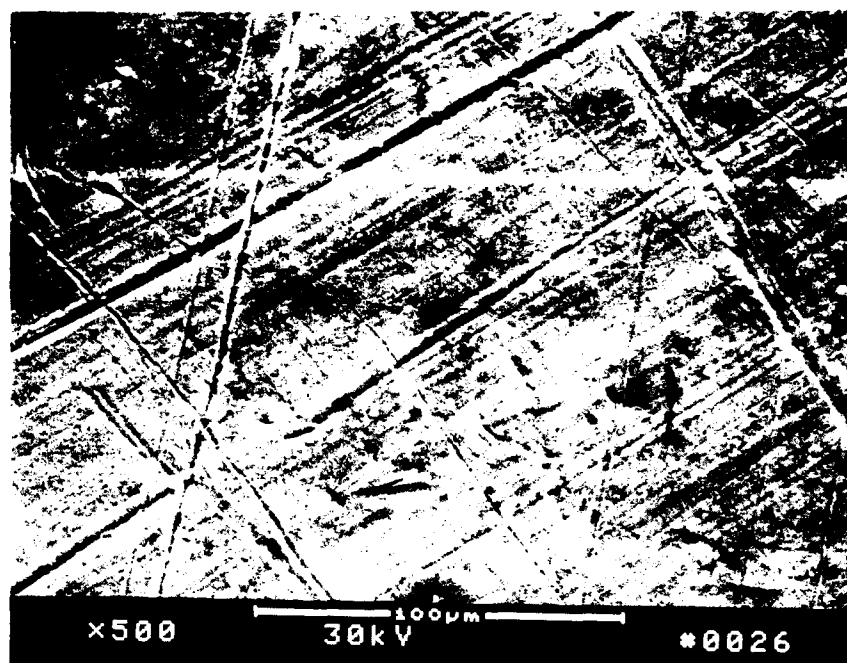
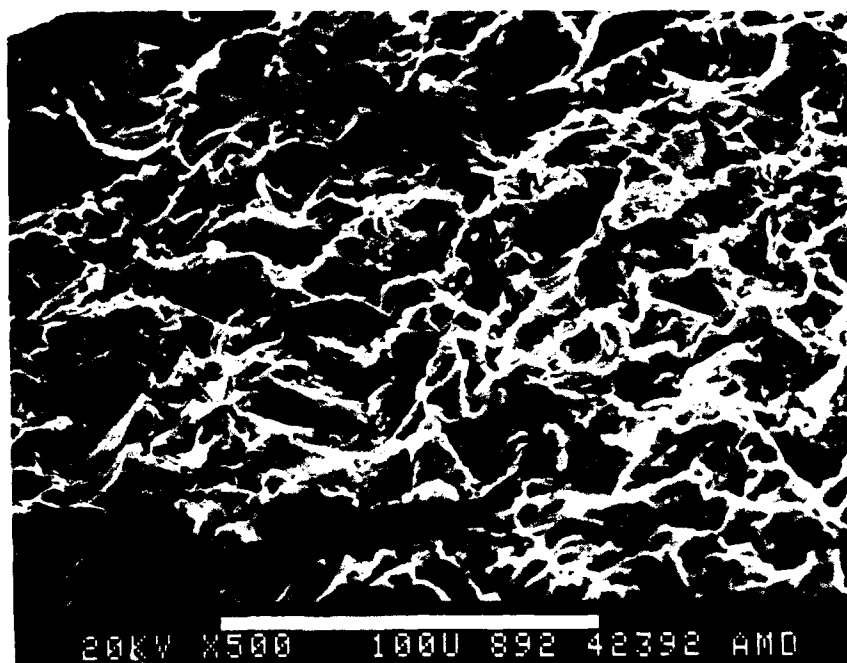


Figure 16. Fatigue Specimens Used for S-N Testing of 8009 Aluminum and 8009/U25 Laminates.



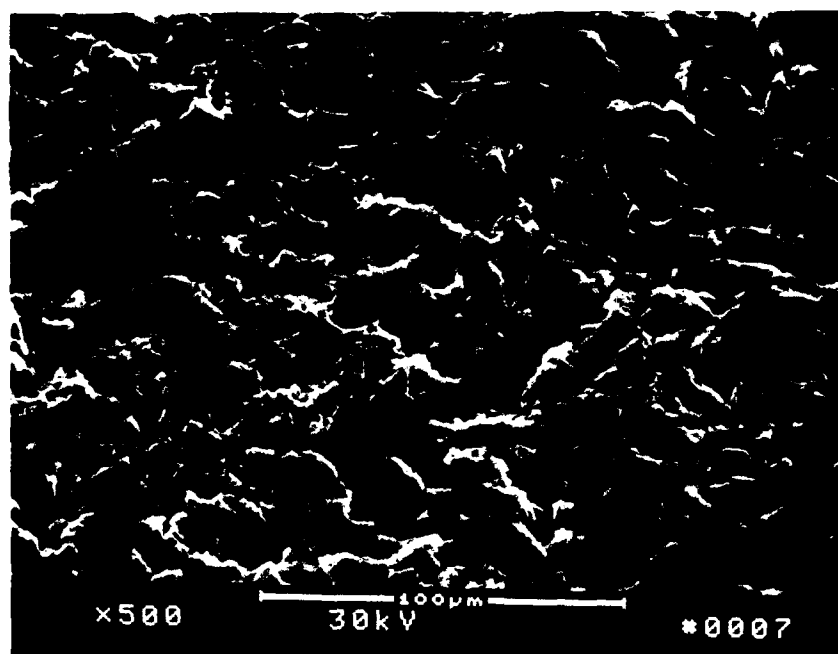
(a)



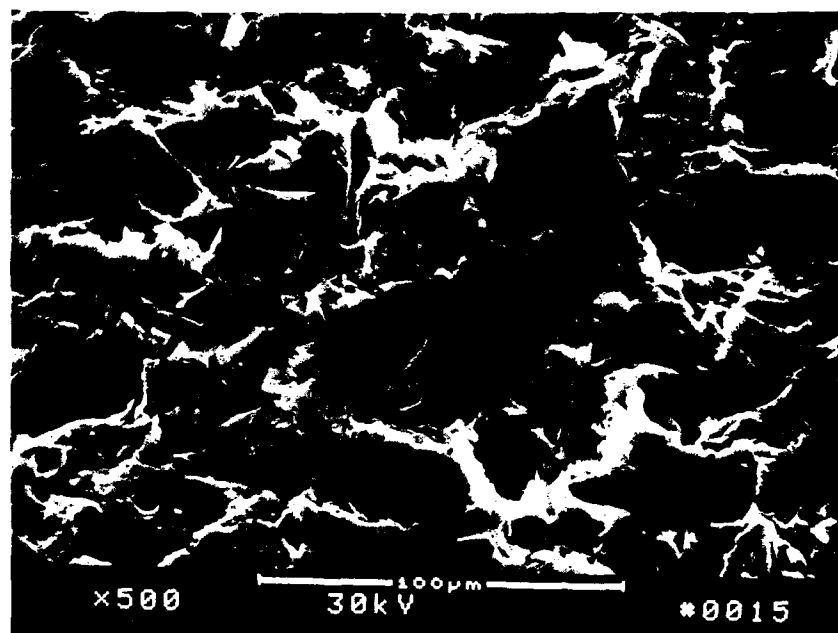
(b)

Figure 17. SEM Images of 2024 Surface Treatments.

- (a) Untreated (UT)
- (b) Dry Alumina Grit Blasted (DA)



(c)

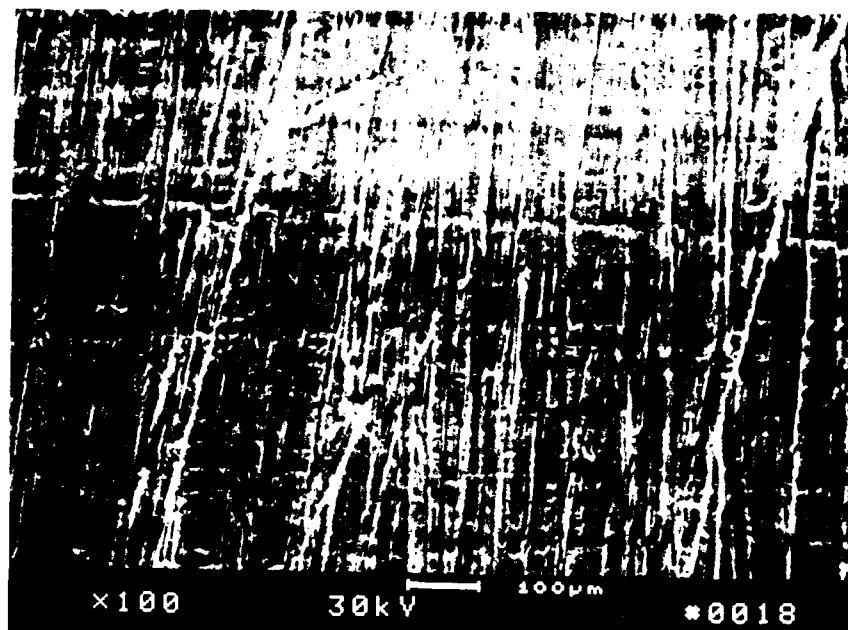


(d)

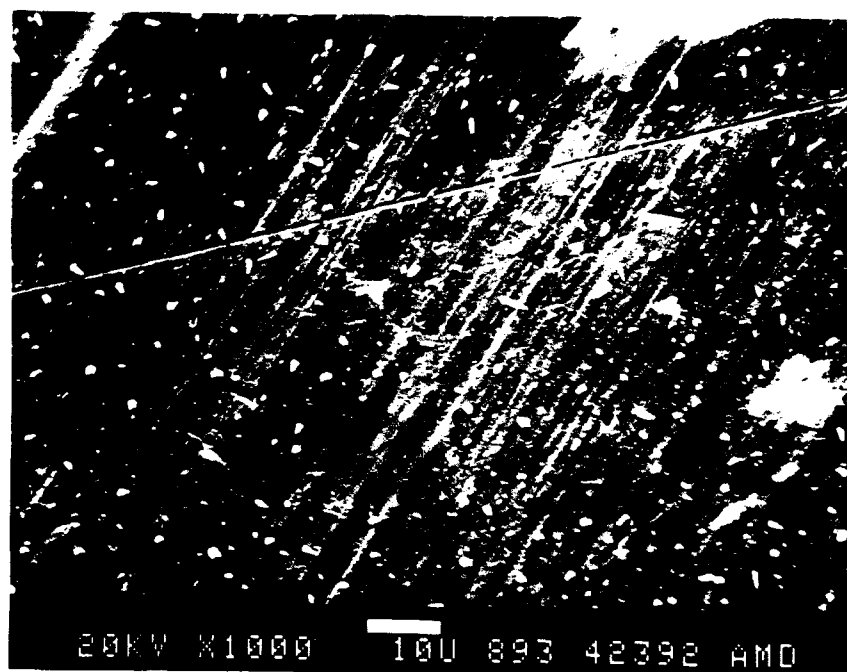
Figure 17 (continued). SEM Images of 2024 Surface Treatments.

(c) Wet Alumina Grit Blasted (WA)

(d) Glass Bead Blasted (GB)



(e)



(f)

Figure 17 (continued). SEM Images of 2024 Surface Treatments.

- (e) Scotch-Brite Abraded (SB)
- (f) Phosphoric Acid Anodized (PA)

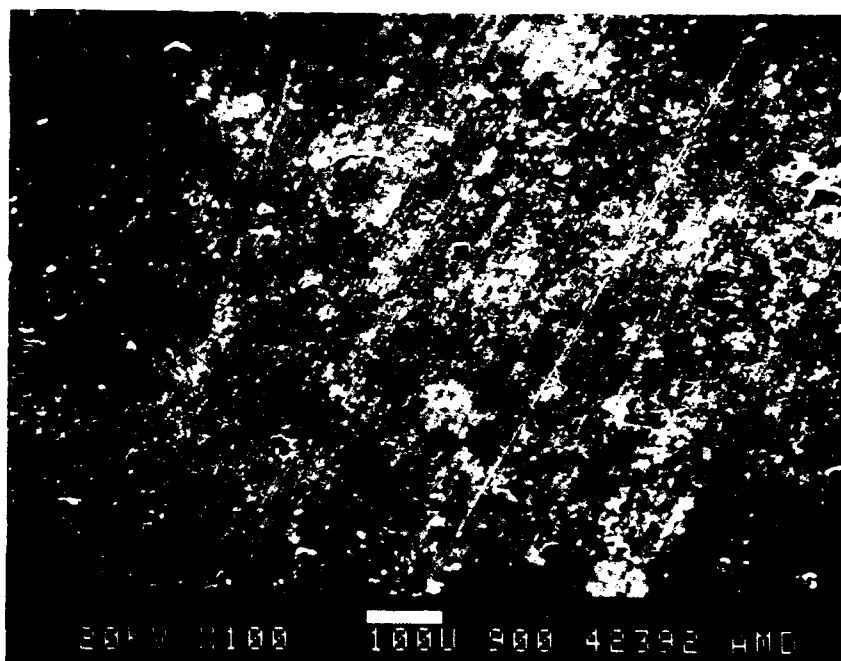
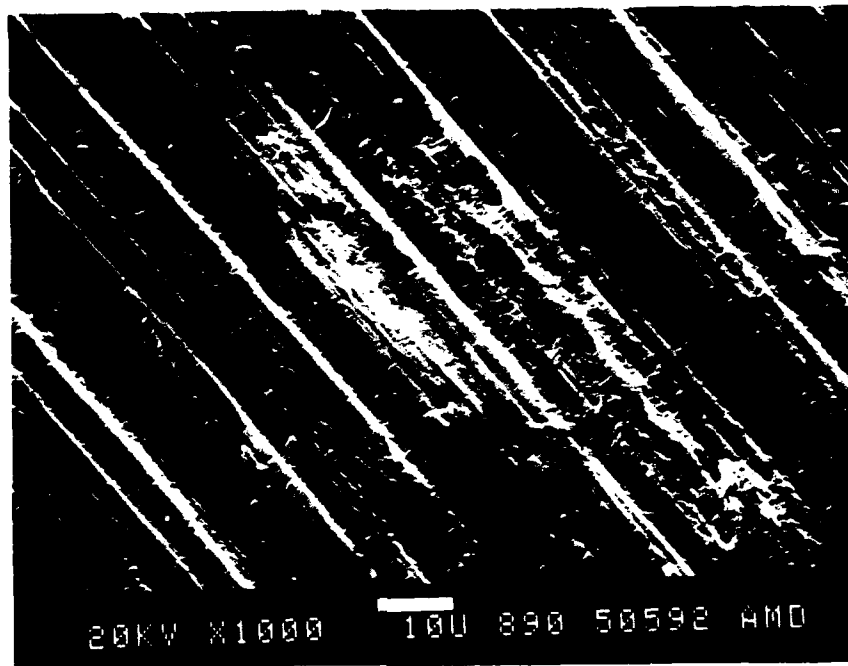
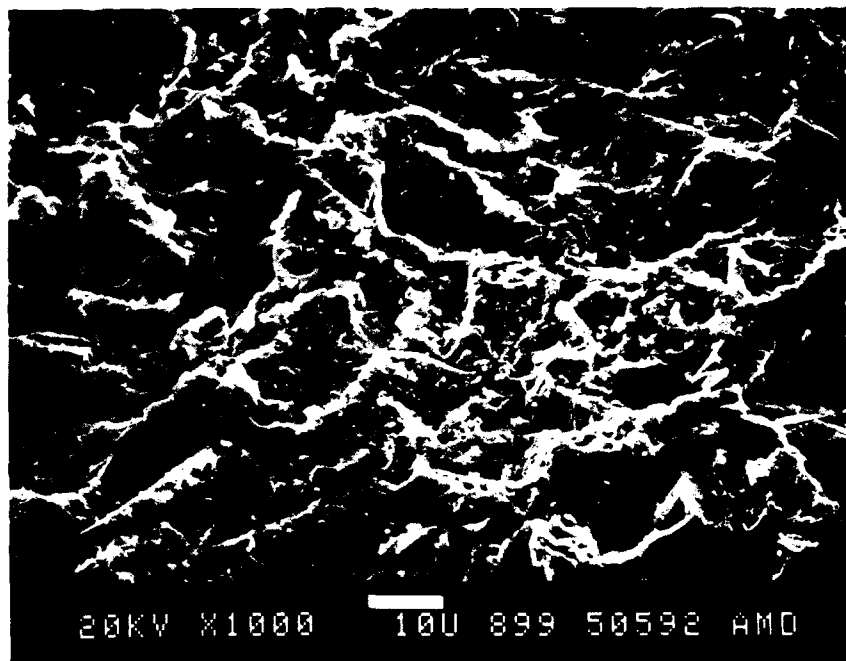


Figure 17 (continued). SEM Images of 2024 Surface Treatments.

(g) Chromic Acid Anodized (CA)



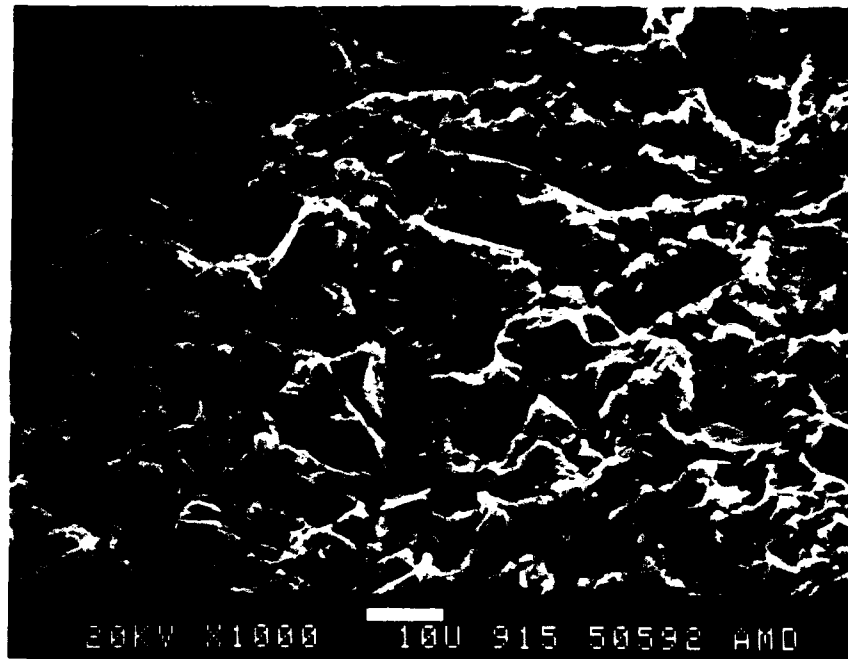
(a)



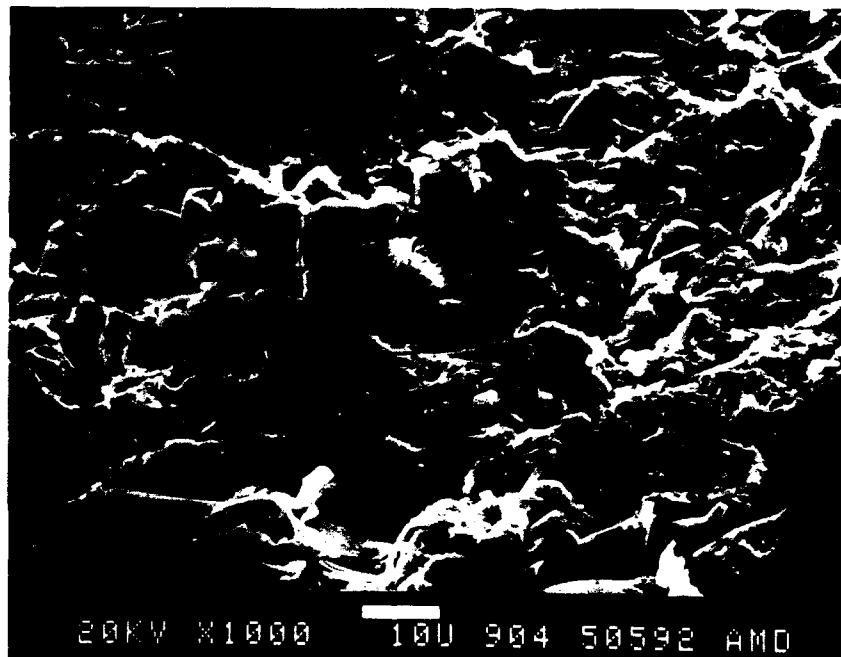
(b)

Figure 18. SEM Images of 8009 Surface Treatments.

- (a) Untreated (UT)
- (b) Dry Alumina Grit Blasted (DA)



(c)



(d)

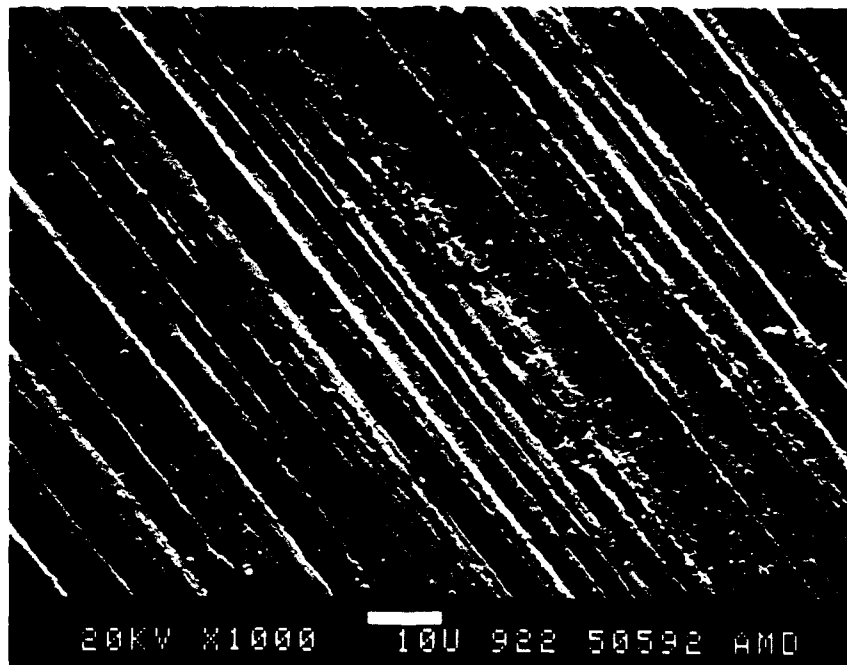
Figure 18 (continued). SEM Images of 8009 Surface Treatments.

(c) Wet Alumina Grit Blasted (WA)

(d) Glass Bead Blasted (GB)



(e)



(f)

Figure 18 (continued). SEM Images of 8009 Surface Treatments.

- (e) Scotch-Brite Abraded (SB)
- (f) Phosphoric Acid Anodized (PA)

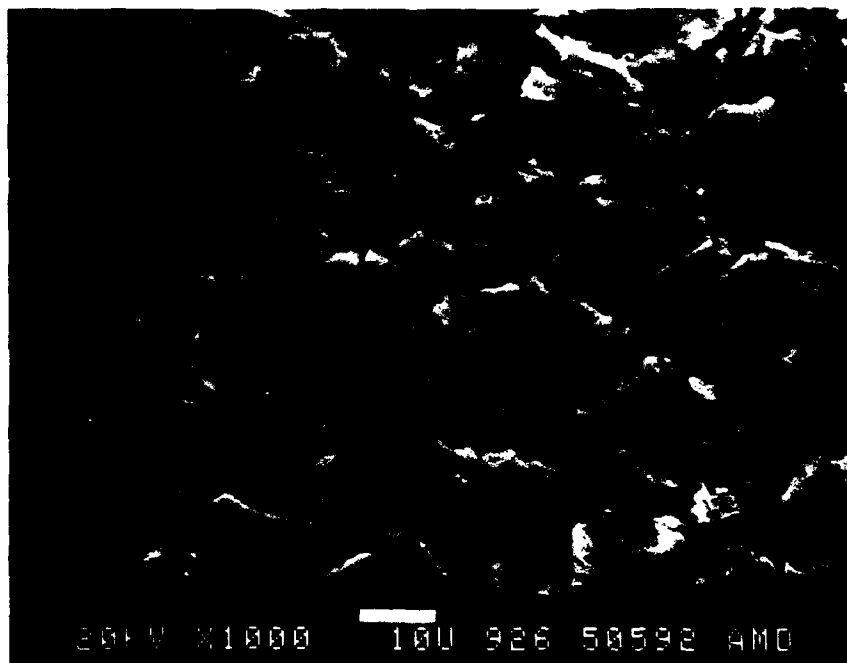


Figure 18 (continued). SEM Images of 8009 Surface Treatments.

(g) Dry Alumina + Phosphoric (DAPA)

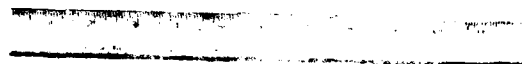


Figure 19. Appearance of a Cured 8009/U25 Laminate Panel (3/2 ply).

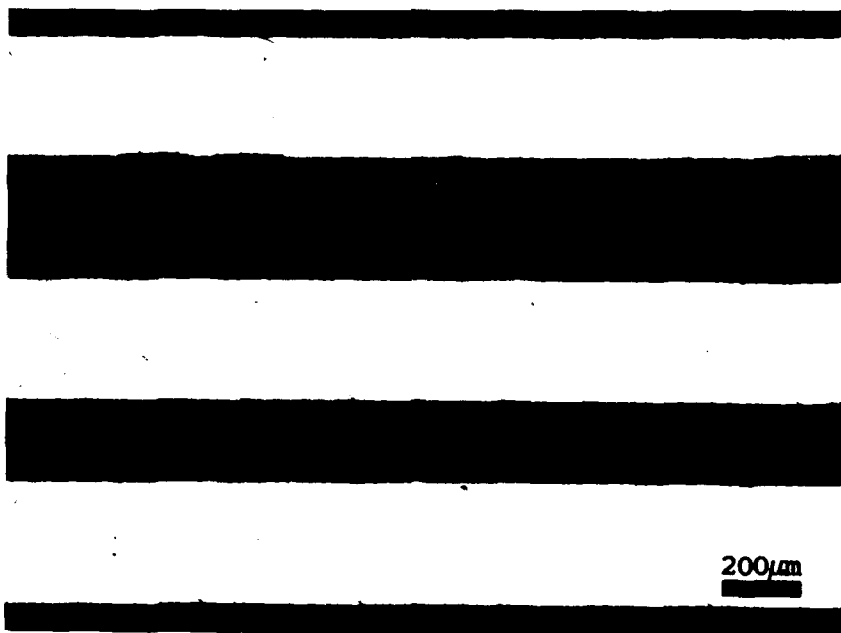


Figure 20. Optical Cross-Section of an 8009/U25 Laminate (3/2 ply, Fiber Direction).



Figure 21. Appearance of a Cured U-25 Composite Panel (5-ply X 0°)

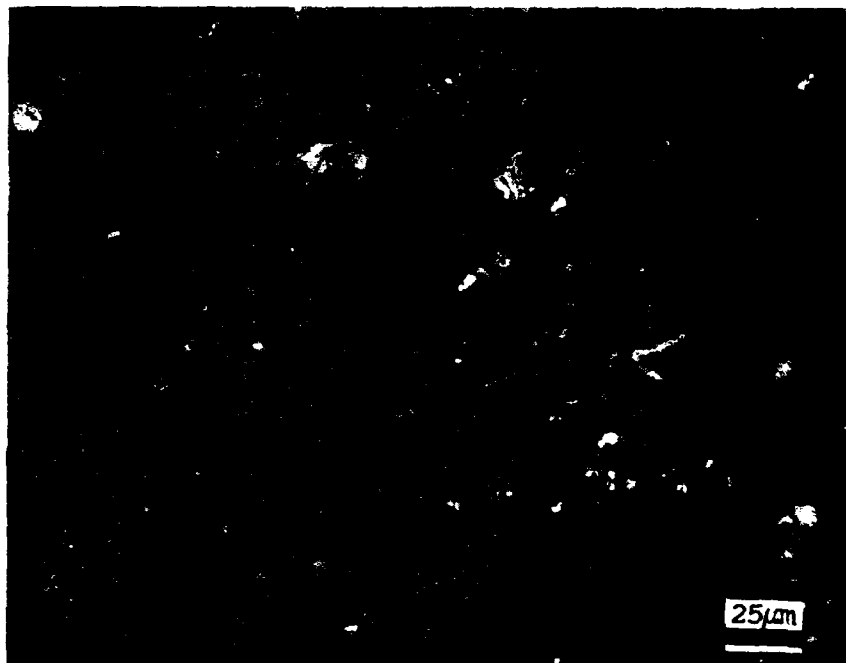


Figure 22. Optical Cross-Section of a U-25 Composite (5-ply X 0°, Fiber Direction).

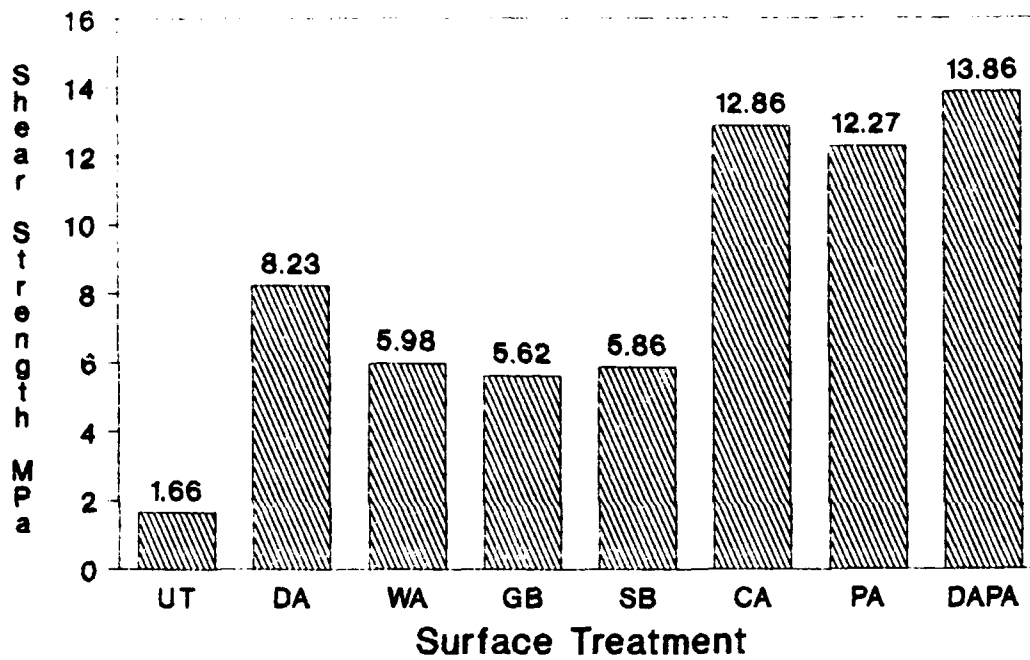


Figure 23. Effects of Surface Treatment on Shear Strength (Dry Condition).

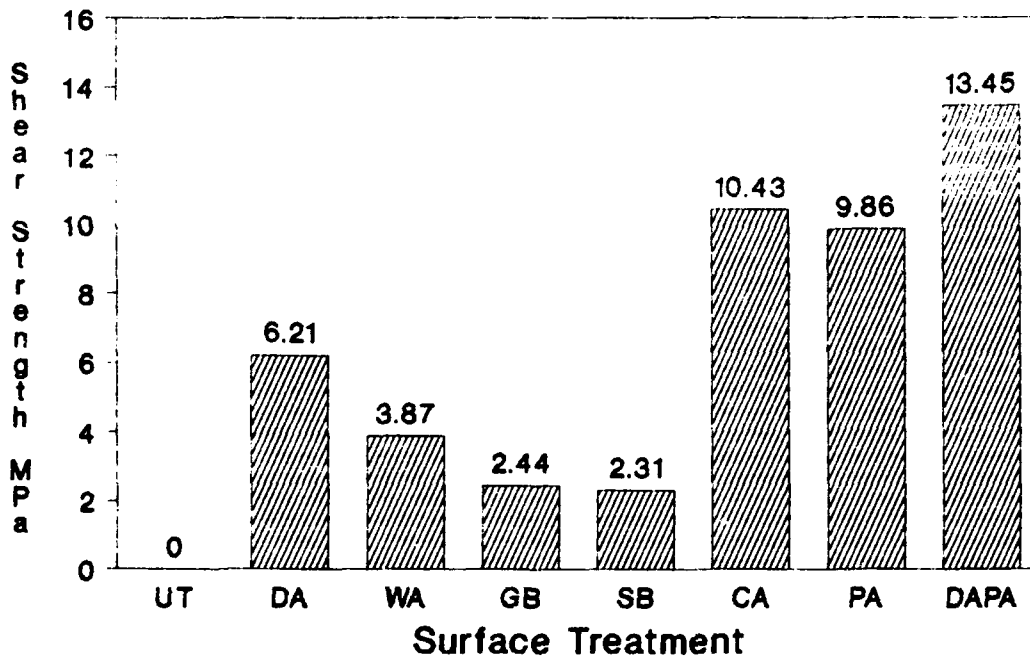


Figure 24. Effects of Surface Treatment on Shear Strength (Wet Condition)

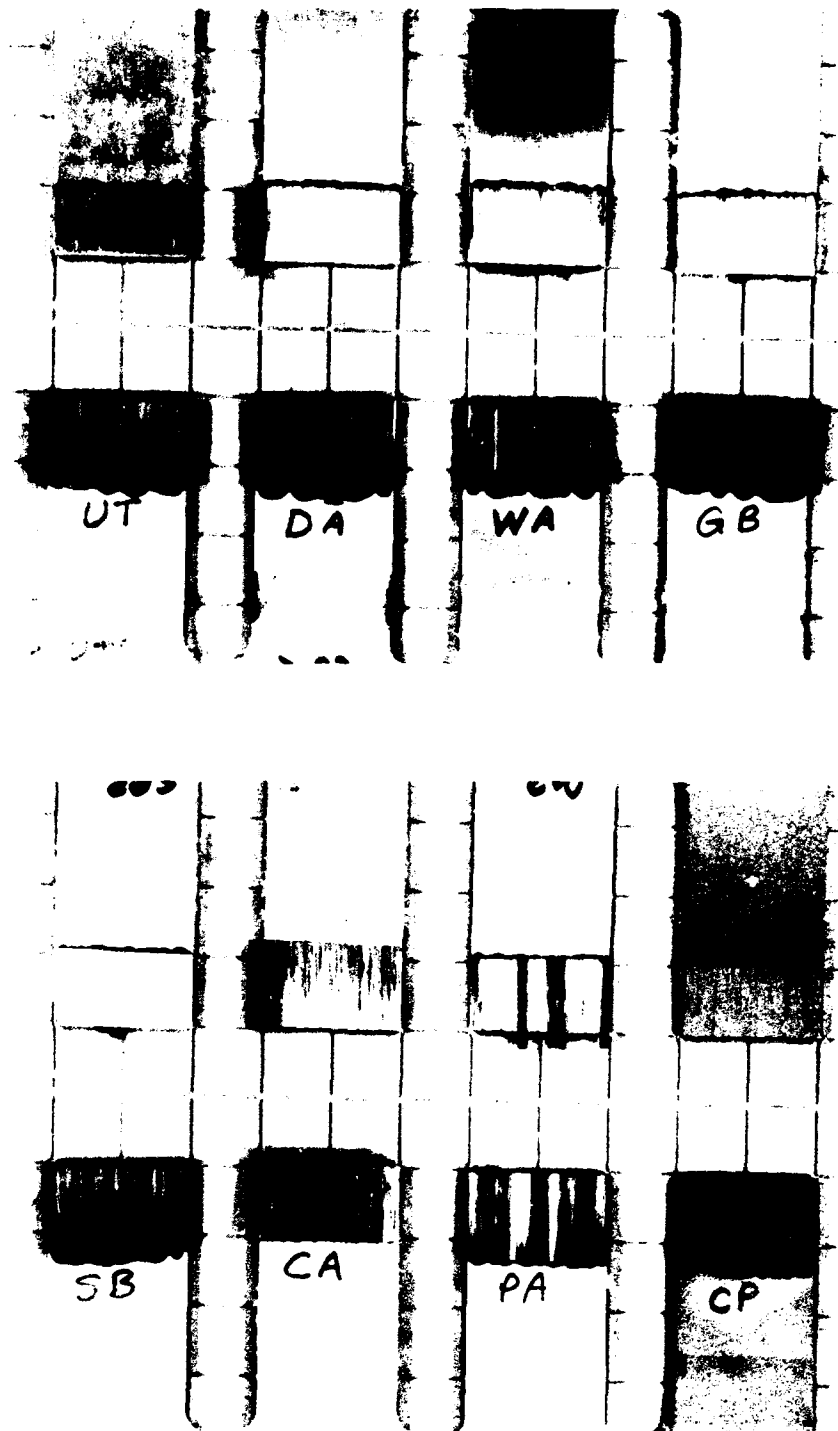
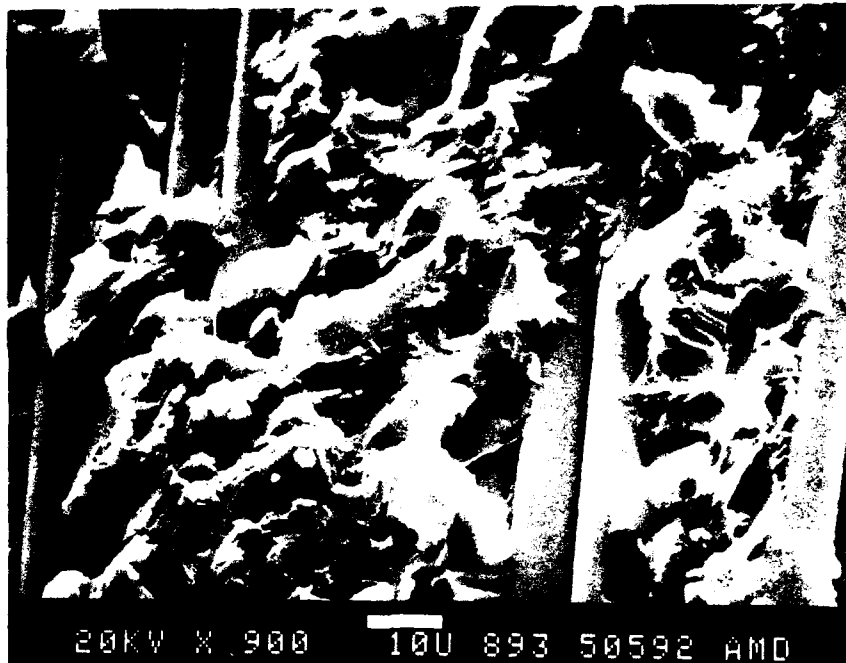


Figure 25. Macroscopic Photographs of 2024/U25 Shear Failures.



(a)



(b)

Figure 26. SEM Images of 2024/U25 Shear Failures.

- (a) Dry Alumina Blasted (DA)
- (b) Chromic Acid Anodized (CA)



(c)



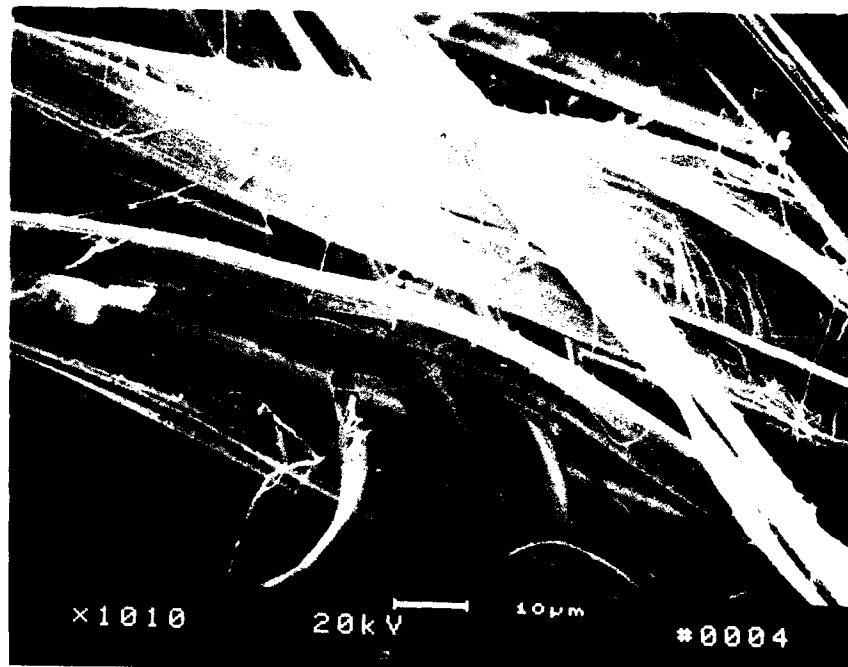
(d)

Figure 26. SEM Images of 2024/U25 Shear Failures.

- (c) Phosphoric Acid Anodized (PA)
- (d) Dry Alumina + Phosphoric (DAPA)



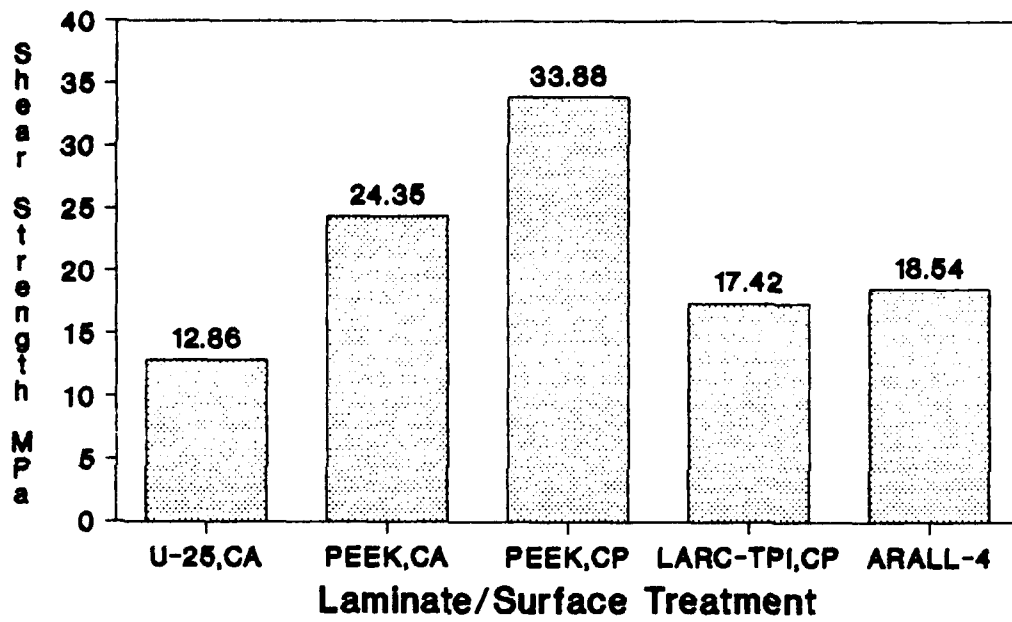
(a)



(b)

Figure 27. ARALL-4 Shear Failures.

- (a) Macroscopic
- (b) SEM Image



CA = Chromic Acid Anodized.
 CP = Anodized + BR35-Primed.

Figure 28. Shear Strength of Various Laminates.

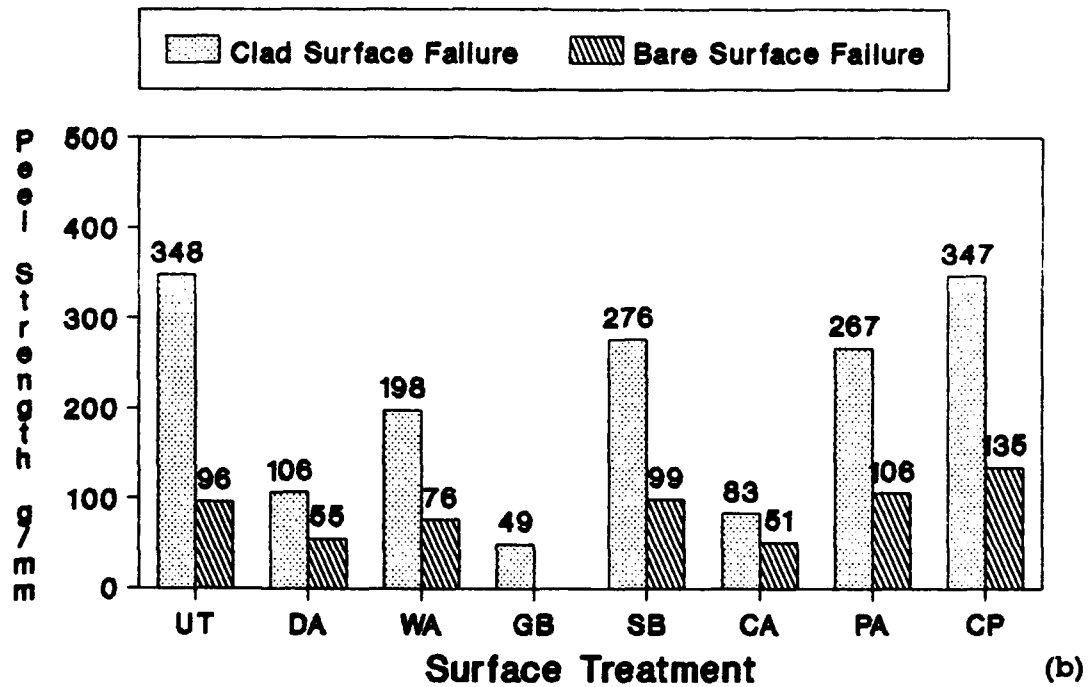
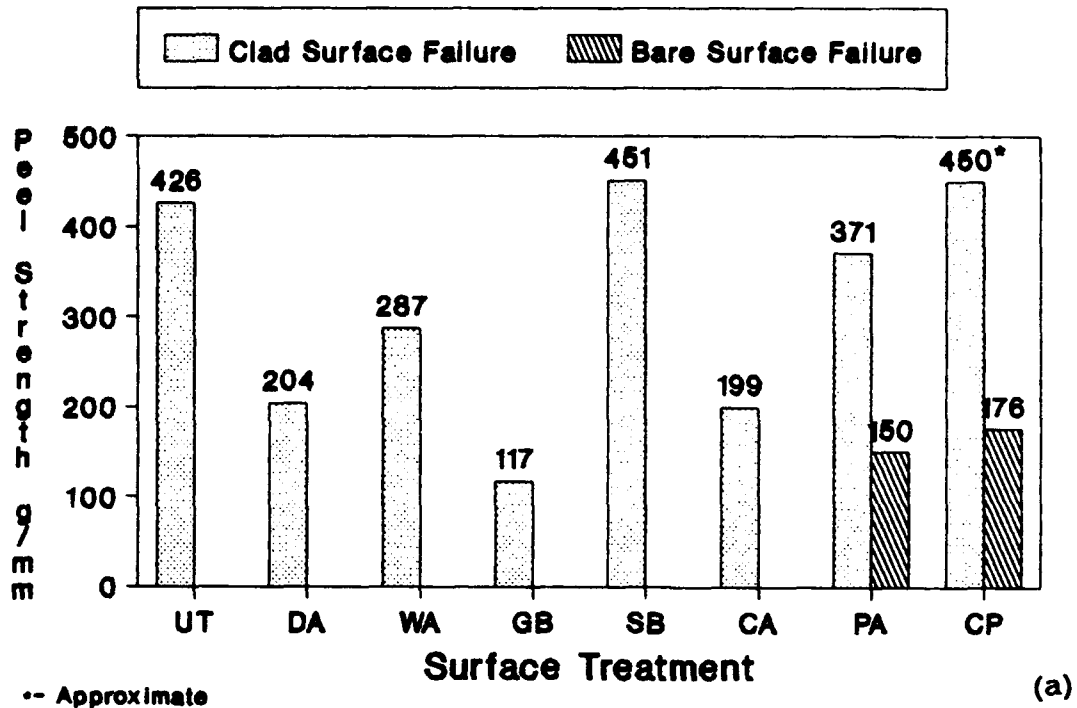
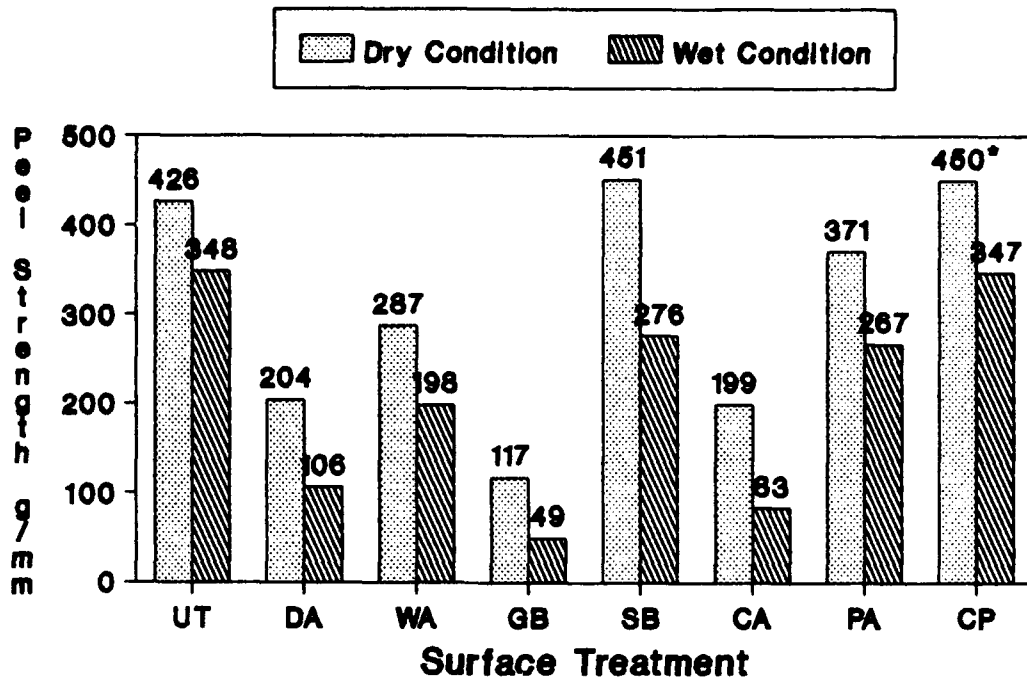


Figure 29. Peel Strength of 2024/U25 Laminates (Incorrectly Processed).
 (a) Clad vs. Bare 2024, Dry Condition.
 (b) Clad vs. Bare 2024, Wet Condition.



-- Estimated

Figure 30. Wet vs. Dry Peel Strength of 2024/U25 Laminates (Incorrectly Processed, Clad 2024).

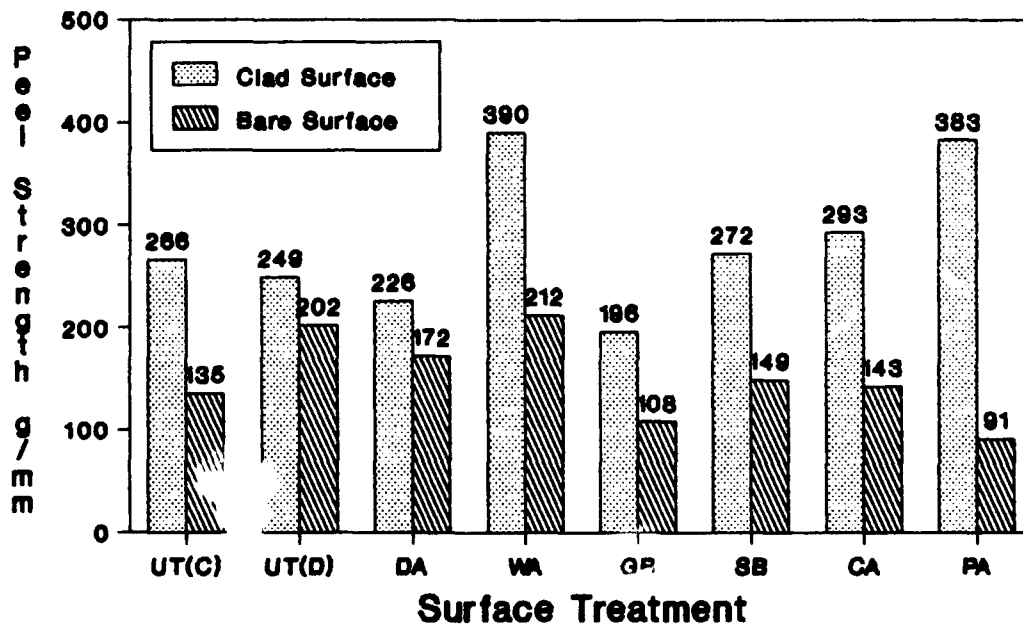
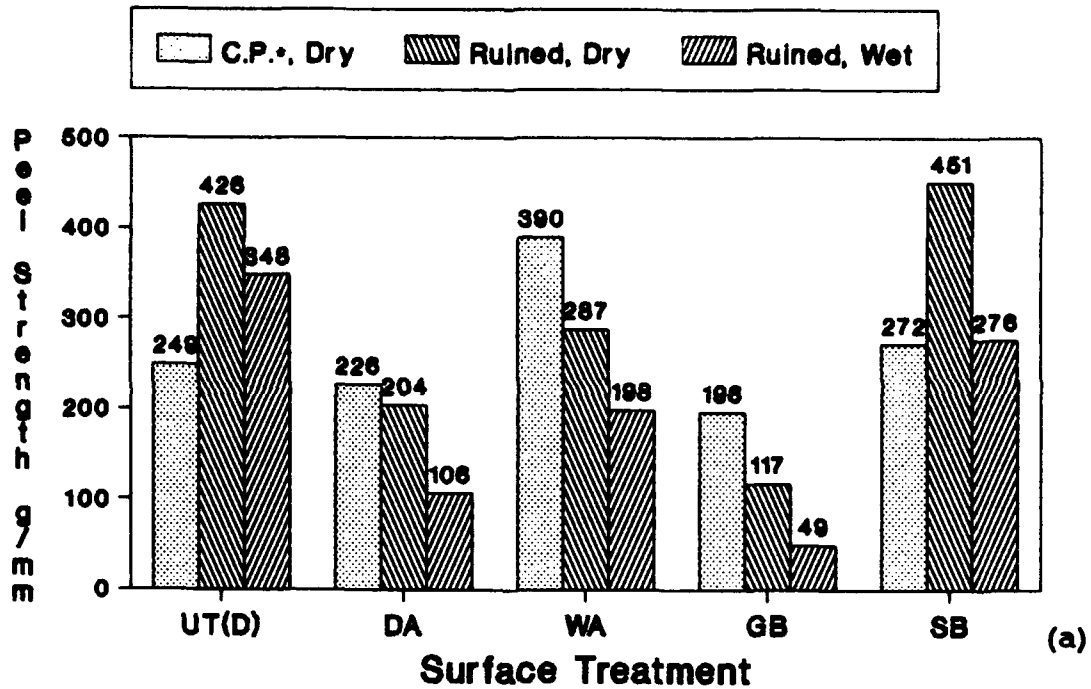
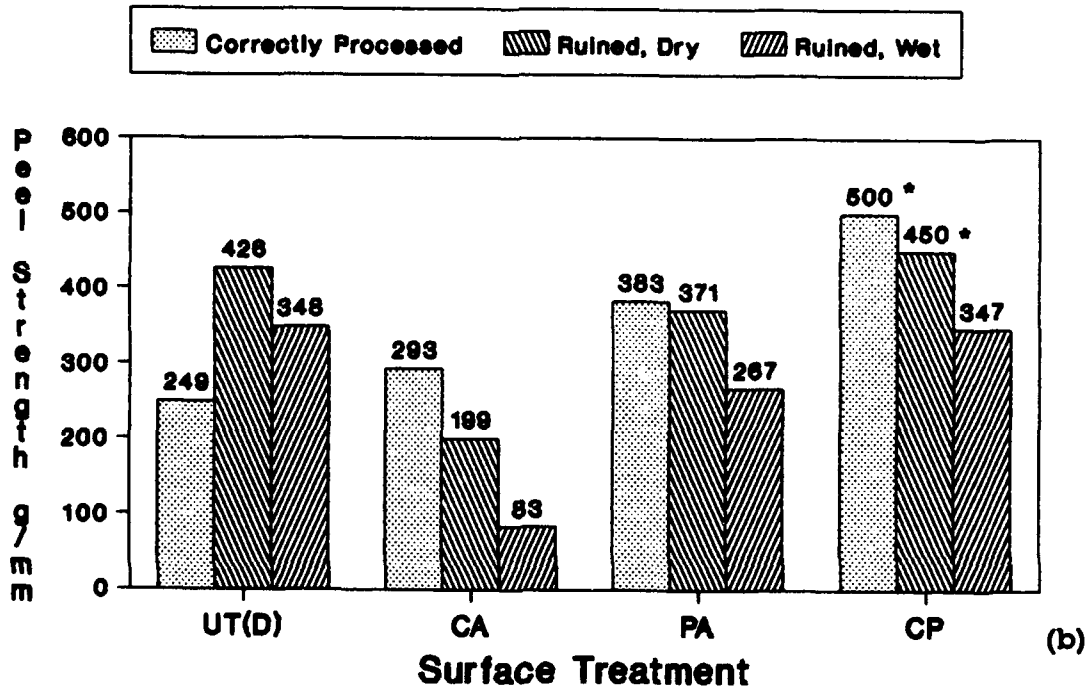


Figure 31. Effects of Surface Treatment on Peel Strength of 2024/U25 Laminates (Correctly Processed, Dry Condition)



• - Correctly Processed



-- Estimated

Figure 32. Effects of Moisture and Processing on Peel Strength of 2024/U25 Laminates (Clad 2024)

- (a) Mechanical Surface Treatments
- (b) Chemical Surface Treatments

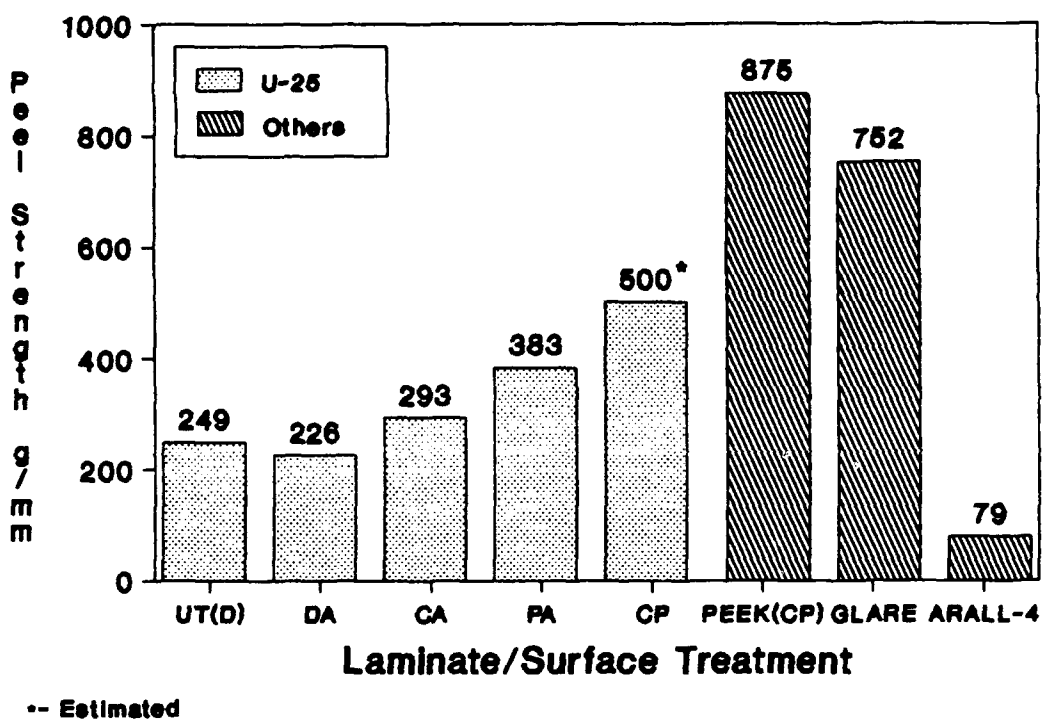
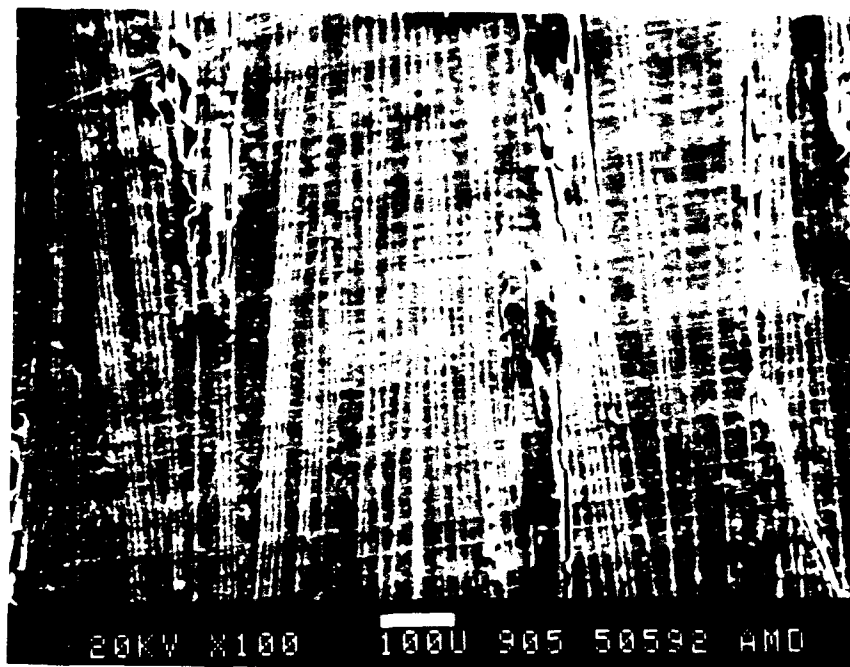
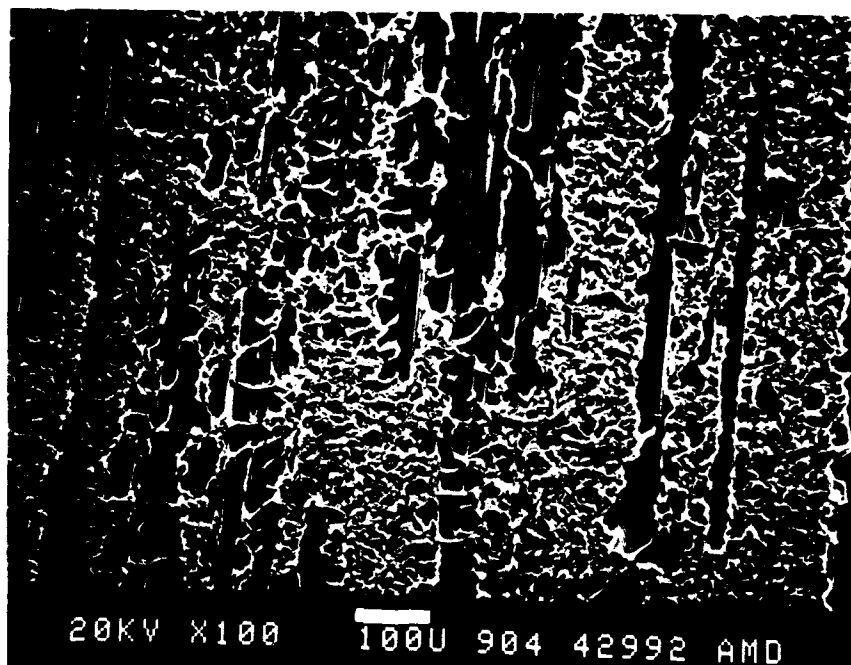


Figure 33. Peel Strength of Various Laminates.



(a)



(b)

Figure 34. SEM Images of 2024/U25 Peel Failures
(Correctly Processed).

(a) UT

(b) DA

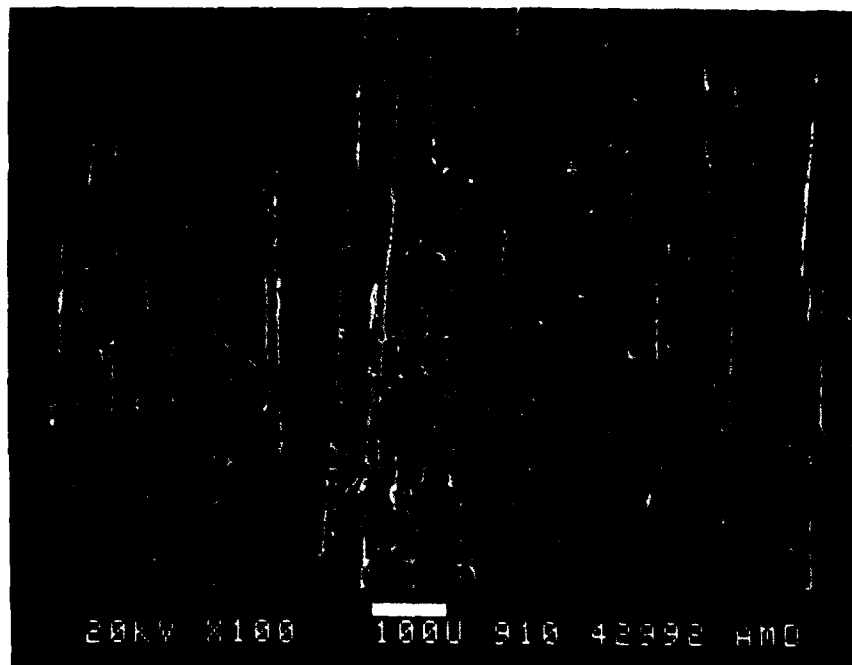


Figure 34 (c). SEM Images of 2024/U25 PA Peel Failures
(Correctly Processed).



(d)



(e)

Figure 35. SEM Images of ARALL-4 and Glare Peel Failures (Correctly Processed).

(d) ARALL-4

(e) Glare

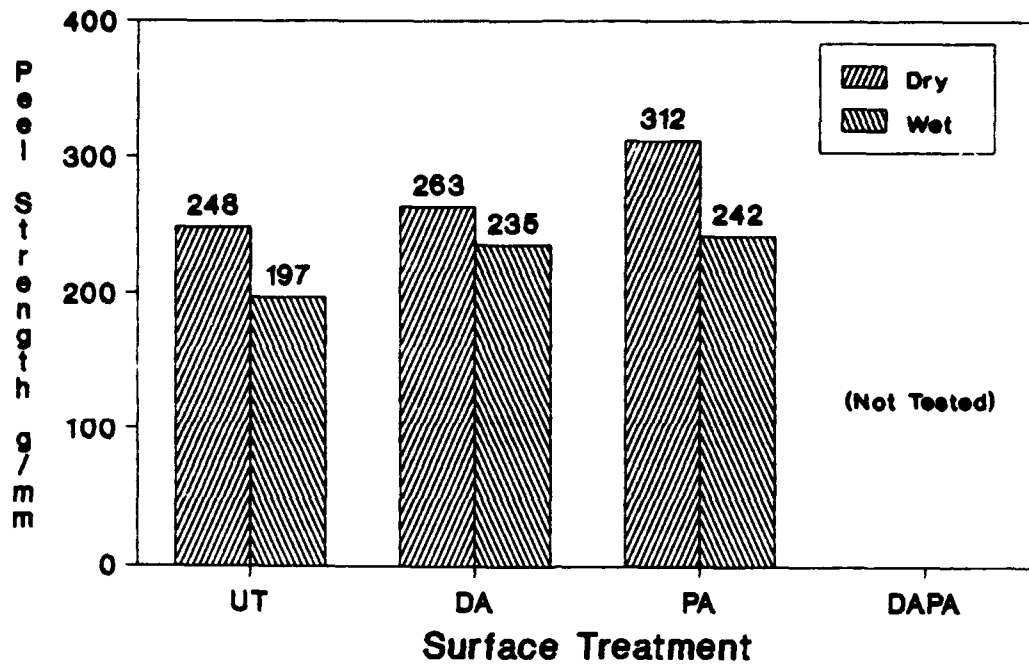


Figure 36. Peel Strength of 8009/U25 Laminates.

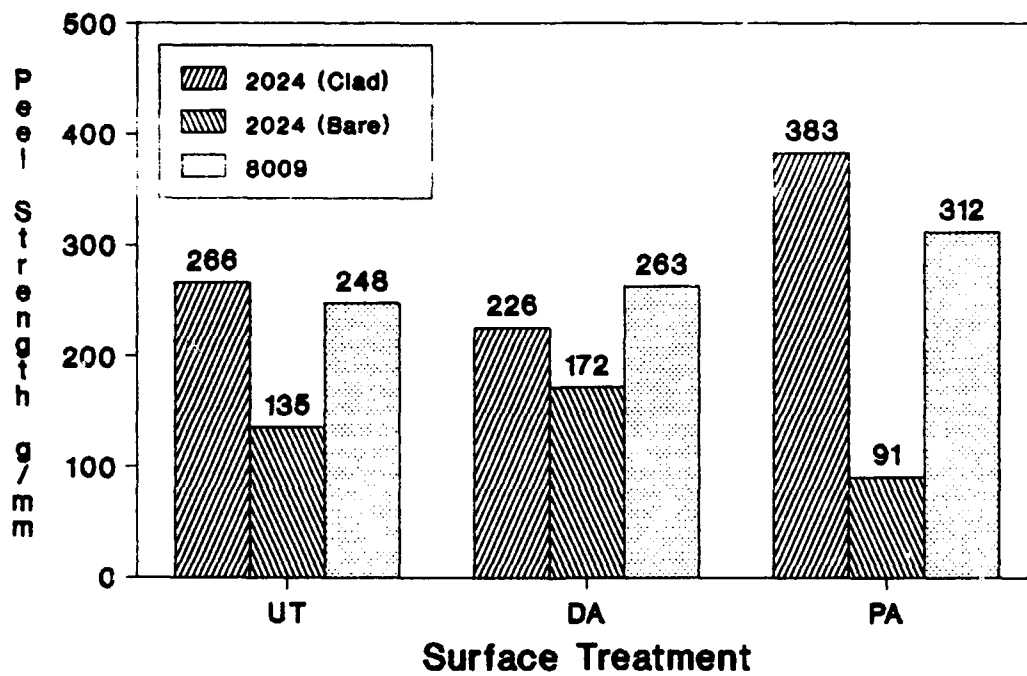
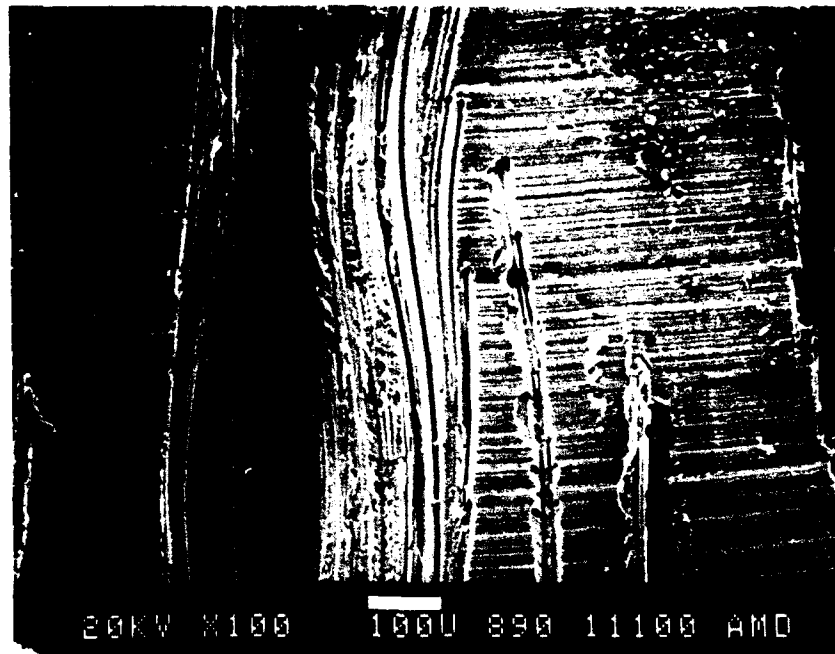


Figure 37. Peel Strength of 8009/U25 vs. 2024/U25 Laminates.



(a)



(b)

Figure 38. SEM Images of 8009/U25 Peel Failures.

(a) UT

(b) DA

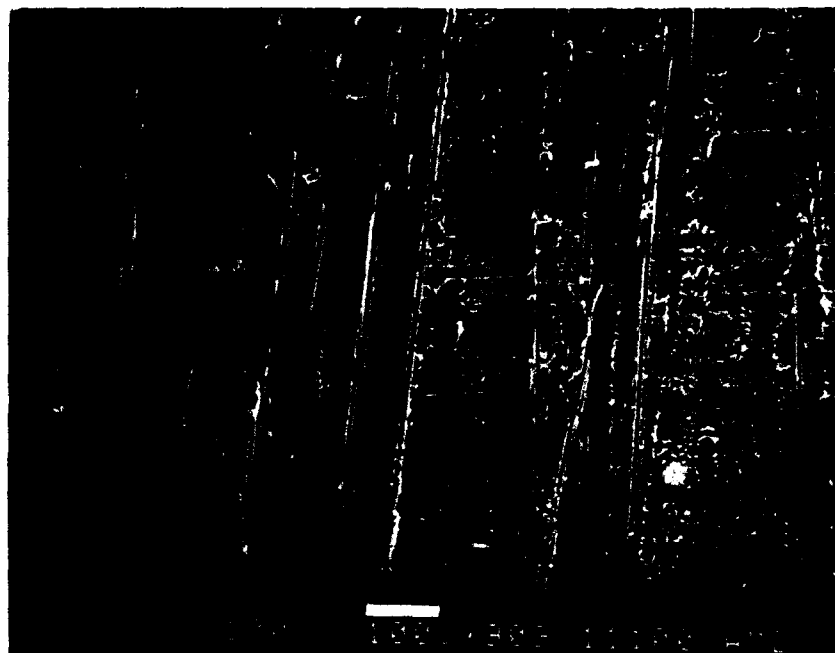


Figure 38(c). SEM Images of 8009/U25 Peel Failures. (PA)

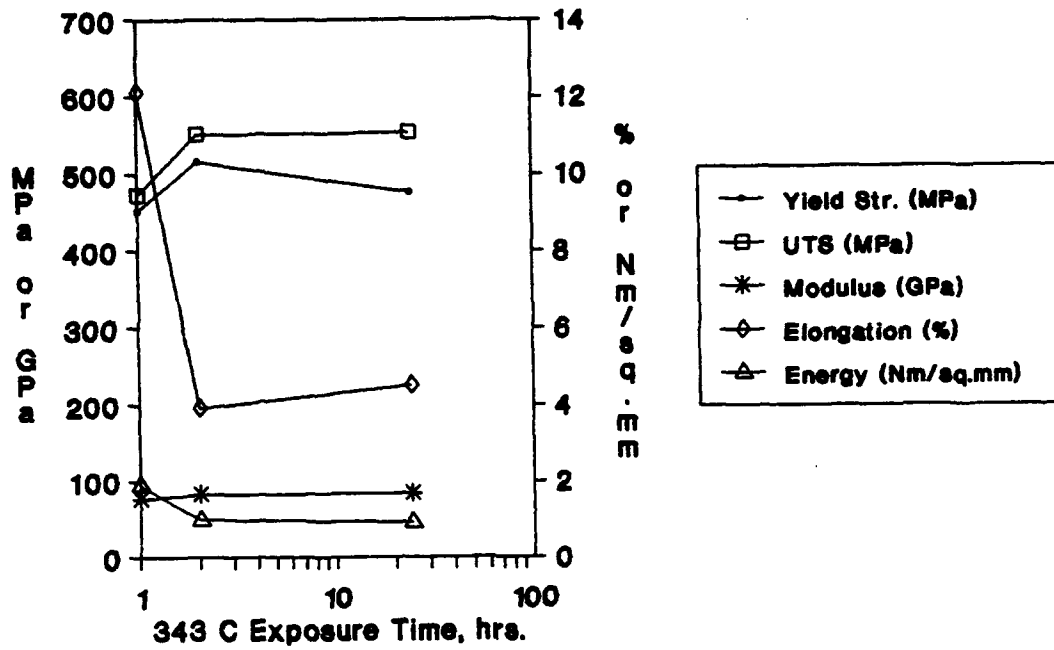


Figure 39. Tensile Properties of 8009 Aluminum as a Function of 343°C Annealing Time.

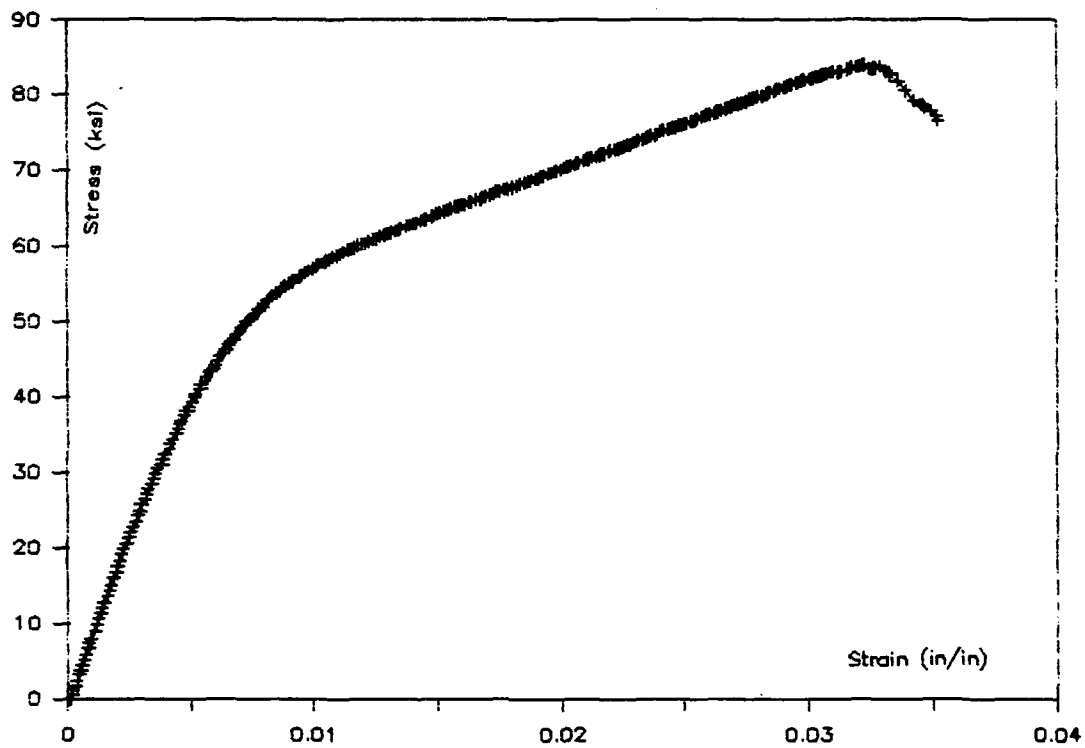


Figure 40. Stress-Strain Diagram for 8009/U25 Laminates.

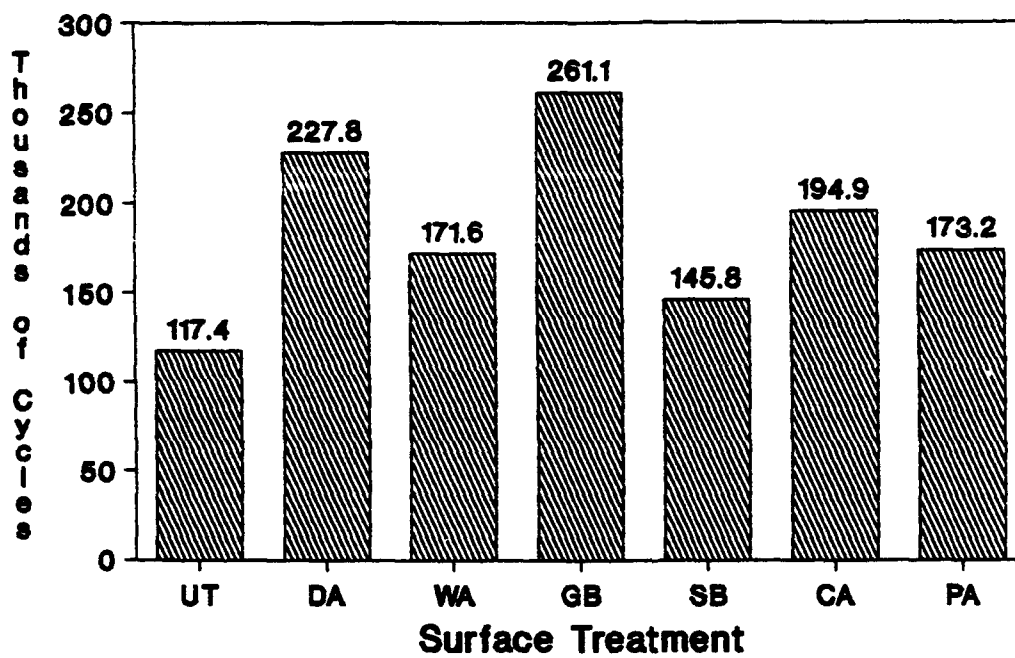


Figure 41. Effects of Surface Treatment on the Fatigue Life of 2024.

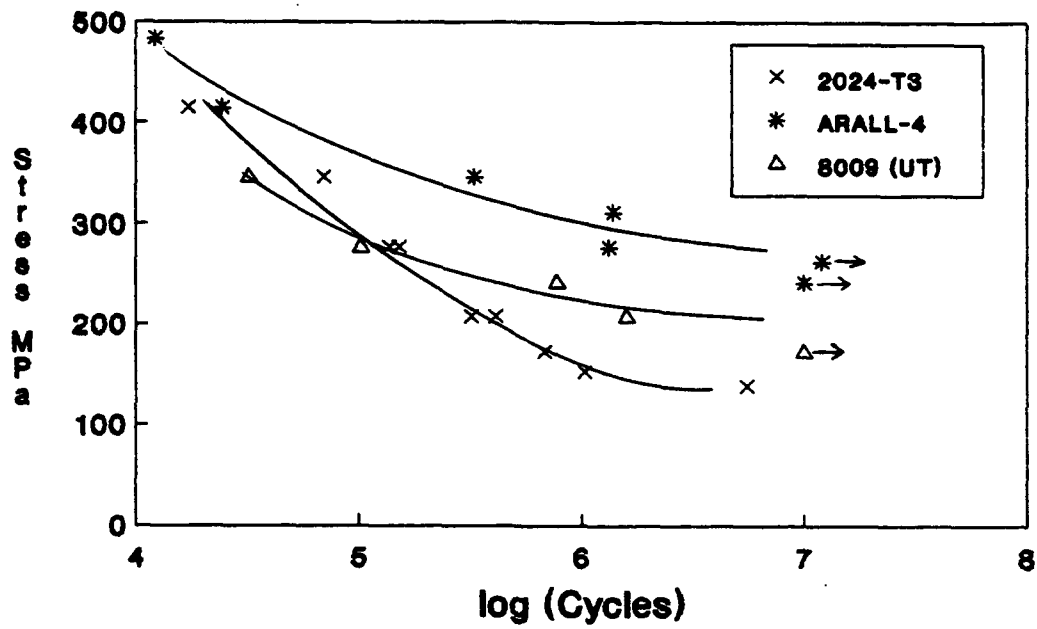


Figure 42. S/N curves for 2024 and 8009 Aluminum.

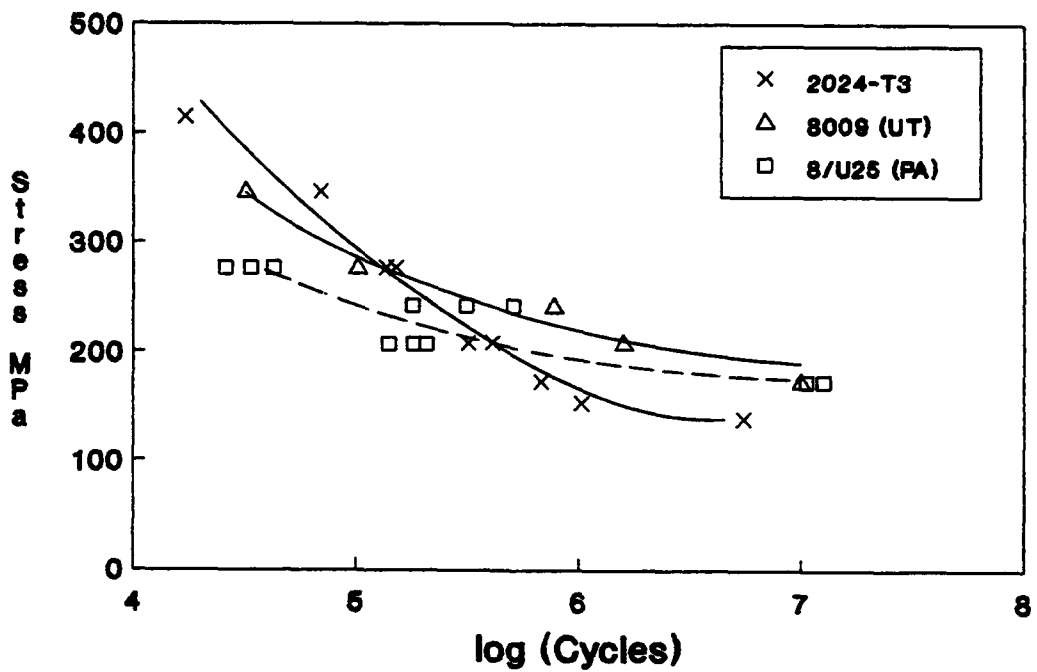


Figure 43. S/N Curves for 8009/U25 Laminates and 8009 Aluminum.

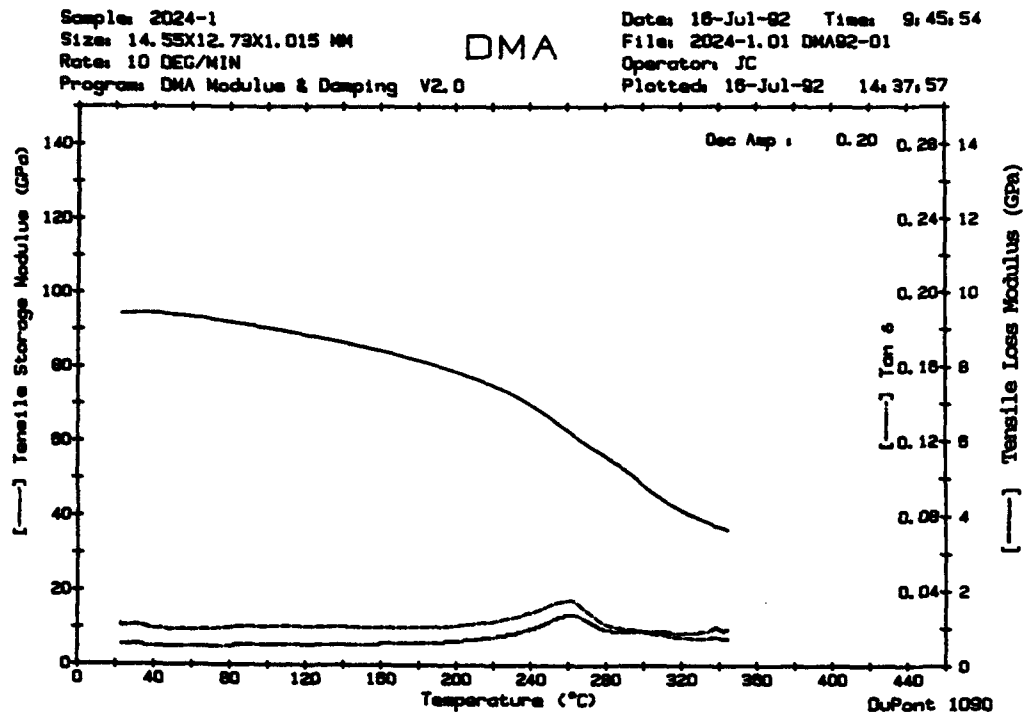


Figure 44. DMA Plot for 2024 Aluminum.

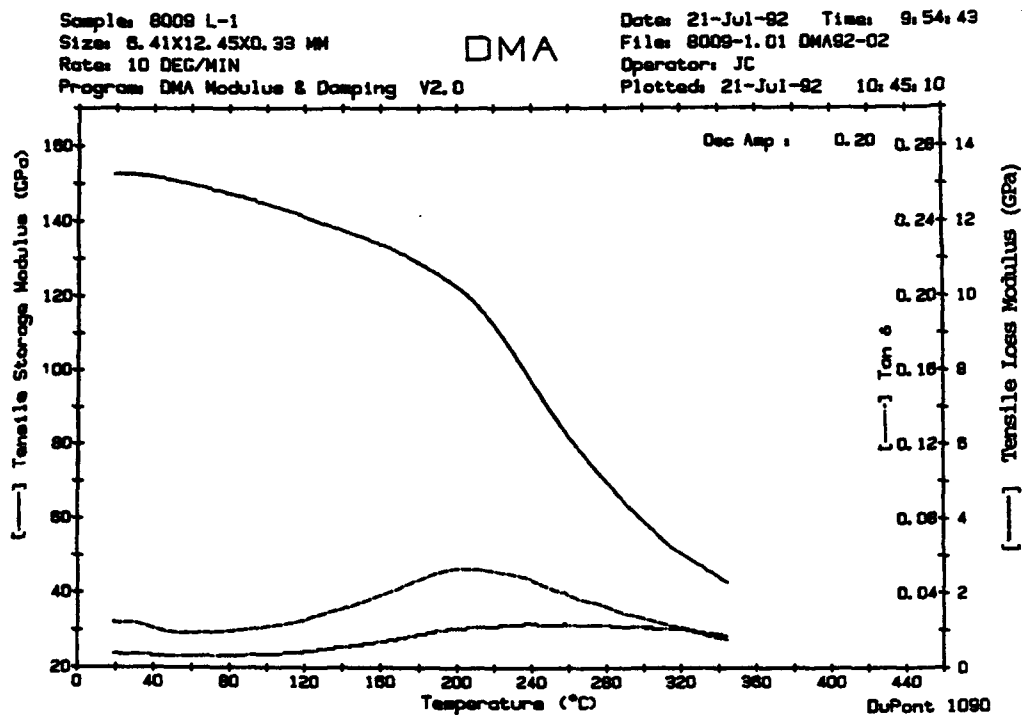


Figure 45. DMA Plot for 8009 Aluminum.

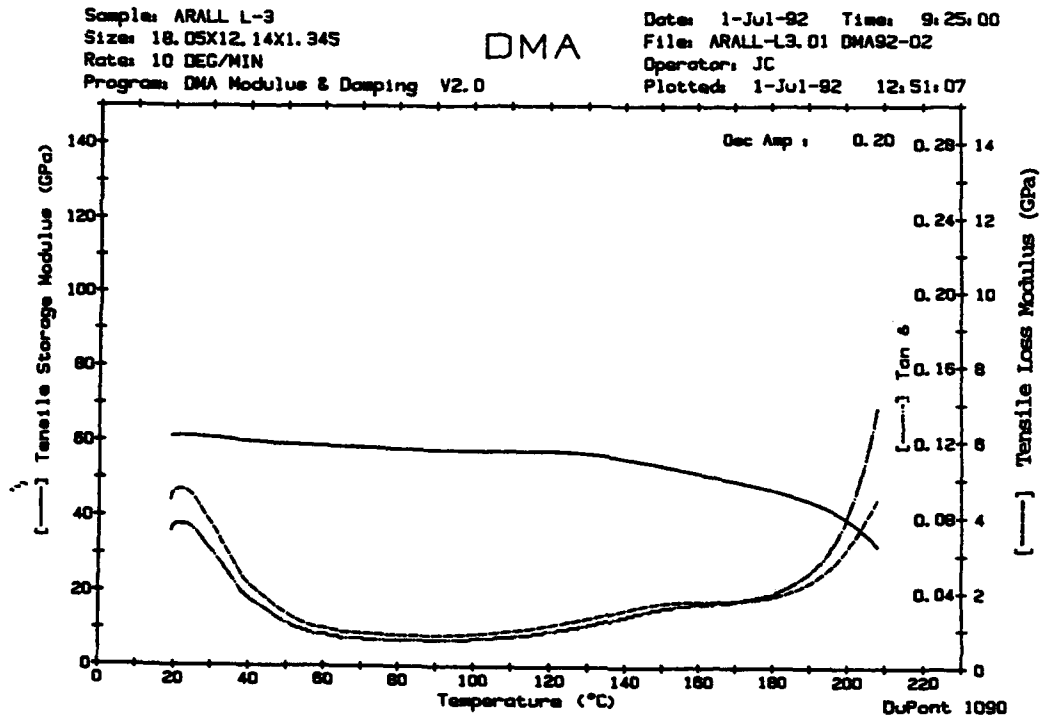


Figure 46. DMA Plot for ARALL-4 Laminate.

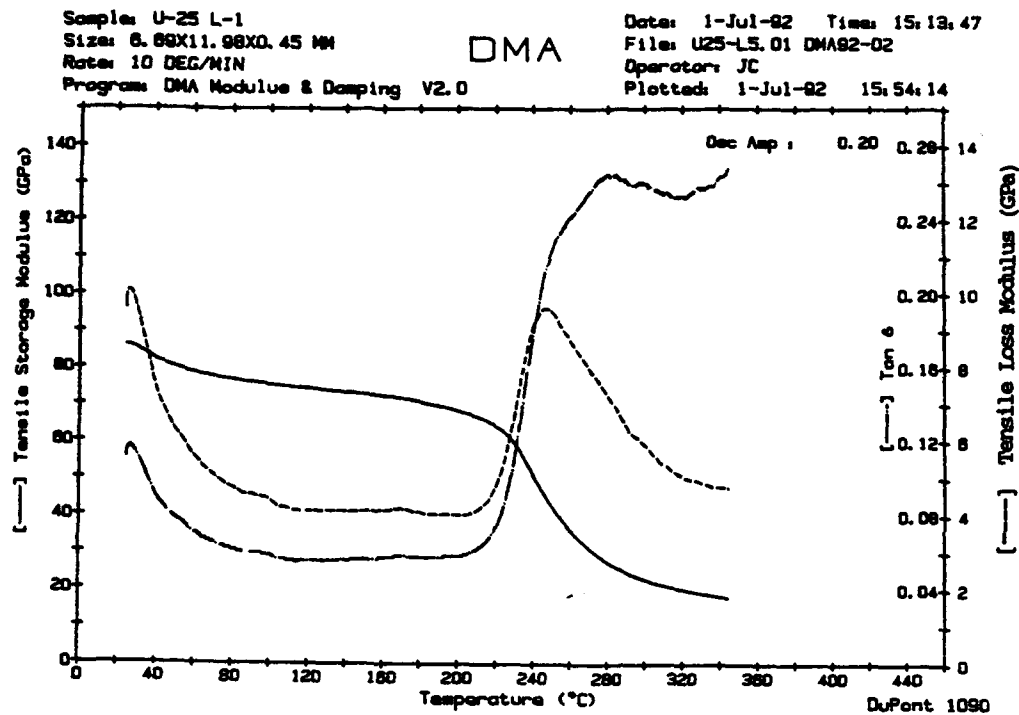


Figure 47. DMA Plot for U-25 Composite (Dry Condition).

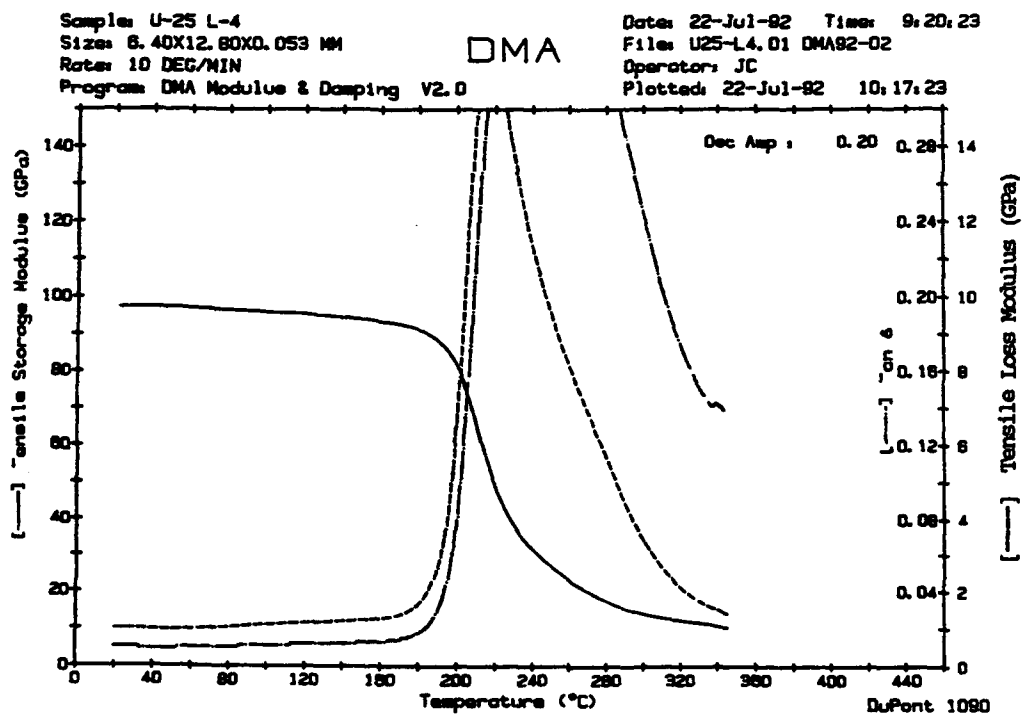


Figure 48. DMA Plot for U-25 Composite (Wet Condition).

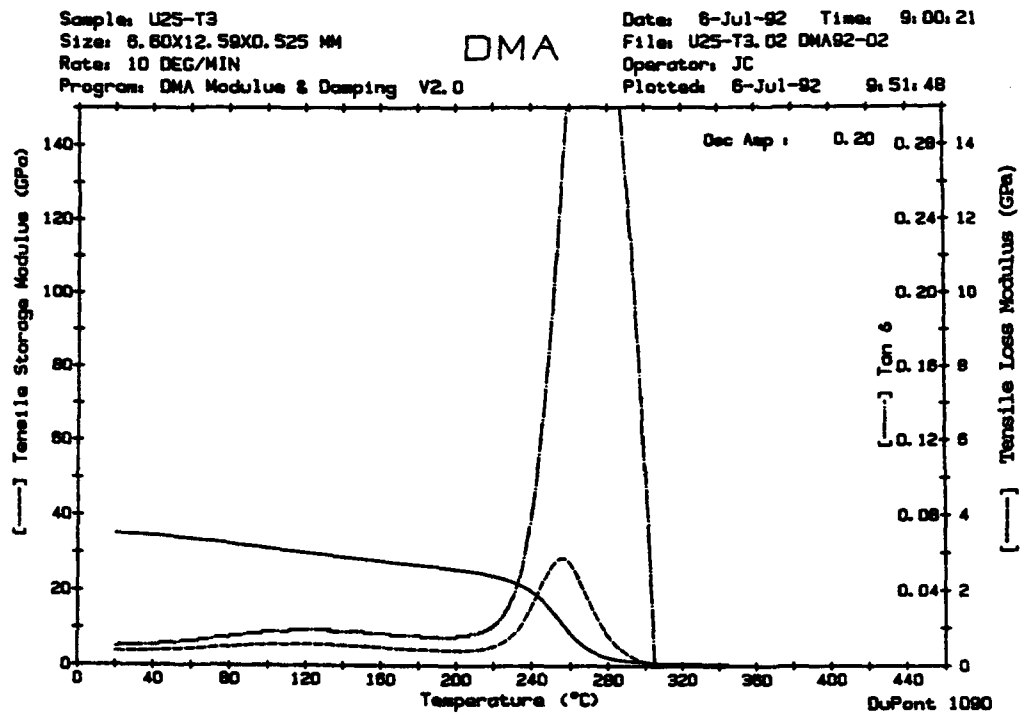


Figure 49. DMA Plot for U-25 Composite (Transverse Direction, Dry).

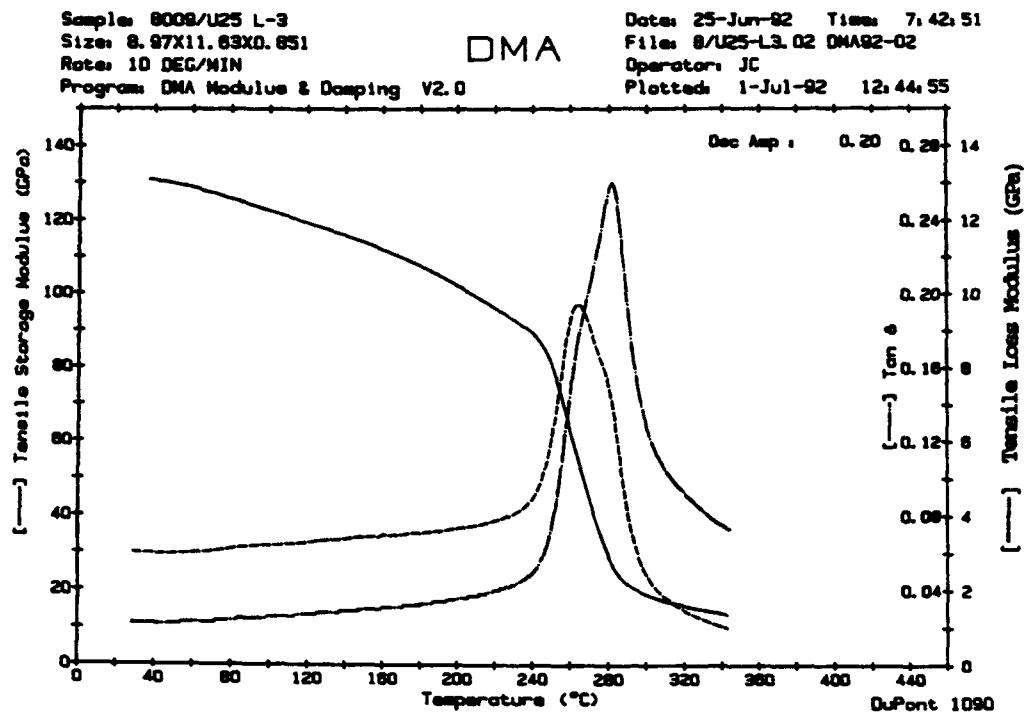


Figure 50. DMA Plot for 8009/U25 Laminate
 (Longitudinal Direction, Dry).

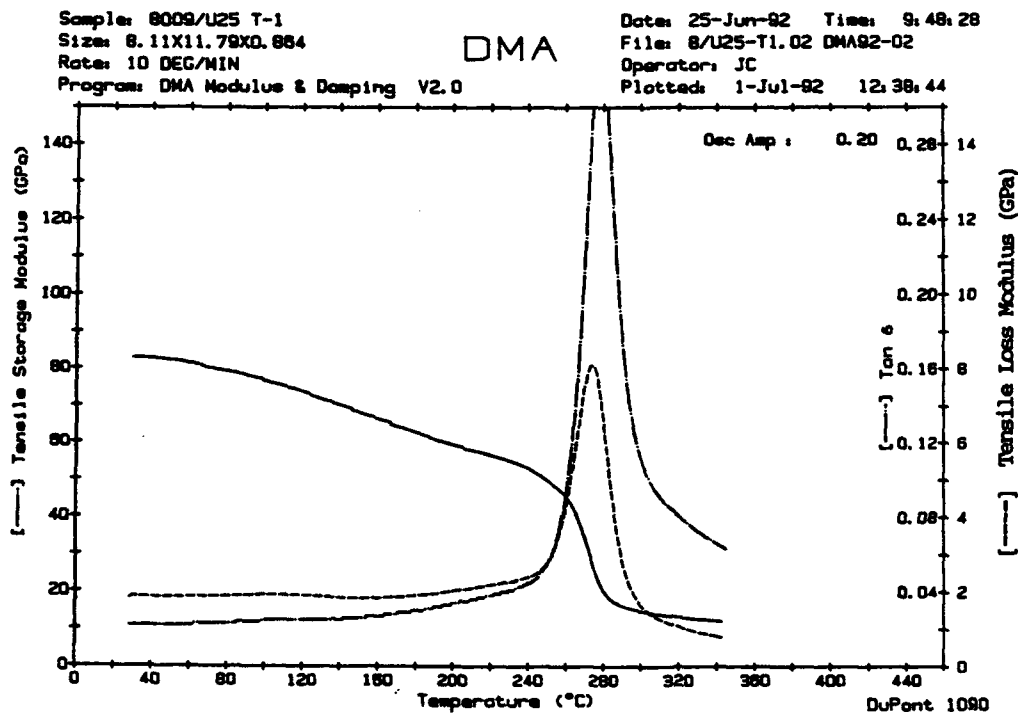


Figure 51. DMA Plot for 8009/U25 Laminate
 (Transverse Direction, Dry).

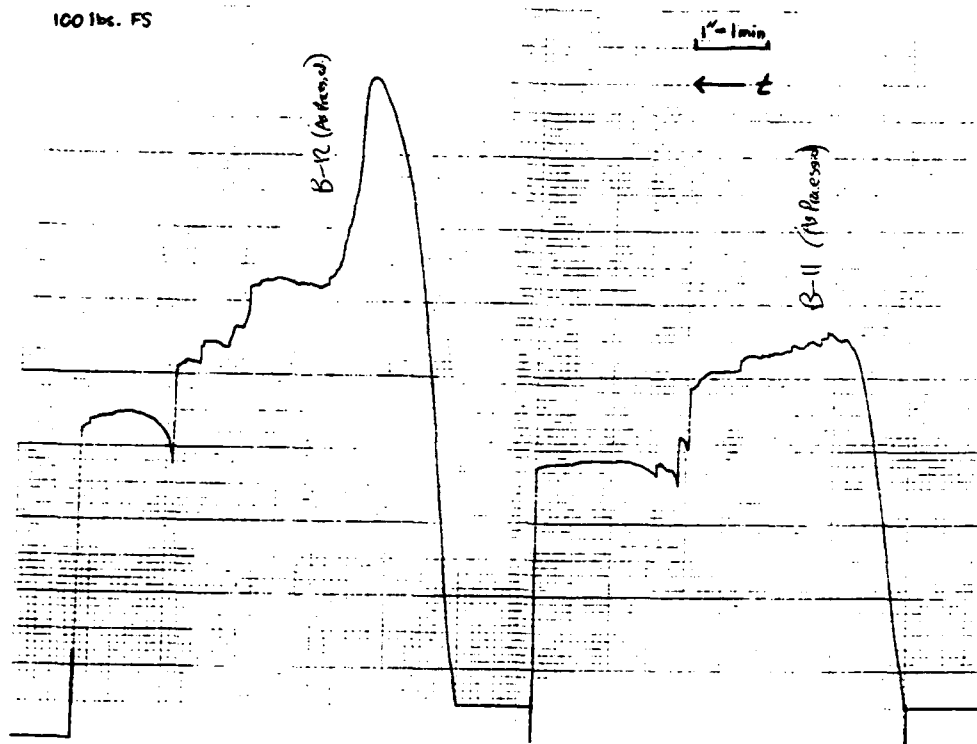


Figure 52. Typical 3-Point Bend Curves for 8009/U25 Laminates.

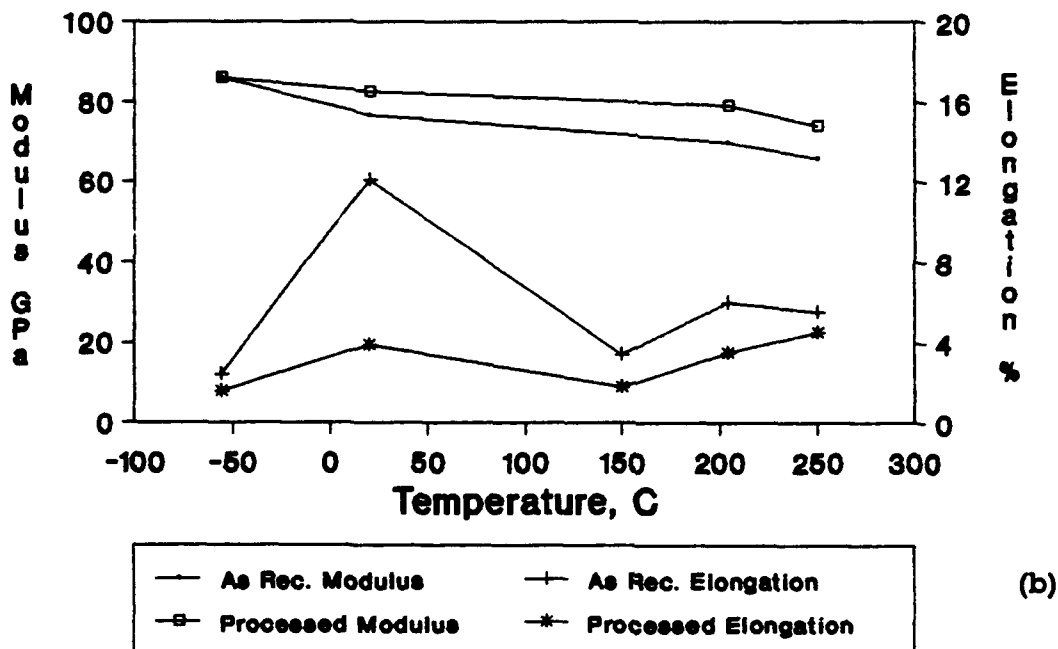
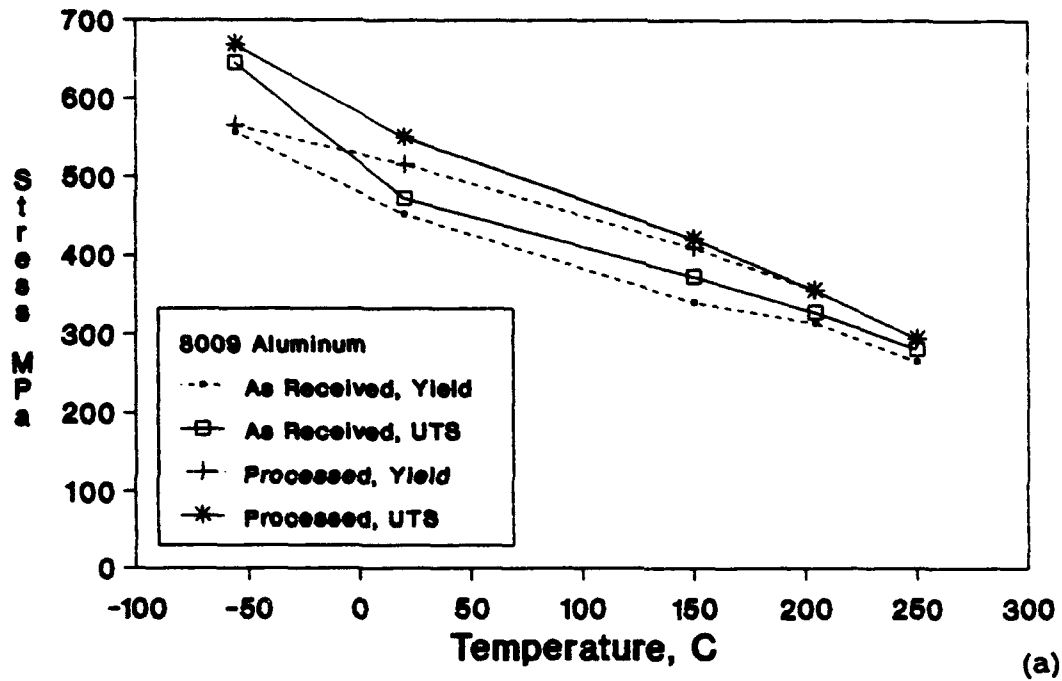
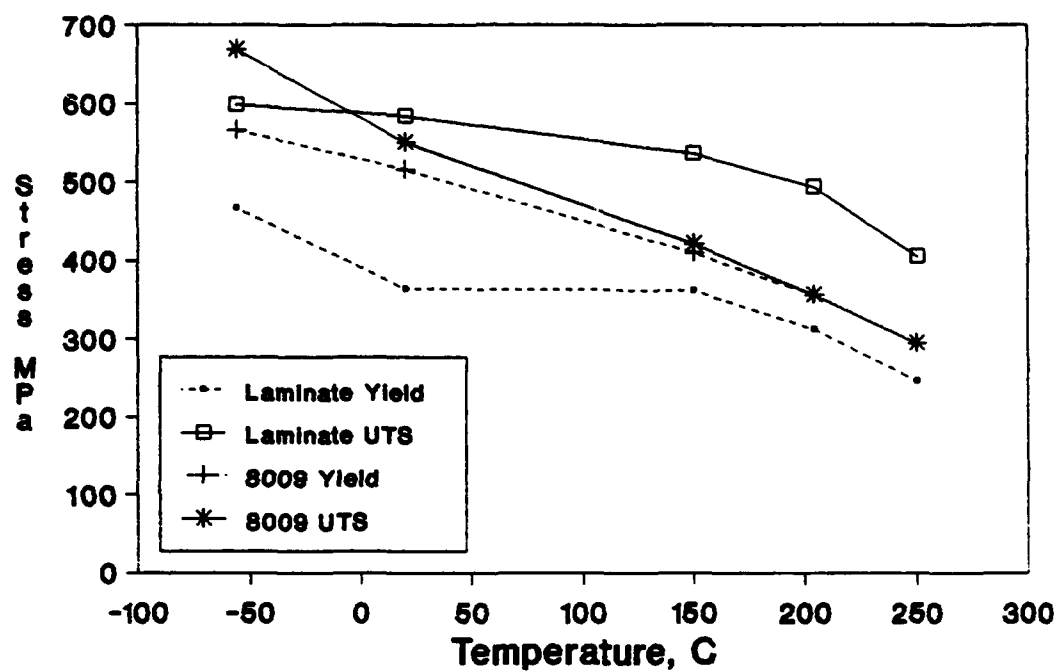


Figure 53. Tensile Properties of 8009 Aluminum.

(a) Yield and Ultimate Strength.

(b) Modulus and Elongation.



8009 in the "Processed" condition.

Figure 54. Tensile Properties of 8009/U25 Laminates vs. 8009 Aluminum.

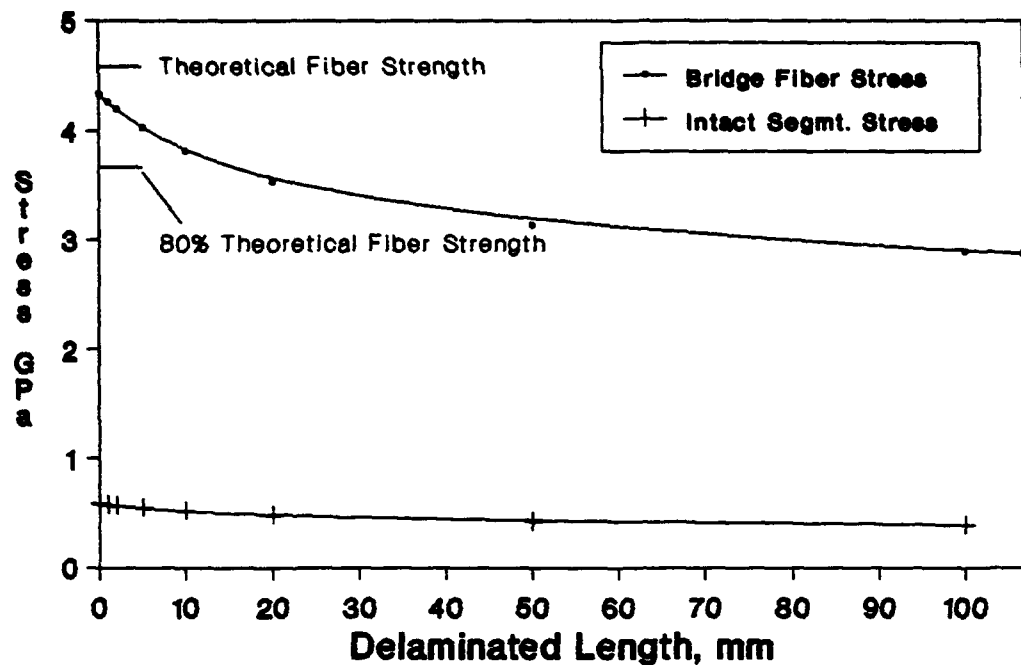


Figure 55. Stress in Crack-Bridging Fibers as a Function of Delaminated Length, Immediately after Failure of the Aluminum Layers.

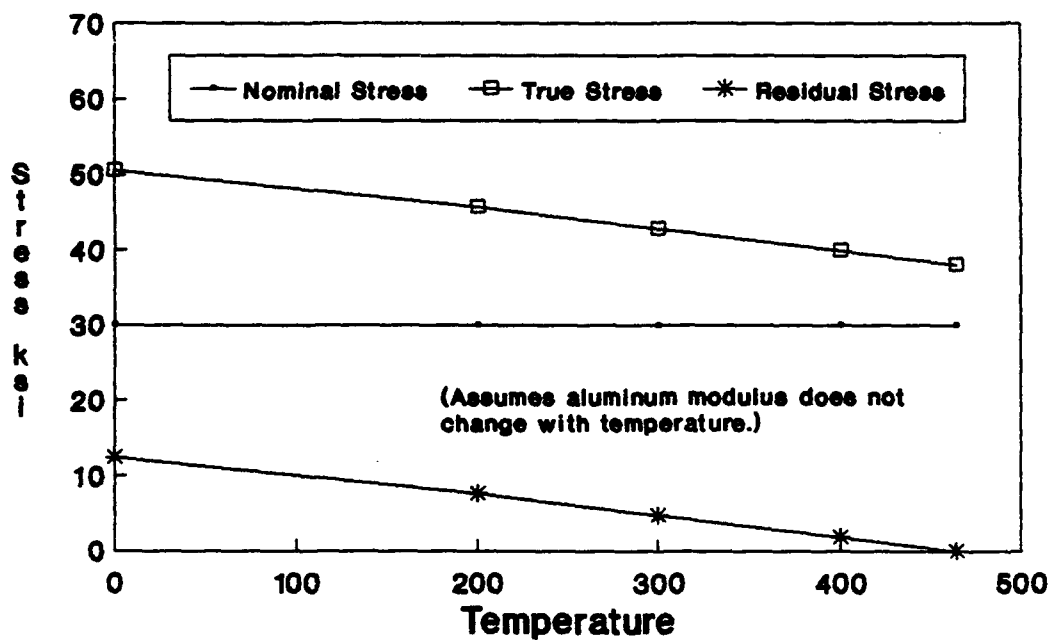


Figure 56. Residual Stress in 8009/U25 Laminate vs. Temperature.

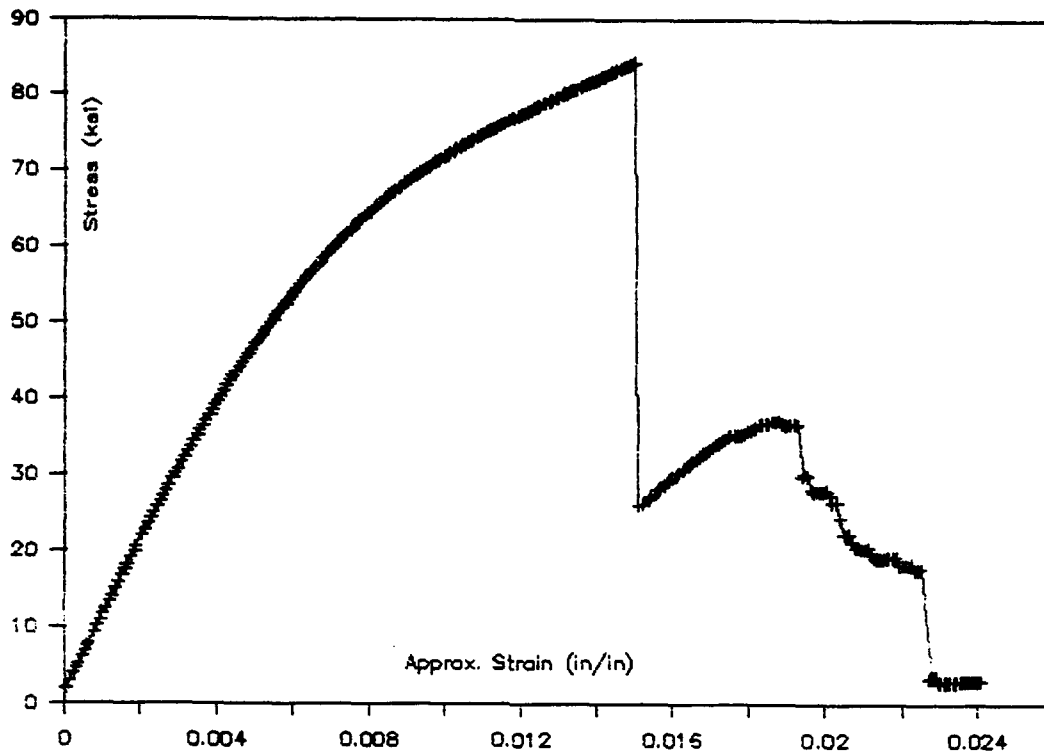


Figure 57. Load-Displacement Curve for -56°C Tensile Failure of 8009/U25 Laminate.

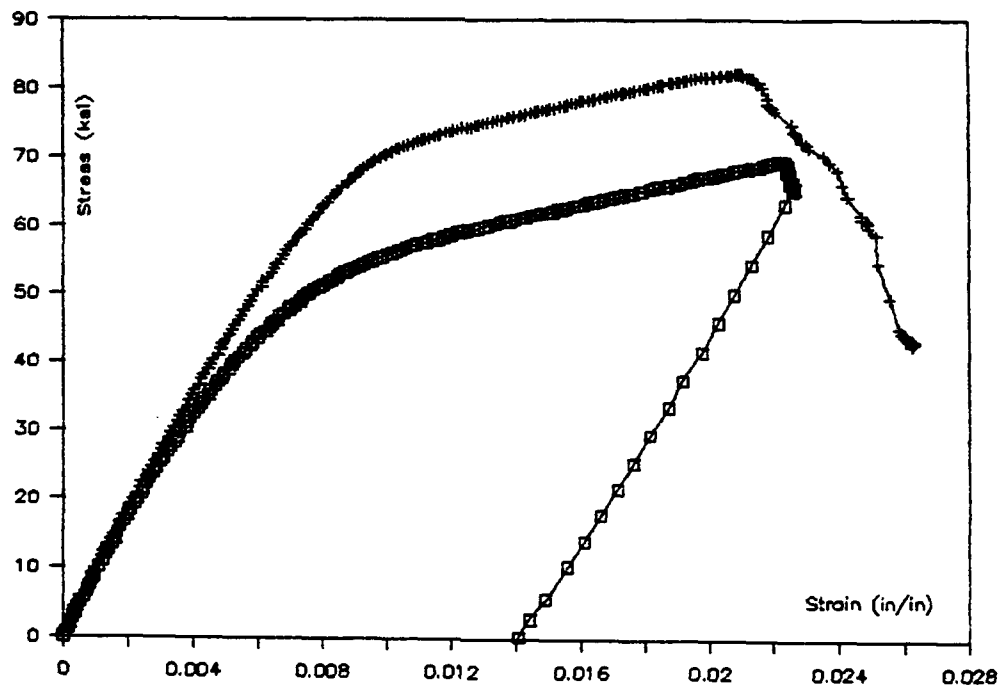
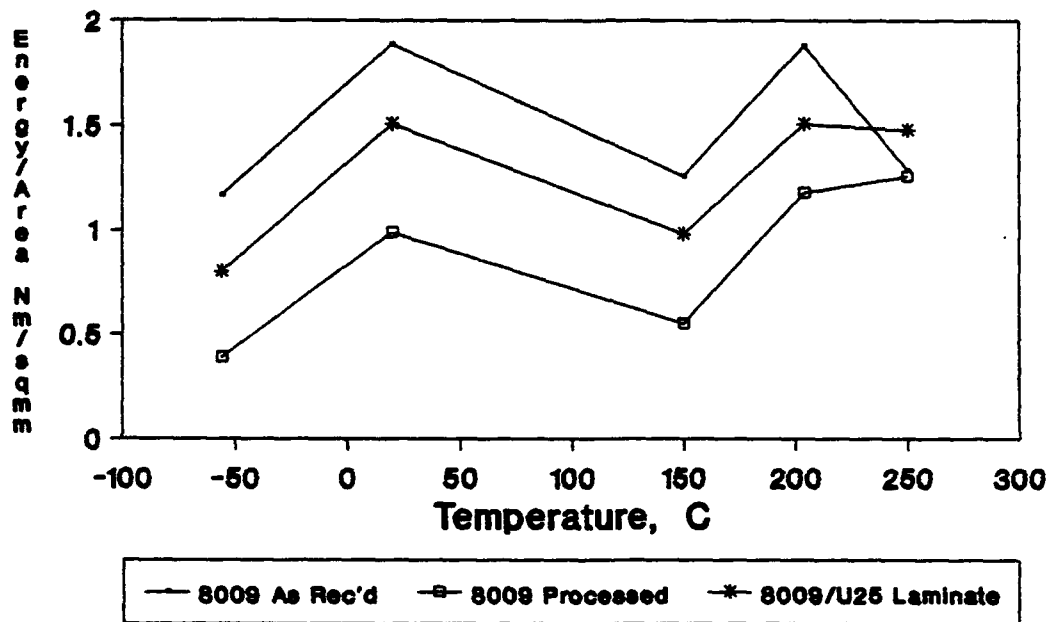


Figure 58. Stress-Strain Curve for Post-Stretching and Subsequent Tensile Testing of 8009/U25 Laminate.



* - Area under Load-Displacement curve
divided by cross-sec. area of specimen

Figure 59. Tensile Fracture Energies* vs. Test Temperature.

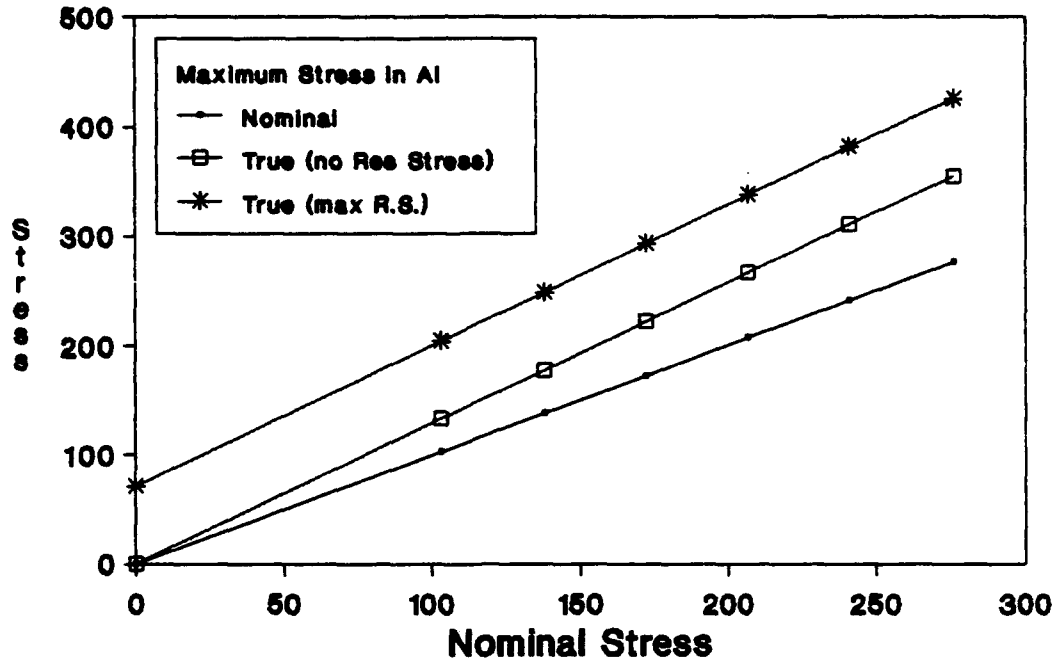


Figure 60. Maximum Cyclic Stress in Aluminum Layers:
8009/U25 Laminate vs. 8009 Aluminum.

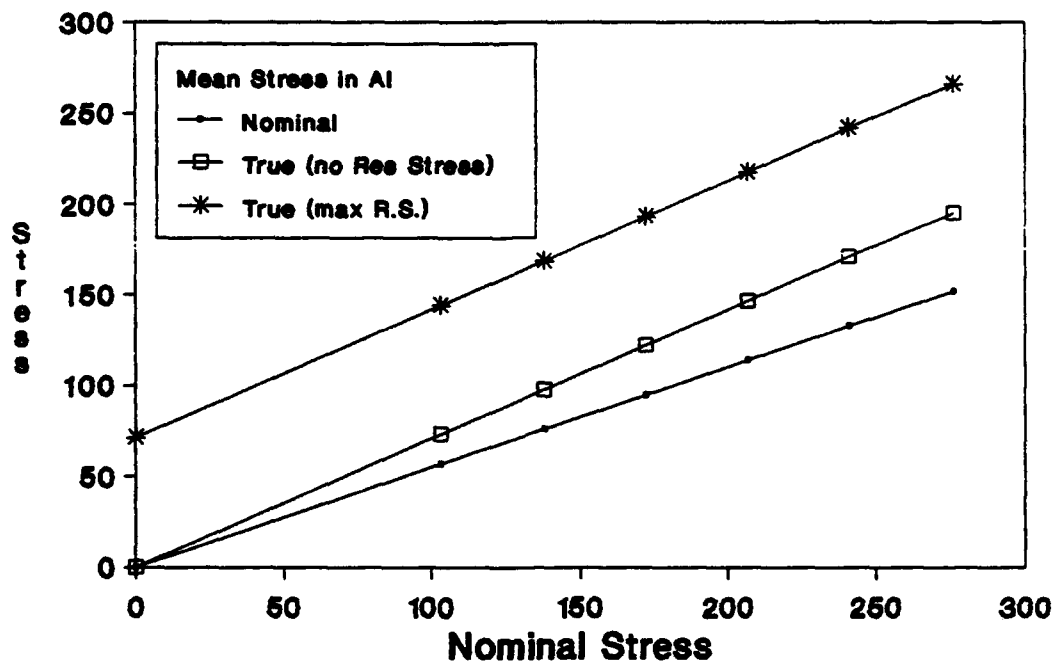


Figure 61. Mean Cyclic Stress in Aluminum Layers:
8009/U25 Laminate vs. 8009 Aluminum.

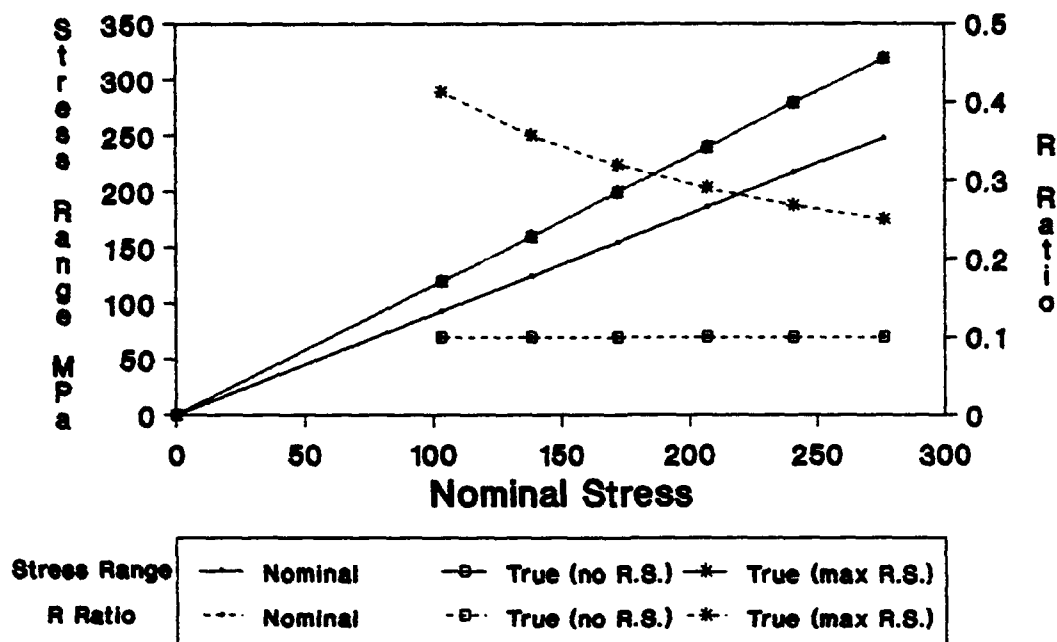


Figure 62. Stress Range and R Ratio in Aluminum Layers: 8009/U25 Laminate vs. 8009 Aluminum.

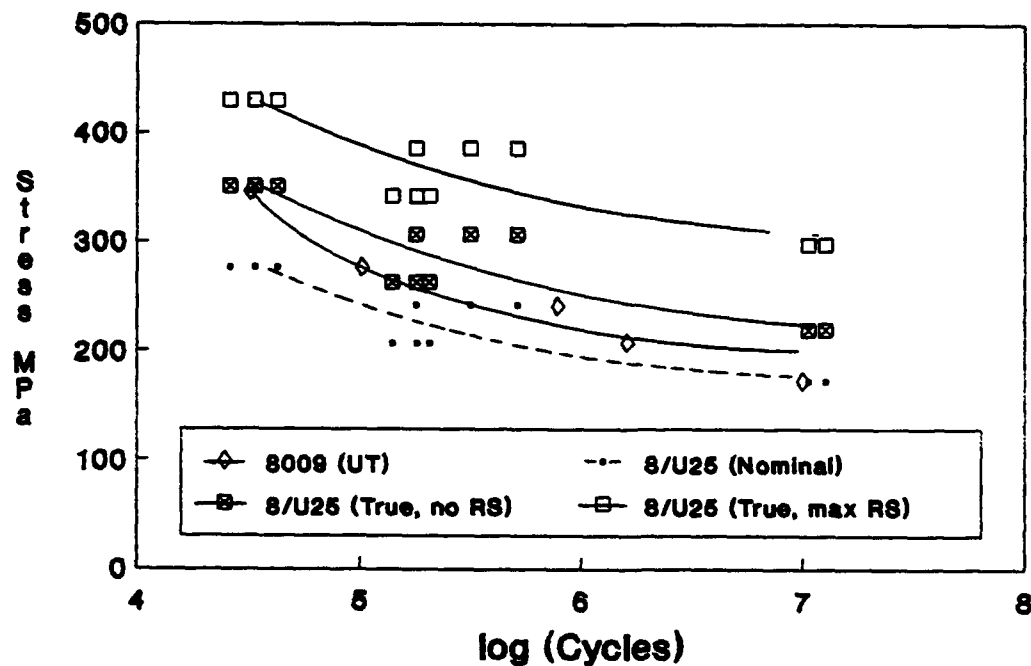


Figure 63. S/N Curves for 8009/U25 Laminate, Corrected for True Stress in the Aluminum Layers.

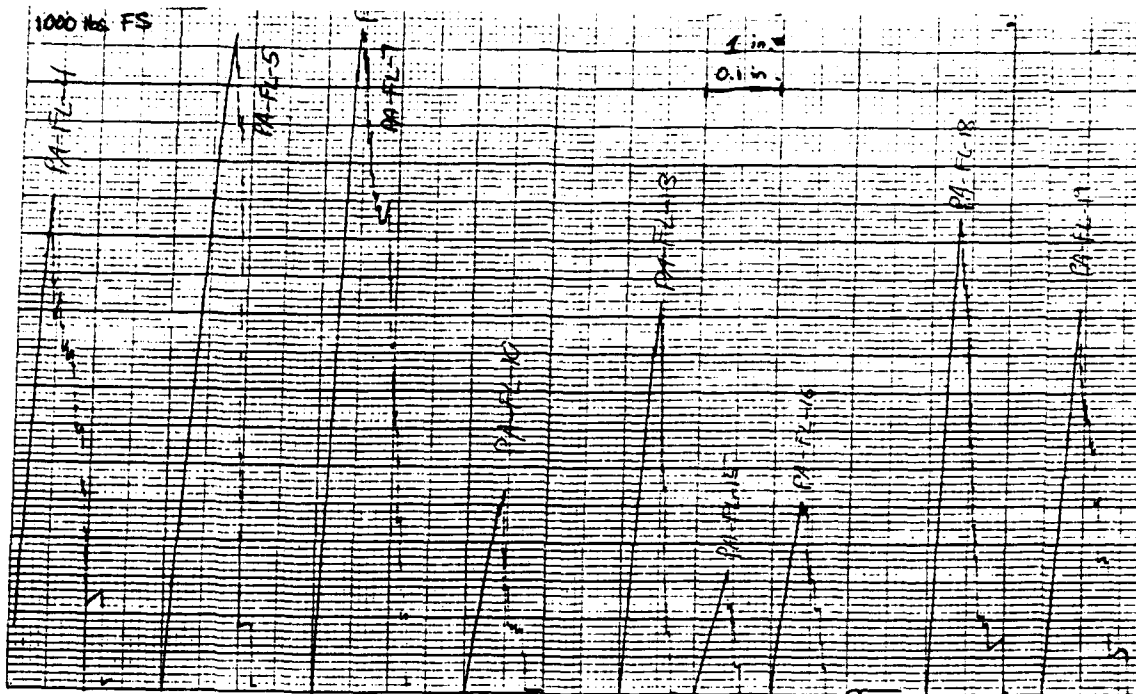


Figure 64. Example Curves for Residual Stress after Fatigue.

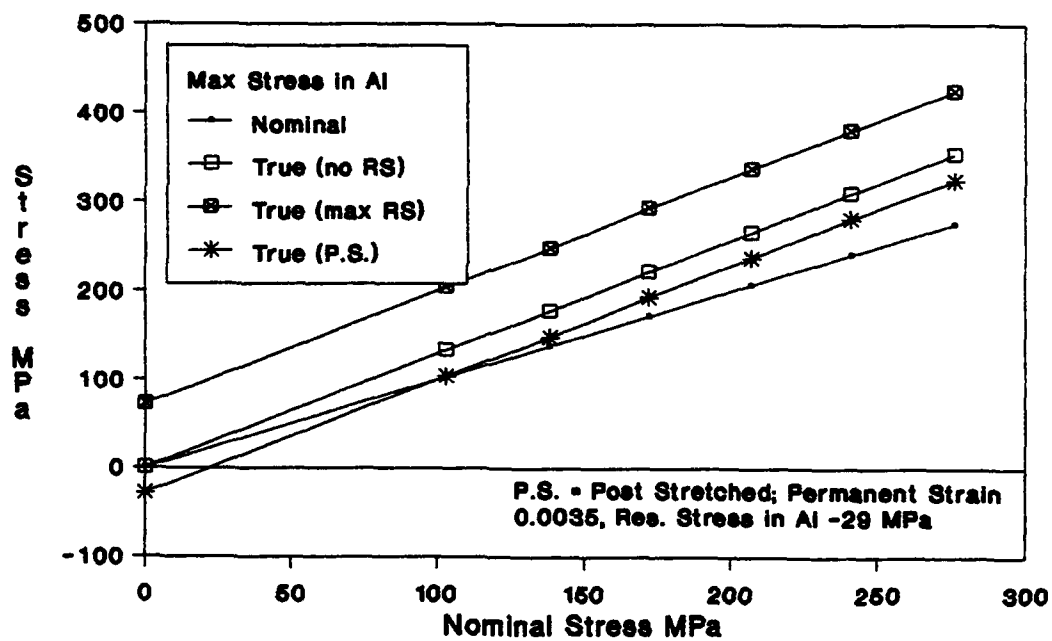


Figure 65. Effects of Post-Stretching on the Maximum Cyclic Stress in the Aluminum Layers.

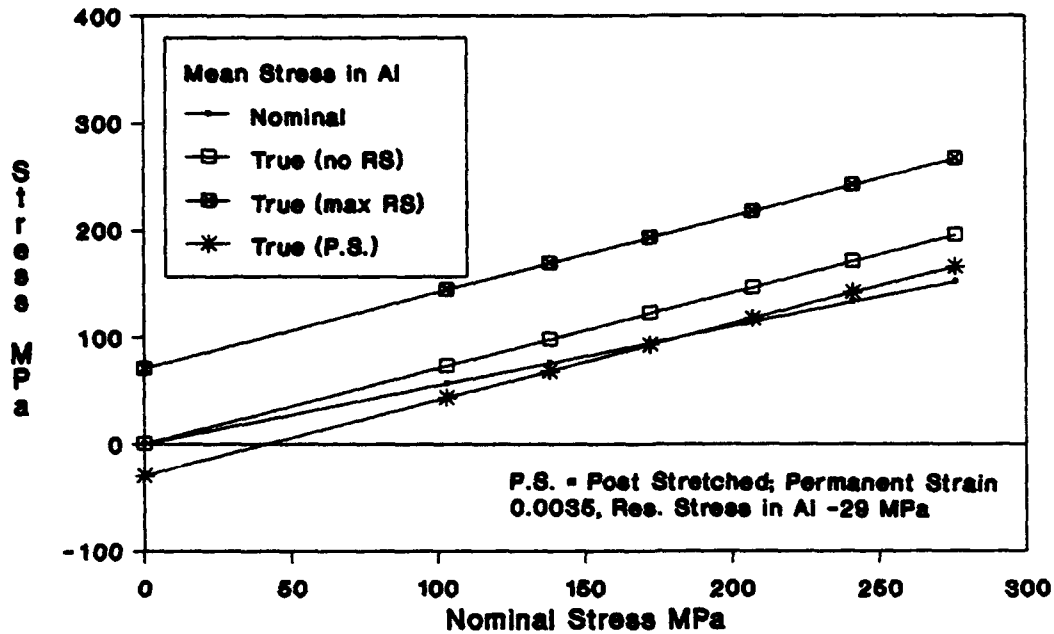


Figure 66. Effects of Post-Stretching on the Mean Cyclic Stress in the Aluminum Layers

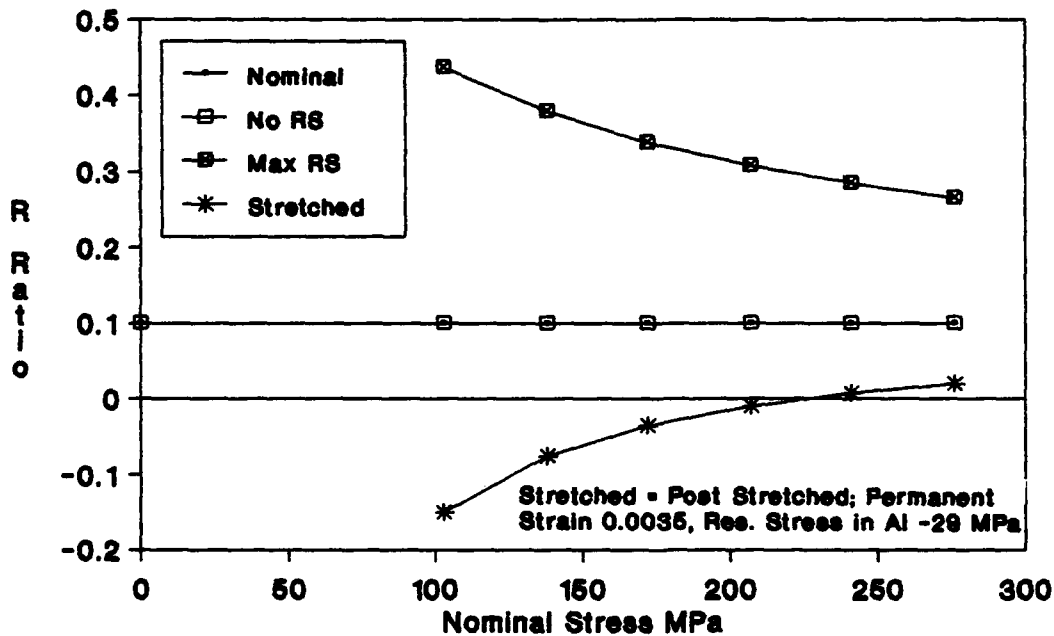


Figure 67. Effects of Post-Stretching on the Stress Range and R Ratio in the Aluminum Layers

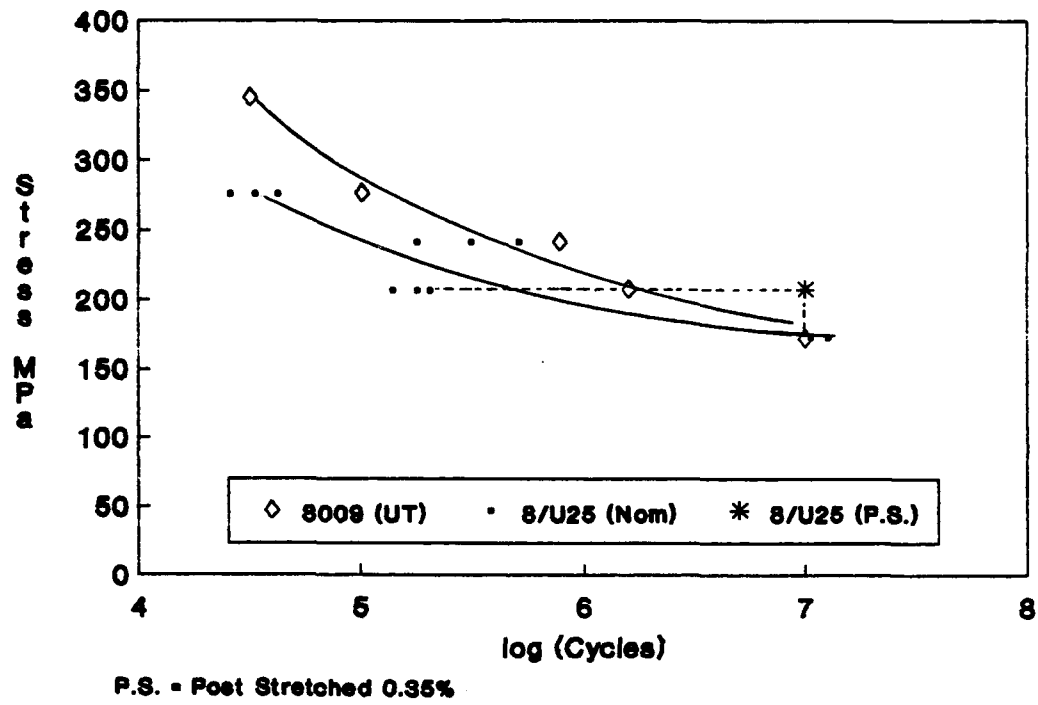


Figure 68. Effects of Post-Stretching on Fatigue Life:
8009/U25 Laminates

APPENDICES

APPENDIX I: 8009/U25 Laminates - Residual Stress.

A) In Aluminum Layers:

$$\sigma_{\text{res.Al}} = \Delta e \frac{E_{\text{Al}} E_f V_f}{E_{\text{Al}} V_{\text{Al}} + E_f V_f} \quad \begin{aligned} E_L &= E_{\text{Al}} V_{\text{Al}} + E_f V_f \\ \Delta e &= \Delta T (\alpha_{\text{Al}} + \alpha_f) \end{aligned}$$

$$\Rightarrow \underline{\sigma_{\text{res.Al}} = \Delta T (\alpha_{\text{Al}} - \alpha_f) (E_{\text{Al}} E_f V_f) / E_L} \quad \begin{aligned} \Delta T &= T_g - 20^\circ\text{C} \\ &= 240^\circ\text{C} - 20^\circ\text{C} \\ &= 220^\circ\text{C} \end{aligned}$$

$$\begin{aligned} * E_L &= 64.2 \text{ GPa} \\ * E_{\text{Al}} &= 82.6 \text{ GPa} \\ E_f &= 88.9 \text{ GPa} \\ * \# V_f &= (E_L - E_{\text{Al}} V_{\text{Al}}) / E_f \\ &= 0.135 \\ \alpha_{\text{Al}} &= 22.5 \times 10^{-6} / ^\circ\text{C} \\ \alpha_f &= 1.6 \times 10^{-6} / ^\circ\text{C} \end{aligned}$$

$$(\Delta e = 0.0046)$$

$$\sigma_{\text{res.Al}} = 220 (22.5 - 1.6) \times 10^{-6} (82.6 \times 88.9 \times 0.135) / 64.2 \text{ GPa}$$

$$\boxed{\sigma_{\text{res.Al}} = 71.0 \text{ MPa (tensile)}}$$

B) In Fibers:

$$\sigma_{\text{res.f}} = -\Delta e \frac{E_f E_{\text{Al}} V_{\text{Al}}}{E_{\text{Al}} V_{\text{Al}} + E_f V_f} \quad \begin{aligned} E_L &= E_{\text{Al}} V_{\text{Al}} + E_f V_f \\ \Delta e &= \Delta T (\alpha_{\text{Al}} + \alpha_f) \end{aligned}$$

$$\Rightarrow \underline{\sigma_{\text{res.f}} = -\Delta T (\alpha_{\text{Al}} - \alpha_f) (E_f E_{\text{Al}} V_{\text{Al}}) / E_L} \quad \begin{aligned} \Delta T &= 220^\circ\text{C} \\ * E_L &= 64.2 \text{ GPa} \\ * E_{\text{Al}} &= 82.6 \text{ GPa} \\ E_f &= 88.9 \text{ GPa} \\ \# V_{\text{Al}} &= 0.632 \\ \alpha_{\text{Al}} &= 22.5 \times 10^{-6} / ^\circ\text{C} \\ \alpha_f &= 1.6 \times 10^{-6} / ^\circ\text{C} \end{aligned}$$

$$\sigma_{\text{res.f}} = -220 (22.5 - 1.6) \times 10^{-6} (88.9 \times 82.6 \times 0.632) / 64.2 \text{ GPa}$$

$$\boxed{\sigma_{\text{res.f}} = -332.5 \text{ MPa (Compressive)}}$$

* = Based on experimental measurements.

= Based on a nominal laminate thickness of 1.47 mm (0.058 in).

APPENDIX II: 8009/U25 Laminates - Yield Strength.

A) Assuming Maximum Residual Stress:

$$\sigma_{YL} = (\sigma_{yAl} - \sigma_{res.Al}) V_{Al} + \sigma_{*f}^* V_f \quad (\sigma_{*f}^* = \sigma_f - \sigma_{res.f})$$

$$\sigma_{*f}^*/E_f = (\sigma_{Al} - \sigma_{res.Al})/E_{Al} \quad (\epsilon \text{ in all layers is assumed equal})$$

$$\Rightarrow \sigma_{*f}^* = (\sigma_{Al} - \sigma_{res.Al}) E_f/E_{Al}$$

$$\sigma_{YL} = (\sigma_{yAl} - \sigma_{res.Al}) V_{Al} + (\sigma_{yAl} - \sigma_{res.Al}) V_f (E_f/E_{Al})$$

$$\Rightarrow \underline{\sigma_{YL} = (\sigma_{yAl} - \sigma_{res.Al}) [V_{Al} + V_f(E_f/E_{Al})]}$$

$$\begin{aligned} * \sigma_{yAl} &= 516 \text{ MPa} \\ \sigma_{res.Al} &= 71 \text{ MPa} \\ \# V_{Al} &= 0.632 \\ * \# V_f &= 0.135 \\ * E_{Al} &= 82.6 \text{ GPa} \\ E_f &= 88.9 \text{ GPa} \end{aligned}$$

$$(\sigma_{*f}^* = 478.9 \text{ MPa})$$

$$\sigma_{YL} = (516 - 71) [0.632 + 0.135 (88.9/82.6)]$$

$$\boxed{\sigma_{YL} = 345.9 \text{ MPa}}$$

B) Assuming No Residual Stress:

$$\sigma_{YL} = (\sigma_{yAl} - \sigma_{res.Al}) [V_{Al} + V_f(E_f/E_{Al})]$$

$$\begin{aligned} * \sigma_{yAl} &= 516 \text{ MPa} \\ \sigma_{res.Al} &= 0 \\ \# V_{Al} &= 0.632 \\ * \# V_f &= 0.135 \\ * E_{Al} &= 82.6 \text{ GPa} \\ E_f &= 88.9 \text{ GPa} \end{aligned}$$

$$(\sigma_{*f}^* = 555.4 \text{ MPa})$$

$$\sigma_{YL} = (516 - 0) [0.632 + 0.135 (88.9/82.6)]$$

$$\boxed{\sigma_{YL} = 401.1 \text{ MPa}}$$

* = Based on experimental measurements.

= Based on a nominal laminate thickness of 1.47 mm (0.058 in.).

APPENDIX III: 8009/U25 Laminates - Ultimate Strength.**A) Accounting for Residual Stress:**

$$\sigma_{uL} = (\sigma_{uAl} - \sigma_{res.Al}) V_{Al} + (\sigma_{uf} - \sigma_{res.f}) V_f$$

$$\begin{aligned} * \sigma_{uAl} &\approx 500 \text{ MPa} \\ \sigma_{res.Al} &= 71 \text{ MPa} \\ \# V_{Al} &= 0.632 \end{aligned}$$

$$\begin{aligned} \sigma_{uf} &= 4585 \text{ MPa} \\ \sigma_{res.f} &= -332.5 \text{ MPa} \\ ** V_f &= 0.135 \end{aligned}$$

$$\sigma_{uL} = (500 - 71) \times 0.632 + (4585 + 332.5) \times 0.135$$

$$\sigma_{uL} = 935.0 \text{ MPa}$$

B) Neglecting Residual Stress:

$$\sigma_{uL} = \sigma_{uAl} V_{Al} + \sigma_{uf} V_f$$

$$\begin{aligned} * \sigma_{uAl} &\approx 500 \text{ MPa} \\ \# V_{Al} &= 0.632 \\ \sigma_{uf} &= 4585 \text{ MPa} \\ ** V_f &= 0.135 \end{aligned}$$

$$\sigma_{uL} = (500 \times 0.632) + (4585 \times 0.135)$$

$$\sigma_{uL} = 935.0 \text{ MPa}$$

* = Based on experimental measurements.

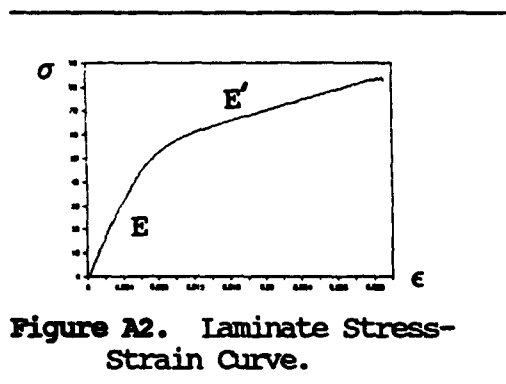
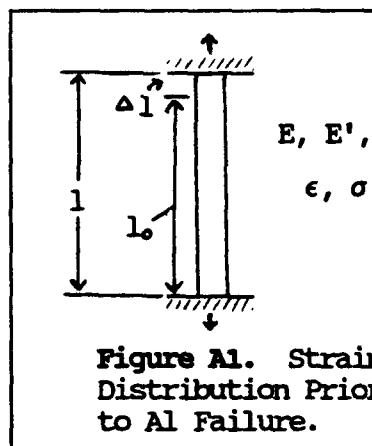
= Based on a nominal laminate thickness of 1.47 mm (0.058 in).

APPENDIX IV(A): 8009/U25 Laminates - Tensile Elongation Just Prior to Failure of the Aluminum Layers.

$$\Delta l = \epsilon l_0$$

$$\epsilon = \epsilon_{\text{elastic}} + \epsilon_{\text{plastic}}$$

$$\epsilon = \sigma_{YL}/E_L + (\sigma_{UL} - \sigma_{YL})/E'_L$$



- l_0 = Effective specimen length
- Δl = Change in specimen length
- ϵ = strain
- * σ_{YL} = Laminate yield strength
- * σ_{UL} = Laminate UTS
- * E_L = Laminate Elastic modulus
- * E'_L = Secondary modulus above the aluminum yield point

$$\Delta l = l_0 \left[\sigma_{YL}/E_L + (\sigma_{UL} - \sigma_{YL})/E'_L \right]$$

* = Based on experimental measurements and a nominal laminate thickness of 1.47 mm (0.058 in).

APPENDIX IV(B): 8009/U25 Laminates - Tensile Elongation and Stress in the Fibers Bridging the Cracked Aluminum Immediately After Failure of the Aluminum Layers.

$$\Delta l = \epsilon_1 l_1 + \epsilon_2 l_2$$

$$l_1 + l_2 = l$$

$$\epsilon_1 = \sigma_{yL}/E_1 + (\sigma_{uL} - \sigma_{yL})/E'_1 - (\sigma_{uL} - \sigma_1)/E_1$$

$$\epsilon_1 = (\sigma_{yL} + \sigma_1 - \sigma_{uL})/E_1 + (\sigma_{uL} - \sigma_{yL})/E'_1$$

$$\epsilon_2 = \sigma_2/E_2$$

$$\Delta l = l_1 \left[(\sigma_{yL} + \sigma_1 - \sigma_{uL})/E_1 + (\sigma_{uL} - \sigma_{yL})/E'_1 \right] + l_2 (\sigma_2/E_2)$$

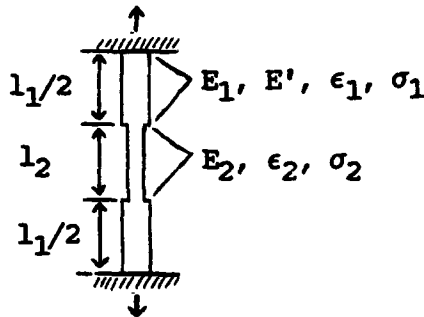


Figure A3. Strain Distribution after Aluminum Layer Failure.

- l = Effective specimen length
- l_1 = Effective specimen length away from delam. zone
- l_2 = Length of the delaminated zone
- * Δl = Change in specimen length
- ϵ_1 = Strain in undelaminated part of the specimen
- ϵ_2 = Strain in fibers in the delaminated zone
- * σ_{yL} = Laminate yield strength
- * σ_{uL} = Laminate UTS
- σ_1 = Stress remaining in the undelaminated part
- σ_2 = Stress in fibers in the delaminated zone
- * $E_1 = E_T$
- * $E'_1 = E'_L$
- E_2 = Fiber Elastic modulus

$$\Delta l = l_1 \left[(\sigma_{uL} - \sigma_{yL}) (1/E'_1 - 1/E_1) + (\sigma_1/E_1) \right] + l_2 (\sigma_2/E_2)$$

Northrop, Aircraft Division, One Northrop Av.,
Hawthorne, CA 90250, S. P. Agrawal and
G. R. Chanani.....2

Office of Naval Research, 800 Quincy St. , Arlington,
VA 22217-5000
G. Yoder (1 copy)
S. Fishman (6 copies).....7

Rice University, MEMF, P.O. Box 1892, Houston, TX
77251, Enrique Berrera.....1

Temple University, Dept. of Mechanical Engineering,
12th & Norris St. Phila., PA 19122, Jim S.J. Chen1

University of California, Dept. of Mechanical
Engineering, Irvine, CA 92717, Enrique J. Lavernia.....1

Wayne State University, 5050 Anthony Wayne Drive,
Detroit, MI 48202, John Benci.....1

Worcester Polytechnic Institute, 100 Institute Road,
Worcester MA 01609-2280, D. Apelian.....1

U.S. Air Force, AFOSR/NE Bldg. 410, Bolling AFB,
Washington, DC 20332-6448, Dr. Allen H. Rosenstein1

The Wichita State University, Dept of Mechanical
Engineering, Wichita, KS 67208, Jorge E. Talia.....1

Metal Working News, 201 King of Prussia Rd., Radnor, PA
 19089, R. R. Irving.....1

Metal Working Technology Inc. 1450 Scalp Avenue,
 Johnstown, PA 15904, W. L. Otto.....1

McDonnell Aircraft Co., Box 516, Saint Louis, MO 63166,
 K. K. Sankaran.....1

NASA Headquarters, 600 Independence Av., Washington,
 DC 20546, N. Mayer, S. Vennesi.....2

NASA Langley Research Center, Hampton, VA 23365,
 A. Taylor, L. Blackburn,2

National Bureau of Standards, Gaithersburg, MD 20899,
 R. Shaffer, J. R. Manning.....2

National Science Foundation, Office of Science and
 Technology Centers Division, 1800 G Street,
 Washington, DC 20550, L. W. Haworth.....1

NAWCADWAR, Warminster, PA, 18974-5000,
 Library, Code 8131 (2 Copies),
 W.E. Frazier, Code 6063 (10 Copies).....12

NAVAIRSYSCOM, Washington, DC 20361, J. Collins Air-
 5304, L. Slotter Air-931.....2

NAWCADWAR, Lakehurst, NJ 08733-5100, R. Celin (AV624-
 2173), R. Jablonski (AV624-2174), G. Fisher (SESD)
 (AV624-1179), B. Foor (02T)4

NAWCADWAR, P.O. Box 7176, Trenton, NJ 08628-0176,
 F. Warvolis (PE34), A. Culbertson,2

Naval Air System Command, Washington, DC 20361-5140,
 R. A. Retta (AIR-51412),1

Naval Air System Command, Washington, DC 20361-5140,
 J. Jarrett (AIR-51412J),1

Naval Industrial Resources Support Activity, Bldg. 75-2
 Naval Base Phila., PA 19112-5078, L. Plonsky
 (NAVIRSA-203).....1

Naval Post Graduate School, Mechanical Engineering
 Department, Monterey, CA 93943, T. McNelly.....1

Naval Research Laboratory, Washington, DC 20375,
 Metallurgy1

DISTRIBUTION LIST

	Copies
Air Force Wright Aeronautical Lab., Wrigth Patterson AFB, OH 45433, W. Griffith (MLTM) and J. Kleek (WL/MLLM),	2
ARPA, 3701 North Fairfax Drive, Arlington, VA 22203, William Barker, Robert Crowe, Benn Wilcox.....	3
Allied-Signal Corp., P.O. Box 1021R, Morristown, NJ 07960, S.K. Das	1
BDM International, Inc., 4001 N. Fairfax Dr. #750, Arlington, VA 22203, P. A. Parrish.....	1
Boeing Commercial Airplane, Seattle WA , W. Quist.....	1
Center for Naval Analyses, 4401 Front Ave., P.O. Box 16268 Alexandria, VA 22302-0268.....	1
Clemson University, Dept. of Mechanical Engineering, Riggs Hall, Clemson, SC 29634-0921, H.J. Rack.....	1
Jeff Cook, 1233 N. Mesa Dr., Apt. 1140, Mesa Arizona 85201.....	5
Defense Technical Information Center, Bldg. #5, Cameron Station, Bldg. 5, Alexandria, VA 22314 (Attn. Adminstrator).....	2
Department of Energy, 100 Independence Av., SW Washington, DC 20585, Code CE142.....	1
Drexel University, Dept. of Materials Engineering, 32nd and Chestnut St., Phila., PA 19104, M. J. Koczak	3
Grumman Areospace Corp., Bethpage, NY 11714, M. Donnellan, P. N. Adler.....	2
Innovare Inc., Airport Road, Commonwealth Park, 7277 Park Drive, Bath, PA 18014, Al R. Austen.....	1
Lockheed Missiles and Space Co., Metallurgy Dept. 93- 10/204, 3251 Hanover St., Palo Alto CA 94304, R. Lewis and J. Wadworth.....	2
Marko Materials Inc., 144 Rangeway Rd., N. Billerica, MA 01862, R. Ray.....	1
Martin Marietta Laboratories, 1450 South Rolling Rd., Baltimore, MD 21227-3898, J. Venables, K.S. Kumar.....	2